MANAGEMENT DECISION SUPPORT SYSTEM OF SOLVENT-BASED POST-COMBUSTION CARBON CAPTURE

Norhuda Abdul Manaf

A thesis submitted in fulfillment of the
requirements for the degree of Doctor of Philosophy

Faculty of Engineering & Information Technology
University of Sydney

2017

Statement of Originality

I hereby declare that this thesis, submitted in fulfillment of the requirements for the award of Doctor of Philosophy, in the School of Chemical and Biomolecular Engineering, the University of Sydney, is my own work unless otherwise referenced or acknowledged. The document has not been previously submitted for the award of any other qualification at any educational institution. Most of the results contained herein have been published, accepted for publication, or submitted for publication, in journals or conferences of international standing. My contribution in terms of published material is listed in "Journal papers" and "Conference papers" chapters.

Norhuda Abdul Manaf

Acknowledgement

First and foremost, I would like to express my sincere gratitude to my advisor, Associate Prof Ali Abbas for his guidance, encouragement and continuous support for the past three years. Your advice on both research as well as on my career have been priceless. Not forgetting a special thanks to all the members of my research group and the administration staff in the School of Chemical and Bimolecular Engineering for their help and support. A special appreciation goes to my family for their love and encouragement. Lastly, for my parents who raised me with love and patience, and supported me in all my pursuits. This thesis is dedicated to both of you.

Thank you.

Norhuda Abdul Manaf

Sydney, NSW, Australia

November 2016

Abstract

Low emissions fossil fuel technologies are of significant importance for short and long term global energy securities. Solvent-based post combustion CO_2 capture (PCC) is well-known as one such technology, and one that is viable and mature for dealing with the excessive amounts of greenhouse gases (GHG) (i.e. CO_2) generated from power plants. While most countries are heading towards 'carbon capture-ready' power plants, comprehensive managerial studies are essential for the implementation of long-term solvent-based PCC commercial scale operations. Such studies would need to cover holistic industrial perspectives and approaches that consider technical, economic, social, policy, safety and environmental challenges.

A management decision-support framework for a coal-fired power plant with solvent-based PCC technology (integrated plant) is proposed and developed in this thesis. It is demonstrated as an appropriate systematic strategy to overcome and tackle key challenges in commercialization of solvent-based PCC technology. In light of the global concern (environmental and energy sustainability), the main objective of this thesis is to provide conceivable decision support and insight to serve the managerial level (investor and government) as well as the operational level (engineer and operator).

This thesis is organized in seven chapters covering four interrelated top-down

management levels including instrumentation, plant, enterprise and policy levels. A brief introduction pertaining to the solvent-based PCC technology, thesis motivations and objectives are given in Chapter 1. Chapter 2 comprises a comprehensive literature review of solvent-based PCC plant from the bottom level (PCC instrumentation level) until the top level (investment and management decision support of PCC system). This covers literature studies on the development of solvent-based PCC dynamic models, application of control and optimization strategies, economic feasibility and plant planning and scheduling.

Chapter 3 describes the development of solvent-based PCC dynamic model via empirical methods. The solvent-based PCC dynamic model is constructed based on actual pilot plant located from Tarong power station in Queensland, Australia. This model is developed and simulated in Matlab's Simulink Environment (Mathworks, USA). Open-loop dynamic analyses are presented to provide a deeper understanding of the dynamic behaviour of key variables in solvent-based PCC plant under variable power plant load conditions.

Chapter 4 presents the design of the control architecture for solvent-based PCC plant. Two control algorithms are proposed and developed, which utilise conventional proportional, integral and derivative (PID) controller and advanced model predictive control (MPC). Controllability analyses are presented subject to servo and regulator problems while considering implications of constraints. These analyses are performed based on actual operation of solvent-based PCC plant while considering the integration with coal-fired power plant. Later on, the performance comparisons between the PID and MPC algorithms are provided in this chapter.

Chapter 5 proposes a conceptual framework for optimal operation of flexible

solvent-based PCC system retrofitted with a coal-fired power plant. The framework consists of a hybridization of control algorithm (Chapter 4) and economic optimization (Chapter 5). The MPC controller is chosen as the control algorithm while mixed integer non-linear programming (MINLP) using genetic algorithm (GA) function is employed in the optimization algorithm. Both algorithms are integrated to produce a hybrid MPC-MINLP algorithm. Capability and applicability of the hybrid MPC-MINLP algorithm is evaluated based on 24 hours operation of power plant retrofitted with solvent-based PCC system. Subsequently, a developed hybrid MPC-MINLP algorithm is used to predict investment opportunity in term of technical operation (investing in control strategy) based on the estimated annual plant net operating revenue for year 2011 and forecast 2020. This investment decisions is applied for fixed and flexible operation mode of solvent-based PCC plant associated with coal-fired power plant subject to Australia electricity market trend and various type of climate/carbon policies.

Chapter 6 extends the scope of Chapter 5 by evaluating the relevance of solvent-based PCC technology in the operation of black coal-fired power plant in Australia. This chapter considers a prevailing climate policy established in Australia namely Emission Reduction Fund (ERF) via Government's Direct Action Plan. Future operational and financial uncertainties of black coal-fired power plant operation under the ERF scheme are evaluated by estimating a feasible price of a tonne of Australian carbon credit unit (ACCU) that can provide financial benefit to the power plant throughout the contract period. A rigorous discussion on deployment of solvent-based PCC plant into large-scale application is made by considering the implication of climate policy (ERF project) towards plant's revenue, national emission target and viability of the solvent-based PCC plant at commercial scale. The analysis is demonstrated via multi-objective constrained optimization problem.

Finally, the concluding remarks and future extensions of this research are presented in Chapter 7.

Journal papers

[J1] N. A. Manaf, A. Qadir, and A. Abbas, "The hybrid MPC-MINLP algorithm for optimal operation of coal-fired power plant with solvent based post-combustion CO_2 capture." *Petroleum*, Accepted. 2016.

[J2] N. A. Manaf and A. Abbas, "Temporal multiscalar decision support framework for flexible operation of carbon capture plants targeting low-carbon management of power plant emissions." *Journal of Applied Energy*, vol. 169, pp. 912–926, 2016.

[J3] N. A. Manaf, A. Cousin, P. Feron, and A. Abbas, "Dynamic modelling, identification and preliminary control analysis of an amine-based post-combustion CO_2 capture pilot plant." *Journal of Cleaner Production*, vol. 113, pp. 635–653, 2016.

[J4] M. T. Luu, N. A. Manaf, and A. Abbas, "Dynamic modelling and control strategies for flexible operation of amine-based post-combustion CO_2 capture systems." *International Journal of Greenhouse Gas Control*, vol. 39, pp. 377–389, 2015.

[J5] N. A. Manaf, A. Cousin, P. Feron, and A. Abbas, "Control analysis of post combustion carbon dioxide capture process (PCC)." *International Journal of Chemical and Environmental Engineering*, vol. 5, pp. 250–254, 2014.

Conference papers

[C1] N. A. Manaf and A. Abbas, "Financial and operational uncertainties of Australian black coal electricity generation under Emission Reduction Fund policy." in *Australasia's Premier Chemical Engineering Conference (CHEMECA)*, Sept 25 - 28, 2016, Adelaide.

[C2] N. A. Manaf, A. Qadir, and A. Abbas, "Agile control of CO_2 capture technology for maximum net operating revenue." in *The 11th IFAC Symposium on Dynamics and Control of Process System, including Biosystems (DYCOPS-CAB)*, June 6 - 8, 2016, Norway.

[C3] N. A. Manaf and A. Abbas, "Off-line optimisation and control of carbon capture operations." in *The 26th European Symposium on Computer Aided Process Engineering (ESCAPE 26)*, June 12 -15, 2016, Slovenia.

[C4] N. A. Manaf, M. F. Zanil, M. A. Hussain, and A. Abbas, "Application of hybird PID-ANFIS controller for post combustion CO_2 capture process." in *Asia Pacific Confederation of Chemical Engineering Congress incorporating Chemeca (APCChE)*, Sept 27 - Oct 01, 2015, Melbourne.

[C5] N. A. Manaf, A. Cousins, P. Feron, and A. Abbas, "Dynamic modelling and simulation of post combustion CO_2 capture plant." in *Australasia's Premier Chemical Engineering Conference (CHEMECA)*, Sept 28 - Oct 01, 2014, Western Australia.

[C6] N. A. Manaf, A. Cousin, P. Feron, and A. Abbas, "Control analysis of post combustion carbon dioxide capture process," in *The 2nd International Renewable Energy and Environment Conference (IREEC)*, July 4 - July 6, 2014, Kuala Lumpur.

Table of Contents

List of Figures

List of Tables

List of Appendix

Glossary

ABS Absorber.

ACCU Australian carbon credit unit.

AEMO Australian energy market operator.

ARX Autoregressive with exogenous input.

AWS Ammonia wet scrubbing.

BAU Bussiness as usual.

CC CO_2 capture rate.

CCS Carbon capture and storage.

CER Clean Energy Regulator.

CFI Carbon Farming Incentive.

CO_2 Carbon dioxide.

CPRS Carbon Pollution Reduction Scheme.

CT Concentration transmitter.

CV Controlled variable.

DEA Diethanolamine.

DES Desorber.

DGA Diglycolamine.

$DIPA$ Diisopropanolamine.

EP Energy performance.

ERF Emission Reduction Fund.

ETS Emission Trading Scheme.

EU European Union.

FAE Forward abatement estimate.

FT Flow transmitter.

GA Genetic algorithm.

$GAMS$ General algebraic modeling system.

GHG Greenhouse gas.

GPC Generic Predictive Control.

GW Gigawatt.

Gg Giga-grams.

HE Heat-exchanger.

$ICSM$ Inexact management model.

$IChemE$ Institution of Chemical Engineers.

IEA International Energy Agency.

$IGCC$ Integrated gasification combined cycle.

MEA Monoethanolamine.

MIC Morari integral contollability index.

$MILP$ Mixed integer linear program.

$MIMO$ Multiple input multiple output.

$MINLP$ Mixed integer non-linear programming.

MPC Model predictive controller.

MS Membrane separation.

MV Manipulated variable.

MW Megawatt.

NDC Nationally Determined Contributions.

NEM National Electricity Market.

$NEPP$ National Energy Productivity Plan.

$NGCC$ Natural gas combined cycle.

NGT Natural gas turbine.

$NLARX$ Non-linear autoregressive with exogenous input.

$NMPC$ Nonlinear Model Predictive Control.

NPV Net present value.

NSW New South Wales.

OXY Oxy-fuel combustion.

$O\&M_{PCC}$ Operation and maintenance costs of PCC plant.

$O\&M_{PP}$ Operation and maintenance costs of power plant.

PCC Amine based (MEA) post combustion CO_2 capture otherwise stated.

PID Proportional, integral and derivative.

PP Power plant.

RE Solar and biomass energies.

RET Renewable Energy Target.

RGA Relative gain array.

RRP Regional reference price.

SS Solid sorbents.

i.e. example.

vs integrate with.

Chapter 1

Introduction

1.1 Global warming and climate change

Low emissions fossil fuel technologies are of significant importance for short and long term global energy securities. Post combustion CO_2 capture (PCC) is well-known as one such technology, and one that is viable and mature for dealing with the excessive amounts of greenhouse gases (GHG) (i.e. CO_2) generated from power plants. While most countries are heading towards 'carbon capture-ready 'power plants, comprehensive managerial studies are essential for the implementation of long-term PCC commercial scale operations. Such studies should cover holistic industrial perspectives and approaches that consider technical, economic, social, policy, safety and environmental challenges.

Global warming and climate change are arguably attributed to the elevation of GHGs particularly CO_2 with an approximate concentration of up to 80% from the total GHGs emissions in the atmosphere [4]. Based on the International Energy Agency (IEA) reports, energy sector (from the consumption of fuels for electricity and heat generation) accounts for more than 40% of CO_2 emissions as

compared to the other sectors as shown in Figure 1.1. From this fraction, coal-based energy is responsible for emitting the highest amount of energy-related CO_2 emissions (at the point of combustion) followed by natural gas and oil. This shapes the world forecast primary energy demand as illustrated in Figure 1.2. It shows that there is high possibility that the demand for coal power plants will rise towards year 2040. Relatively, oil will keep dominating the major energy demand by fuel throughout the coming decades. Though, energy-related CO_2 emissions from oil are less than those derived from coal and natural gas, its price which is relatively more expensive and its uncertainty in resource supply in part of the world contributes to the operation limit. Thus, it is realistically possible that coal-based energy will be the most viable electricity generation in the near future.

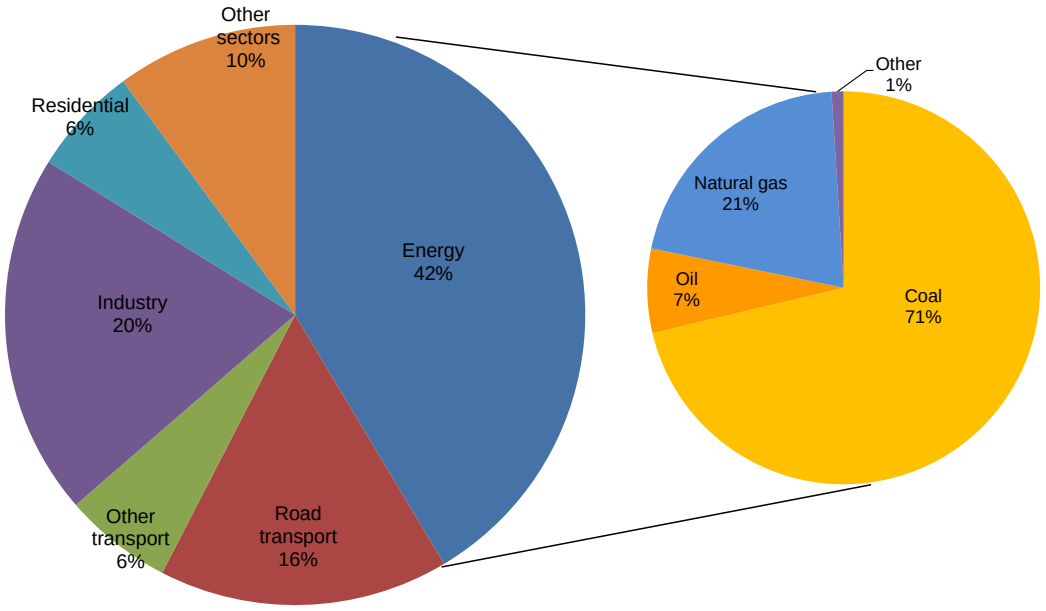

Figure 1.1: World CO_2 emission by sector [1].

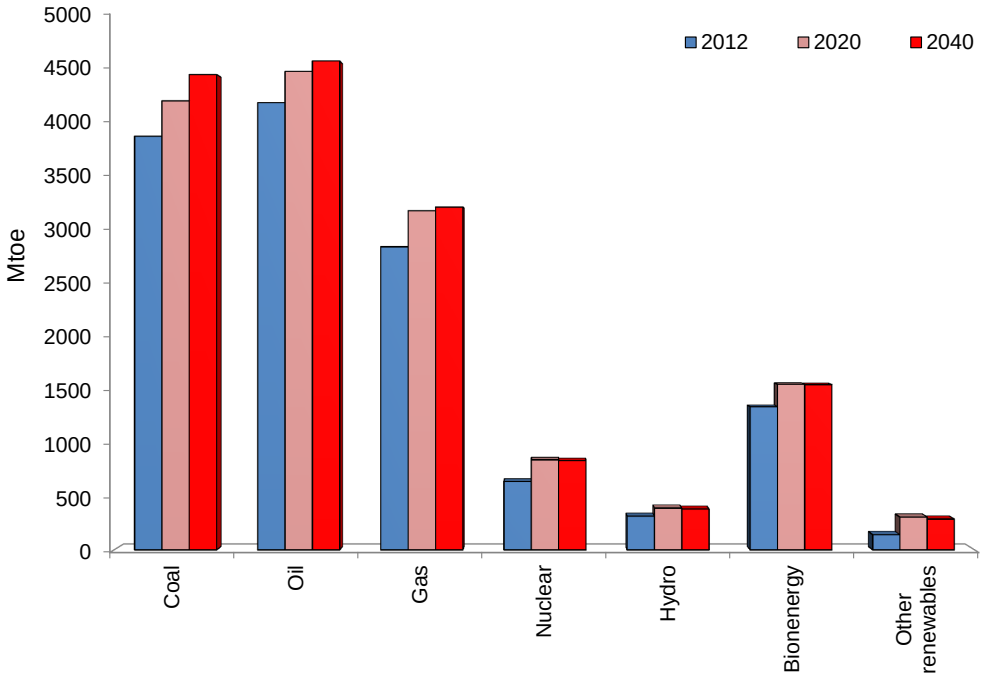

Figure 1.2: World primary energy demand by fuel [2].

In line with the Paris Climate Conference, Australia as one of the conference parties pledged to reduce its national GHGs emissions to 5% below 2000 levels by 2020. Based on the National Greenhouse Gas Inventory, Australia emitted about 550 000 Gg CO_2 in 2012 with an imperceptible reduction compared to the previous reported years [5]. From this value, the energy sector was identified as the largest CO_2 emitter which accounted for 76% of Australia total emissions. On the other hand, Figure 1.3 illustrates the historical and forecast trends of fossil-fuel power plants (energy sector) installed capacity in Australia [3]. In 2015, Australia had 19 GW installed capacity of black coal power plants which made up 40% of overall total installed power capacity [3]. Although coal-fired power installed capacity shows a large stagnant over the outlook period, it is expected that black-coal will be the major source of energy at least in the ten years ahead surpassing all other power technologies.

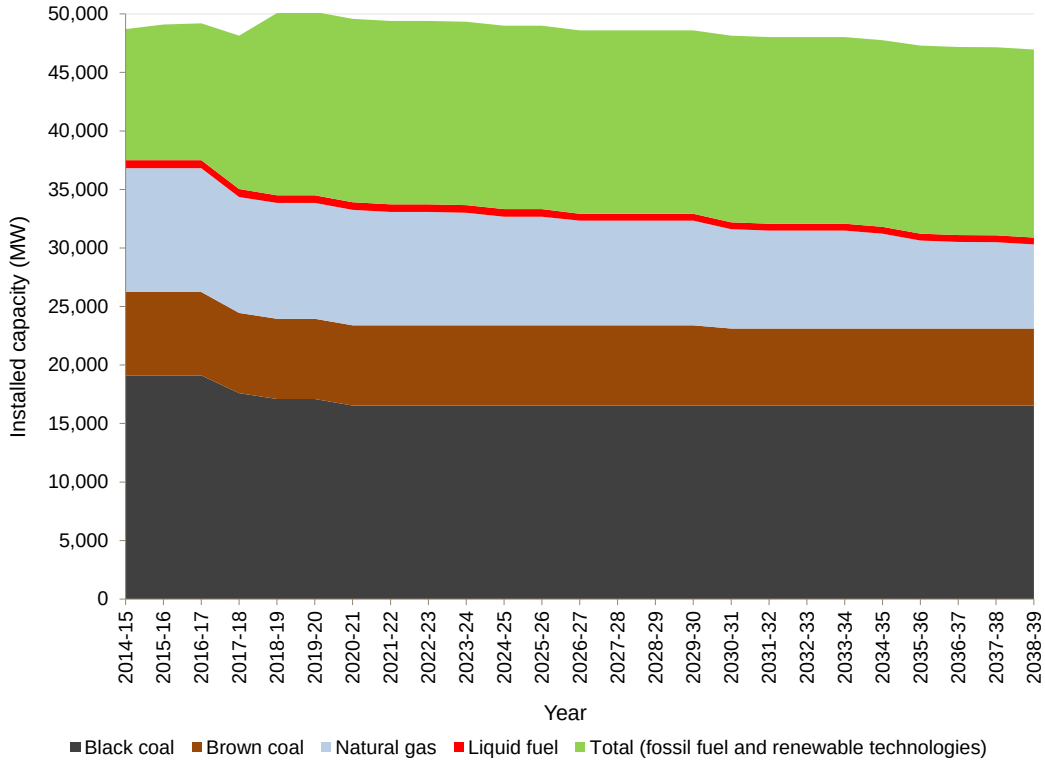

Figure 1.3: Total NEM installed capacity by technology in Australia [3]

To date, Australia has relatively high per capita annual emissions approximately 19 tonnes CO_2-e/person in New South Wales (NSW), compared to other developed countries, which have average per capita emissions around 12 tonnes CO_2-e/person [6]. One of the main factors influencing this high value is due to the large recoverable coal reserves resulting in dependency on coal-based electricity generation now and in a near future [6, 7]. This scenario indirectly compromises the national and global environmental and energy sustainability hence increases Australia's carbon footprint. Therefore, it is of significant importance for Australia to develop sound and effective CO_2 abatement technologies in line with concerted international action on climate change and energy policy to overcome this situation.

1.2 Link between energy security and climate change policy

Energy security refers to the uninterrupted availability of energy sources at an acceptable cost in terms of economic and environmental perspectives [8]. It can be divided into two dimensions, which are short-term, and long-term energy securities. Short-term energy security emphasizes on the robust and flexible operation of energy systems towards abrupt perturbation within the supply-demand balance. While, long-term energy security focuses on the perpetual energy supply consistent with the economic enhancement while satisfying environmental sustainability [8].

Essentially, energy security plays a vital role towards the growth of world economic activities. However, the introduction of existing and new climate change policy that stresses energy sustainability (i.e. via Carbon capture storage (CCS) and renewable energy technologies) is impacting on the structure and efficiency of the global energy system. Generally, climate change policy is manifested to control the excessive increment of GHGs emissions (i.e. CO_2) produced from energy sectors by implementing various measures, for instance, through fuel switching and demands reduction. Apparently, these measures provide negative impacts to the national and international energy portfolios in terms of fuel and technology mix. While, the security of energy system is always associated with the unprecedented risks such as monopoly/oligopoly of energy market prices, depletion of fossil fuel resource supplies and inadequate market structure [9], therefore efficient interaction and bilateral understanding between government and industry are imperative. This is to ensure that the objectives of climate change policy and security of the energy system are achievable and working commendably.

At present, CCS installation is part of the predominant EU climate change policy as a measure to tackle the national energy insecurity [9]. The directive aims to sustain the overall consumption of fossil fuels in power generation technologies in a near future by incentivizing various CO_2 mitigation technologies. Subject to this directive, it is expected that more coal-based power generations will be operated beyond 2020 as compared to oil and gas due to the coal's invulnerability towards natural and technical hazards and no pipeline transportation is required. This scenario not only applies to European Union (EU) but may be extended to other countries which use coal as their primary energy generation.

1.3 The evolution of Australia's policy on climate change

The Carbon Pollution Reduction Scheme (CPRS) is one of the earliest climate legislations enacted in Australia on December 2008 after several political contentions. It featured the Government's initial thinking on the establishment of an Australian Emission Trading Scheme (ETS) with the main objective to reduce greenhouse gas emissions [10]. However, the CPRS collapsed in 2009 due to political transition. On July 2012 under the Gillard Labor Government, Australia employed a new climate change policy via the carbon pricing mechanism. This policy employed fixed price period by providing emission permit or carbon tax at the $AUD 23/tonne of CO_2-e with a 2.5% increment each year. Following that, Gillard planned to make a transition from carbon pricing mechanism to ETS (adapted from the EU climate change policy), which was scheduled to be launched on 1^{st} July 2014.

However, after the end of the electoral cycle, a new climate policy replacing the

carbon price scheme emerged through the Direct Action Plan of the then new Liberal Government. In Australia, financial support to reduce emissions is available from various sources for instance, the Clean Energy Finance Corporation, the Australian Renewable Energy Agency and the Emissions Reduction Fund (ERF).

The ERF provides an incentive to businesses to reduce their emissions by purchasing Australian Carbon Credit Units (ACCUs). It operates through a reverse auction where organisations can bid their existing and future ACCUs and the Australian Government selects only those bidders that offer low cost ACCUs. Financial support is also available via the Safeguard Mechanism, where large greenhouse gas emitters are required to keep emissions below a defined baseline through the purchase and surrender of offsets such as ACCUs. ACCUs are created by undertaking certain activities that reduce emissions. Activities include avoided clearing of native forest protection project, reforestation, changes in land management, early savannah burning, fuel savings in the transport sector and industrial electricity and fuel efficiency [11]. Few industrial businesses have been involved in the creation of ACCUs or bidding in an ERF auction.

The ERF and Safeguard Mechanism are key components of the Australian Government's climate change policy suite. The related Carbon Farming Initiative (CFI) is the mechanism for creating ACCUs. Other elements of government policy that contribute to emission reduction include the Renewable Energy Target (RET) and the National Energy Productivity Plan (NEPP) [12]. The objective of these instruments is to support national efforts to meet Australia's Nationally Determined Contributions (NDC) of a 26 to 28% reduction in emissions relative to 2005 by 2030. The ERF establishes a market for ACCUs through the use of public funds to purchase ACCUs, with an initial AUD 2.55 billion being

made available up to 2020. It is anticipated that the Safeguard Mechanism will eventually drive the market for ACCUs as facilities whose emissions exceed their baselines are required to purchase ACCUs to offset their excessive emissions. All coal-fired generators are covered by the Safeguard Mechanism, and the proposed ERF project acts either to reduce the emissions of the power station so that emissions do not exceed its baseline or allows the power station to create ACCUs if emissions fall below the baseline.

1.4 CO_2 mitigation technology: Amine-based solvent post-combustion CO_2 capture (PCC)

By far, CCS technology is a mature and promising technology in capturing and mitigating the CO_2 emissions. One of the reliable technologies for reforming the carbon intensity in coal-fired power plants is PCC. To date, the most reliable process for CO_2 recovery from flue gas in PCC is by using conventional chemical absorption/desorption via aqueous solvents. The most widely used of aqueous solvents are alkanolamine, such as Monoethanolamine (MEA),Diglycolamine (DGA), Diethanolamine (DEA) and Diisopropanolamine (DIPA). Among them, MEA-based solvent gives more advantages in term of higher absorption rate, enhanced CO_2 capture efficiency and low cost.

In the PCC process (Figure 1.4), the resulting flue gas from the primary fuel combustion (coal-fired power plant) is treated to separate CO_2 in a PCC process which typically consists of two columns; absorber and desorber (known as stripper or regenerator columns). In the absorber column, the flue gas is contacted counter-currently with aqueous MEA, at 40 - 60^{o}C, atmospheric pressure where the MEA solvent is fed from the top of the column. The amine solvent absorbs

CO_2 via chemical absorption mechanism. Subsequently, a gas with reduced CO_2 content is exhausted at the top of the absorption tower (vent gas/off-gas) while CO_2-rich amine solution leaves from the bottom to pass through a cross heat exchanger before entering the desorber column at 1.5 - 2 atm and 100 - 120^{o}C. The rich stream loading is typically 0.4 - 0.5 mole CO_2/mole MEA. Regeneration of solvent by application of heat in the desorber releases the CO_2 gas. The regenerated amine solution is passed through cross heat exchanger and cooled to 40^{o}C before returning to the absorber. The CO_2 that is captured is then purified via various methods and transported for storage and utilization.

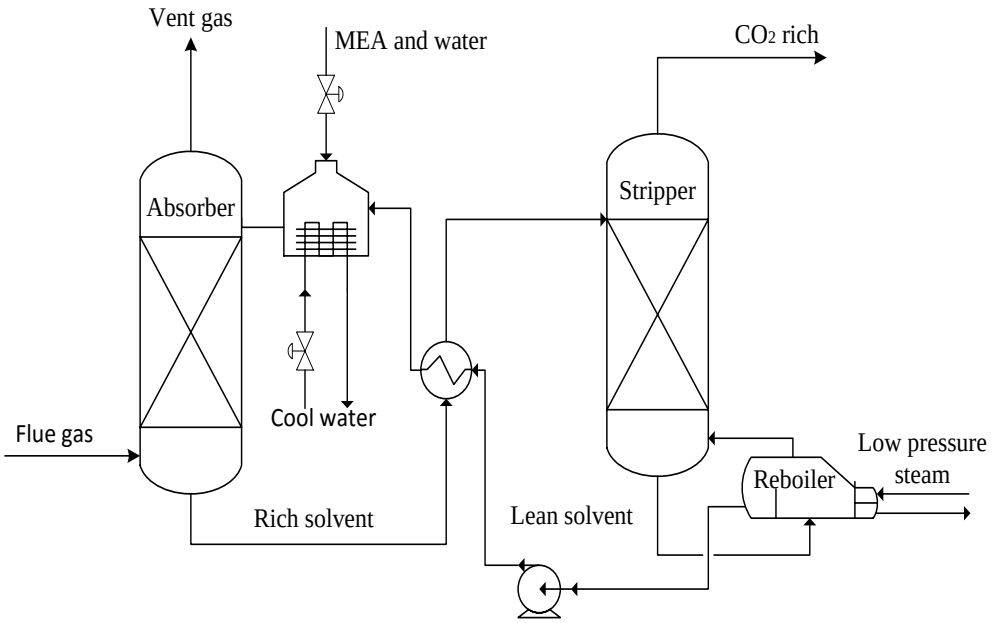

Figure 1.4: Process flow diagram for post-combustion CO_2 capture with MEA solvent.

Generally, PCC plant involves the addition of a downstream process to a conventional coal-fired power plant as illustrated in Figure 1.5. The integration involves low-pressure steam turbine (in power plant) and the reboiler system (in PCC

plant). Whereby, the steam extraction from the turbine system is utilized for solvent regeneration process in PCC plant.

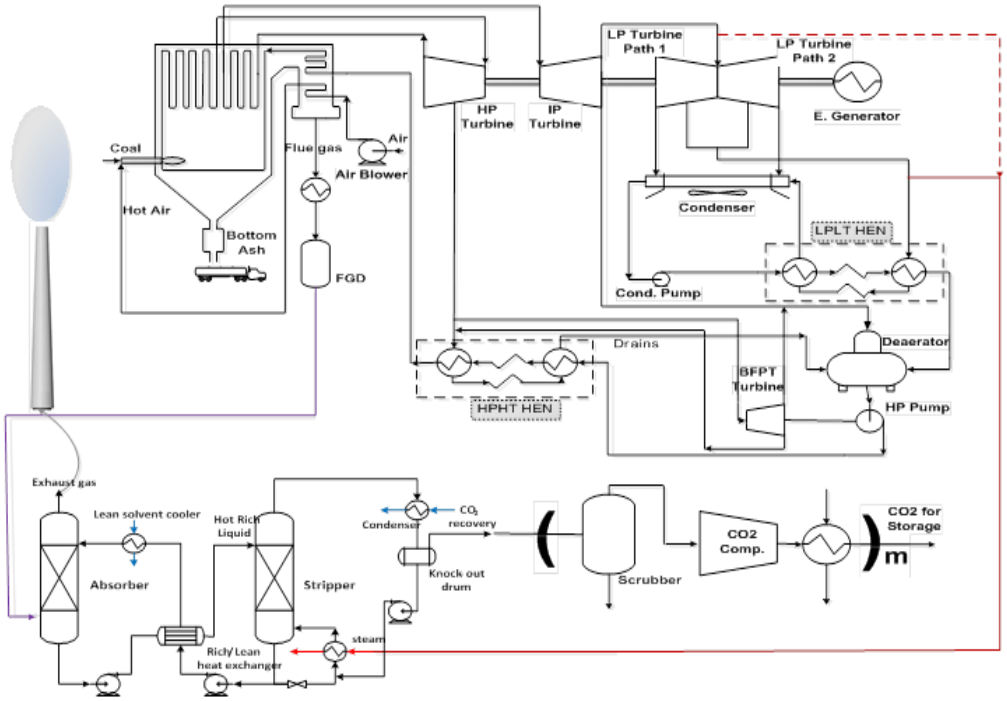

Figure 1.5: A schematic diagram of coal-fired power plant associated with amine-based PCC system with storage system.

1.5 Thesis motivation

The intriguing window in mitigating the GHGs (to limit global warming to 2^{o}C) and promoting sustainable energy has been a topic of debate globally. This challenge entails acceleration of decarbonisation of industrial emissions especially in electricity production where deployment of CCS can offer a robust solution to decouple the strong linkage between fossil fuel and climate change.

As of now, only few CCS technology (i.e. PCC plant) have been developed and commercialized to reduce CO_2 emission from the coal-fired power plant for in-

stance, one located in Regina, Canada [13]. However, operation of this technology back in 2011 had led to severe financial damage and a miniature environmental benefit to the power plant company thus jeopardized the long-term viability of PCC system. This situation was influenced by the operational and technical challenges particularly when PCC system is retrofitted into coal-based power plant. This might includes large energy and capture penalties, space constraints for carbon sequestration and the absence of robust climate change mitigation policy [14]. Additionally, uncertainty in economic (high operating and capital costs) and financial viability of PCC plant have also influenced and thus likely hindered the investment of the PCC plant into large-scale deployment. This is swayed by the volatility of national and international markets such as in CO_2 emission allowance, commodity prices (fuel and coal) and electricity price.

Essentially, integration of PCC into coal-fired power plants demands efficient control system and operational flexibility which particularly occur at the operation level (plant and instrument levels). This is due to the dynamic nature of the coal-fired power plant operation whereby plant particularly operates in a full load during peak hours (higher prices) and part load in off-peak hours (lower prices). These circumstances contribute to the fluctuation of flue gas emitted from the power plant consequently affecting the subsequent process, the PCC plant. Additionally, external interruptions from power plant and auxiliary systems can also contribute to the unstable operation of power plant. Thus resulting in transient behavior of PCC plant where eventually the overall performance of PCC plant is reduced.

Uncertainty in energy demand, electricity and carbon prices may cause interruption in the operation of coal-fired power plant with PCC system. Where, these uncertainties are usually unpredictable because they depend on the socio-economic

and political structure/status of the related countries. This can be featured during the abolishment of existing climate change policy due to the major political transition, fluctuation of electricity and carbon prices due to power outage and volatility on commodity markets (abrupt change in carbon/fuel prices).

These combined hurdles require effective interaction between the operational and management levels of coal-fired power plants if PCC plant is to be considered for a large scale deployment on site. In light of these circumstances, it is of crucial importance to explore and fill in the technological and knowledge gaps available in this area. This may include a comprehensive and holistic study focusing on the technical, economic, social, political, safety and environmental perspectives subject to different management levels (plant, instrument, government and policy levels).

This thesis has been motivated by the tremendous demands in clean-coal technologies by constructing an overarching computational framework consisting of multiscale modelling of the integrated plant (coal-fired power plant associated with PCC facility) embedded with an advanced plant-wide control and optimization algorithm at high temporal resolution. Moreover, this thesis fills in the gap in the existing research studies by utilizing real-time data subject to relevant scenario for targeting the low-carbon management of power plant emissions and yet still consider substantial plant revenue. This motivation is in sync with one of methodologies for CCS deployment as reported by the IChemE, where they proposed development of computational framework to forecast the effects of socio-economic and energy market when deploying the CCS technology [15].

1.6 Research objective

The management decision-support framework presented in this thesis encompassing of coal-fired power plant integrated with PCC technology (integrated plant). It is an appropriate strategy to overcome and tackle the challenges in commercialization of PCC technology. Concurrently, to ensure feasibility and profitability of coal-fired power plants when considering this technology. In light of the global concern (environmental and energy sustainability), the main objective of this thesis is to provide a conceivable decision and idea to the managerial (investor and government) and operational (engineer and operator) personnel pertaining to the future value of CCS technology (flexible retrofit PCC system) rather than providing a solution or methodology for the deployment of CCS technology. Where, eventually, this thesis may be able to answer the current predicament:

> "Is CCS technology (flexible retrofit PCC system) financially and technically worth doing in order to achieve future clean coal technology and how is CCS technology to be operated to attain the low-carbon energy generation in real-time situation?"

The developed management decision support framework consists of four interrelated levels which include policy, enterprise, plant and instrumentation levels as illustrated in Figure 1.6. The scope of each level is briefly explained below.

1. Instrumentation level: Development of PCC dynamic model using actual pilot plant data via system identification method (empirical method). This level provides a deeper understanding of the behaviour of key variables in PCC plant under variable power plant load conditions.
2. Plant level: Development of control algorithm for flexible operation of PCC plant subject to upstream perturbation from the coal-fired power plant.

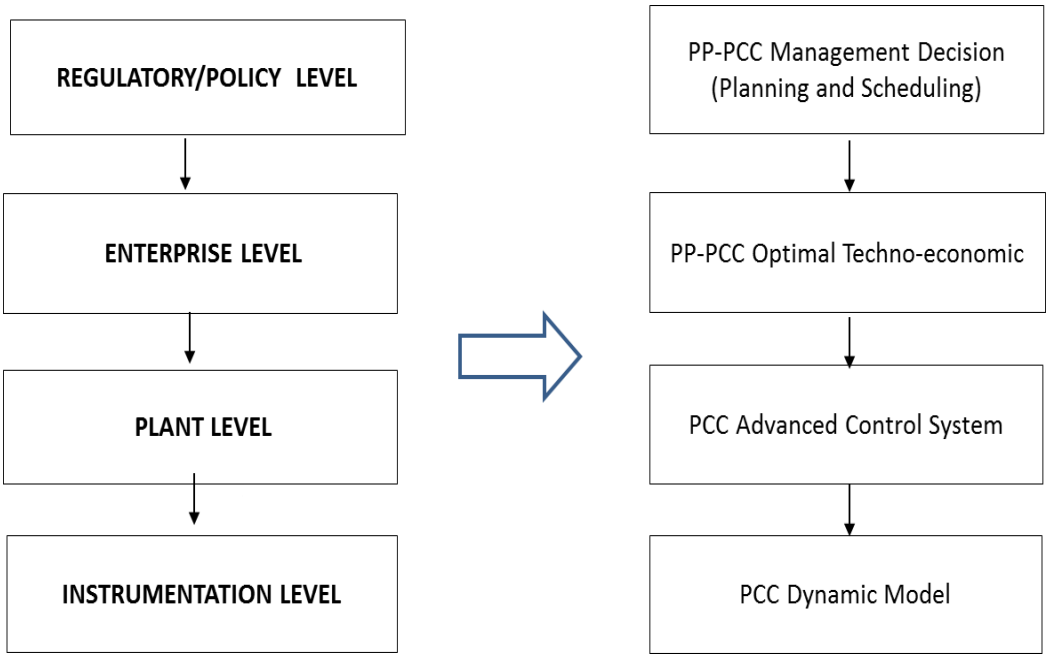

Figure 1.6: The management decision-support framework for coal-fired power plant retrofitted with PCC (PP-PCC).

This level exhibits actual plant-wide control operation of PCC plant by combining three aspects which include emission constraint, optimal energy and economic benefit.

3. Enterprise level: Development of the optimization algorithm integrated with control algorithm (from Plant level) for optimal operation of coal-fired power plant associated with PCC system. This level predicts power plant load trends and CO_2 capture rates subject to real-time electricity prices and various climate change policies.

4. Regulatory/Policy level: Evaluating the implication of prevailing climate change policy towards country's emission reduction and financial outcome of coal-fired power plant associated with PCC system.

Chapter 2

Literature review

In this chapter, a comprehensive literature survey of previous works is presented. It covers dynamic modelling and control of CO_2 capture system, not limited to only PCC process, optimization of capture system which include management decision-making (planning and scheduling) of various energy generations retrofitted with multi-technique of CO_2 capture system.

2.1 Process modelling, control and optimization of CO_2 capture plant

Many studies have focused on the development of steady state model of CO_2 capture plant including standalone column models and whole plant models. Nevertheless, steady state models convey limitations in imitating the actual PCC process (i.e. process dynamics), which exhibits highly nonlinear behavior. This features by the intricate interaction between process variables that are inherently impacted by numerous process uncertainties due to impulsive disturbances, particularly those coming from the power plant. Thus, development of a PCC dynamic model is of significant importance to overcome those limitations and

shortcomings.

For the past few years, several dynamic studies corresponding to amine-based PCC plant have been demonstrated, either it involves individual unit operation or complete PCC unit operation, for instance in [17-38]. In solvent-based PCC process, flue gas flow rate is considered as one of the critical variables in the absorber column and CO_2 capture plant as a whole. Since PCC plant will be integrated with power plant, which may suffer load fluctuation concomitant with the current electricity demand, many studies pertaining to the dynamic flue gas flow rate, have been conducted and published. For example, disturbance of flue gas in ramp-change[16], step change [17, 18, 19, 20], sinusoidal change [16] and linear perturbations [21, 22, 23]. According to the aforementioned studies, perturbation in flue gas flow rate (regardless of the disturbance configuration) in escalating magnitude will lead to a deficiency in PCC plant performance and ultimately to a reduction in Liquid/Gas (L/G) ratio. However, due to the fact that PCC variables have intricate relationships, inconsistencies in predicted dynamic behaviour are expected to emerge. This is underpinned by studies conducted by [24, 25], in which they perceived that the efficiency of PCC plant (or they named CCS%) is highly effected by the solvent flow rate. This is contrary to the work of [17] where they state that solvent flow rate did not have any significant impact on CO_2 removal efficiency.

Previously, Lawal et al.[26] determined L/G ratio as an important variable compared to flue gas and solvent flow rate in terms of PCC efficiency. They observed that the efficiency of the absorber was influenced by the L/G ratio and the efficiency of the regenerator by the reboiler heat duty. In a separate study, Gaspar and Cosmos [27] found that desorber feed stream temperature and column feed stream loading had more impact on CO_2 capture efficiency than L/G ratio. Posch

and Haider [22] also revealed another different outcome where they noticed that low absorber temperatures might influence the efficiency of CO_2 separation performance. On the other hand, other studies [23, 28, 29] concluded that to sustain the PCC plant performance and inventory, maintaining water balance or moisture content is critical. Besides that, Harun et al. [16] introduced a sinusoidal disturbance to the flue gas flow rate whereby, at the maximum flue gas flow rate, CO_2 removal efficiency decreased to 83% whilst at the minimum flue gas flow rate CO_2 removal efficiency reached a maximum of 99%.

Additionally, plant wide control strategy is employed to sustain a process at the desired operating conditions, securely and efficiently, while providing adequate environmental and product quality requirements. CO_2 capture plant specifically amine-based absorption PCC plant involves multifaceted process interactions (highly non-linear process) and thus requires understanding of the dynamics operation of the plant. Moreover, external interruptions from the power plant and auxiliary systems can contribute to the unstable operation of the plant. Thus resulting in transient behavior of PCC facility (as a downstream process) where eventually diminish the overall performance of the integrated plant (coal-fired power plant with PCC plant). A flexible operation of PCC plant features a potentiality to cope with those uncertainties and concurrently it can be benefited from the process control strategies in the face of process set point changes and disturbance rejections.

For instance, control strategies for flexible operation of power plant with CO_2 capture plant were demonstrated by Lin et al. [26]. Two dynamic strategies were analyzed to obtain the best strategy thus to enhance the flexibility of the capture plant by restricting the hydraulic fluctuations. The respective strategies were variation of lean solvent flow rate (VLSF) and variation of lean solvent loading

(VLSL). Based on that study, they concluded that the VLSL strategy outperformed the VLSF strategy in terms of plant flexibility and performance. Posch et al. [23] employed conventional PID controller in their dynamic simulation study, which was implemented on the absorber system. Ramp and continuous load changes were introduced to the system model and their work indicated that L/G ratio and CO_2 removal rate took substantial time to achieve the set point targets. A similar study was conducted by Lawal et al. [19]; five loops of P/PI controllers were deployed to regulate each respective variable which involved condenser temperature, reboiler temperature, reboiler level, water ratio in lean solvent, CO_2 capture level in absorber and condenser heat duty.

A reboiler model with a control strategy based on Generic Predictive Control (GPC) was presented by Arce et al. [29] while Akesson et al. [25] employed a Nonlinear Model Predictive Control (NMPC) strategy which was integrated with an optimization strategy [29, 25]. The study by Arce et al. was carried out on a reboiler with 78 kW capacity with circulation rate up to 690 kg/hr. The objective of their study was to determine energy and CO_2 costs by means of minimizing the operating cost concomitant with solvent regeneration. The control objective of the strategy developed by Akensson et al. was to regulate the PCC performance by minimizing the amount of steam required in the reboiler. They proposed NMPC with two degree of freedom which involves two manipulated variables; heat flow to reboiler and solvent flow. In their study, a trade-off between efficiency losses and capture rate within economic boundary conditions was considered. Table 2.1 shows the overview of literature survey on PCC research area (i.e. modelling, control and optimization), input-output variables employed for model development and type of modelling implementation tools used in the studies.

Table 2.1: An overview of literature survey on PCC plant modelling, control and optimization.

Ref.	Model section	Model/Control implementation tool	Application			CO_2 Efficiency	Input variable	Output variable
			Modelling	Control	Optimization			
[30]	CO_2 capture plant	gPROMS	✓	✓		90% & 95%	1. Lean solvent temperature 2. Reboiler heat duty 3. Temperature reboiler 4. Flue gas flow rate 5. Temperature condenser 3. Temperature reboiler	1. CO_2 removal rate
[24]	CO_2 capture plant	gPROMS	✓			90%	1. Flue gas flow rate 2. Steam rate 3. Lean solvent temperature 4. Lean solvent flowrate	1. CO_2 removal rate
[31]	CO_2 capture plant	gPROMS	✓				1. Flue gas flowrate 2. Reboiler heat duty	1. Lean loading 2. L/G (lean solvent/flue gas) 3. CO_2 removal rate
[22]	Absorber and desorber	Fortran	✓			90%	1. Lean solvent flow rate 2. Reboiler heat duty	1. CO_2 removal rate
[32]	Absorber and desorber	gPROMS	✓			96%	1. Flue gas molar flowrate 2. V/L fraction of reboiler 3. Lean solvent volume rate	1. Lean loading 2. Rich loading 3. CO_2 removal rate
[33]	Absorber and desorber	Aspen Plus	✓	✓			1. Reboiler heat duty 2. Lean solvent flowrate	1. CO_2 removal rate

Table 2.1: An overview of literature survey on PCC plant modelling, control and optimization (cont.).

Ref.	Model section	Model/Control implementation tool	Application			CO_2 Efficiency	Input variable	Output variable
			Modelling	Control	Optimization			
[17]	Absorber and desorber	gPROMS	✓				1. Lean solvent flowrate 2. Flue gas molar flowrate	1. CO_2 removal rate
[21]	Absorber and desorber	gPROMS	✓				1. CO_2 concentration in flue gas 2. Flue gas temperature 3. Lean solvent flowrate	1. CO_2 mass fraction in treated gas 2. Reboiler heat duty
[25]	Absorber and desorber	Modellica	✓	✓	✓	90%	1. Flue gas flowrate 2. Reboiler heat duty 3. Lean solvent flowrate 4. Flue gas molar composition	1. CO_2 removal rate 2. Reboiler temperature
[26]	Absorber and desorber	Aspen Plus	✓	✓	✓	90%	1. Flue gas flowrate 2. CO_2 composition in flue gas 3. H_2O composition in flue gas 4. Lean solvent flowrate	1. CO_2 removal rate 2. Lean loading 3. Reboiler heat duty
[16]	Absorber and desorber	Matlab	✓				1. Power plant load	1. Rich stream temperature 2. CO_2 removal rate
[27]	Absorber and desorber	gPROMS	✓	✓			1. Water balance control 2. Flue gas flowrate 3. Reboiler heat duty 4. CO_2 concentration in flue gas	1. Lean loading 2. CO_2 removal rate
[23]	Absorber	Aspen Custom Modeller	✓	✓		90%	1. Flue gas temperature 2. Flue gas volume rate 3. Lean solvent temperature	1. L/G (lean solvent/flue gas) 2. CO_2 removal rate

Table 2.1: An overview of literature survey on PCC plant modelling, control and optimization (cont.).

Ref.	Model section	Model/Control implementation tool	Application			CO_2 Efficiency	Input variable	Output variable
			Modelling	Control	Optimization			
[34]	Absorber	gPROMS			✓	95%	1.Flue gas temperature 2.Flue gas pressure 3. Flue gas molar flowrate 4.Flue gas molar composition	1. L/G (lean solvent/flue gas)
[18]	Absorber	Matlab	✓				1. Flue gas flowrate 2. Lean solvent flowrate	1. CO_2 removal rate
[20]	Absorber	Matlab	✓			90%	1. Column's feedstream loading	1. L/G (lean solvent/flue gas) 2. CO_2 removal rate
[35]	Absorber	Matlab	✓				1. Flue gas flowrate 2. Lean solvent flowrate	1. CO_2 removal rate
[36]	Absorber	Matlab	✓				1. Flue gas flowrate	1. CO_2 removal rate 2. Rich loading
[19]	Absorber	Aspen Plus	✓				1. Power plant load	1. Lean loading
[28]	Absorber	gPROMS	✓				1. Flue gas flowrate 2. Flue gas temperature 3. Lean solvent temperature 4. Lean solvent flowrate	1. L/G (lean solvent/flue gas)
[37]	Desorber	Aspen Custom Modeller	✓	✓			1. Reboiler heat duty	2. Lean loading 3. CO_2 removal rate
[29]	Reboiler	gPROMS	✓	✓			1. Solvent inlet flowrate	1. CO_2 removal rate 2. Reboiler level 3. Reboiler temperature

2.2 Management decision support of electricity generation associated with carbon capture system

The implementation of flexible low emissions technologies such as amine-based PCC at coal-fired power generations is of significant importance for the long term and short term global energy securities. Achieving this requires systematic carbon emissions control and planning in power generations (retrofitted with PCC system) which involves implementation of optimal techno-economic strategies (plant planning and scheduling) and highly flexible operations. Table 2.2 summarizes the studies that have been conducted in the management decision-making (planning and scheduling) of various energy generations retrofitted with multi-technique of CO_2 capture systems.

Table 2.2: A summary of previous studies on the management decision-making (planning and scheduling) of various energy generations retrofitted with CO_2 mitigation strategies.

Ref.	Plants	Technique	Objective function/ constraint	Planning horizon	Strategy	Outcome
[38]	Coal PP + Petroleum PP + Steel plant vs CCS (AWS + SS + ABS + MS)	ICSM	1.To minimize total system cost of CCS.	30 years	1.With carbon emission trading (CO_2 emission permits for each source are tradable within the entire CCS system rather than being set at a pre-determined level).	1.Total system cost under a trading mechanism is less than without trading mechanism.
			2.To develop optimal strategies for CCS which involved multiple emission sources, capture technologies and project time span.		2.Without carbon emission trading.	
[39]	Coal PP vs PCC (2 trains)	MILP (GAMS)	To maximize total income.	1 month	1.Company has no constraint in carbon management approach and predefine maintenance schedule.	Strategy 1:Guarantee maximum income for the company.
					2.Company has no constraint in carbon management approach and let program define the maintenance schedule.	Strategy 2:Improve power plant income by 9.5% and require carbon permit to be secured.

Table 2.2: A summary of previous studies on the management decision-making (planning and scheduling) of various energy generations retrofitted with CO_2 mitigation strategies (cont.).

Ref.	Plants	Technique	Objective function/ constraint	Planning horizon	Strategy	Outcome
					3.Same as Strategy 2 but government provides one free permit for every tonne of CO_2 captured.	Strategy 3:The benefit of saving in carbon taxes outweighs the loss due to the net power load reduction.
					4.Same as Strategy 2 but the company want to capture 1 million tonne of CO_2 per annum.	Strategy 4:Feature uneconomical operation schedule.
					5.Same with Strategy 2 with the difference that the company desires to study the impact of projected carbon and electricity prices at -20%, -10%, +20%, +10%.	Strategy 5:Increased electricity prices makes it beneficial for the coal PP to generate more electricity and capture less CO_2 (regardless of carbon price rate).
[40]	Coal PP vs PCC	MILP (GAMS)	To maximize net present value by either investing in PCC or pay carbon tax.	25 years	1.The government introduces free emission permits with CO_2 emission intensity of higher than 1.2 tonnes/MWh. Annual escalation factor for the electricity price and carbon permit price are escalated by 5% annually.	Strategy 1:Not suggested to install PCC plant but rather paying the tax.

Table 2.2: A summary of previous studies on the management decision-making (planning and scheduling) of various energy generations retrofitted with CO_2 mitigation strategies (cont.).

Ref.	Plants	Technique	Objective function/ constraint	Planning horizon	Strategy	Outcome
					2.The government provides certain amount of free emission to the company. Annual escalation factor for the electricity price and carbon permit price are 0.05 and 0.10 respectively.	Strategy 2:Suggested to install PCC plant.
					3.The company sets a plan for certain amount of CO_2 capture over the planning horizon. Annual escalation factor for the electricity price and carbon permit price is 0.05.	Strategy 3:Suggested to install PCC plant.
[41]	Coal PP + Solar PP vs PCC	MINLP (MATLAB)	To maximize profit	1 month (January)	1. PP vs PCC	Strategy 1:Increased electricity prices would result in decreased of capture rate. The lowest cumulative operational revenue compare to all four cases.

Table 2.2: A summary of previous studies on the management decision-making (planning and scheduling) of various energy generations retrofitted with CO_2 mitigation strategies (cont.).

Ref.	Plants	Technique	Objective function/ constraint	Planning horizon	Strategy	Outcome
					2.PP vs solar assisted PCC	Strategy 2:Cumulative revenue for Strategy 2 is more than Strategy 1, but less than revenue for Strategy 3.
					3.PP vs PCC vs solar repowering (power boosting: variable net electricity output)	Strategy 3:Increased electricity generation would result in increment of plant revenue. The most profitable strategy with the lowest carbon emissions.
					4.PP vs PCC vs solar repowering (load matching: fixed net electricity output)	Strategy 4:Cumulative operational revenue is almost the same as Strategy 3 for a carbon price \$25/tonne-CO_2.
[42]	Coal PP vs PCC	Not available	To maximize power plant's short run marginal cost profitability	24 hours	1.Base case:Load following operation of the power plant.	All strategy were compared with the base case (Strategy 1).
					2.Exhaust gas venting.	Strategy 2:Unikely to be a cost effective strategy.

Table 2.2: A summary of previous studies on the management decision-making (planning and scheduling) of various energy generations retrofitted with CO_2 mitigation strategies (cont.).

Ref.	Plants	Technique	Objective function/ constraint	Planning horizon	Strategy	Outcome
					3.Solvent storage.	Strategy 3:Provide marginal benefit.
					4.Times varying solvent regeneration.	Strategy 4:The most profitable.
[43]	Coal PP + New Coal PP + RE + IGCC + NGT + NGCC vs PCC	MILP (GAMS)	To minimize cost of the energy generating system with following constraints: 1.CO_2 emission. 2.Energy demand. 3.Capacity of the power plant's boilers.	20 years	1.BAU (Base case study).	1.Increment of CO_2 avoidance could lead to the increase of electricity cost.
					2.BAU and fulfill targeted energy demand regardless of CO_2 emission limit.	2.NGCC + PCC and new coal PP + CCS are more favorable for improving the CO_2 avoidance.
					3.Variability CO_2 emissions (20%, 30%, 40% and 50% from the projected CO_2 emission)	

Table 2.2: A summary of previous studies on the management decision-making (planning and scheduling) of various energy generations retrofitted with CO_2 mitigation strategies (cont.).

Ref.	Plants	Technique	Objective function/ constraint	Planning horizon	Strategy	Outcome
[44]	Coal PP + Gas fired PP + Petroleum fired PP vs CCS	Inexact Two-Stage Chance-Constrained Programming Approach	To maximize system benefits through allocating the electricity generation under the policy of emission trading.	15 years	1.Emission allowances are free for power plants.	1.Increased restrictions on CO_2 emission would result in decreased system benefits.
					2.Emission allowances are free at 90%, 40%, and 10% of CO_2 emissions generated in a power plant during period 1, 2, and 3. 3. Emission allowances are free in period 1, 2, and 3 at all 10% of CO_2 generated in each power plant.	2.The optimized electricity generated by the coal-fired power plant would reduce as free emission allowances diminish.
[45]	Coal PP vs PCC	MILP (GAMS)	To maximize NPV and optimize CO_2 capture capacity.	30 years	1.Invest in PCC plant (include operating cost and initial investment cost).	1.PCC plant might make different capture capacity selection depending on their expected CO_2 price and their value for flexibility.

Table 2.2: A summary of previous studies on the management decision-making (planning and scheduling) of various energy generations retrofitted with CO_2 mitigation strategies (cont.).

Ref.	Plants	Technique	Objective function/ constraint	Planning horizon	Strategy	Outcome
					2.Not invest in PCC plant but paying the carbon tax.	2.Capturing at low capacity is less expensive and not capture at full scale may enable a faster development of CCS.
[46]	Coal PP vs PCC + OXY	MINLP (GAMS)	To minimize cost of electricity.	1 year	1.Buying or selling emission allowances.	1.Oxyfuel combustion is more cost effective than PCC in a cap and trade framework.
					2.Reducing emission by investment in abatement technology.	
[47]	Coal PP + Oil PP + Nuclear PP + NG PP + Hydroelectric PP vs CCS	MILP (GAMS)	1.Economic mode: To satisfy a CO_2 emissions reduction target while maintaining and enhancing power to the grid.	Not available	2 Options: 1.Fuel balancing 2.Fuel switch	1.Fuel balancing contributes to the reduction of the amount of CO_2 emission by up to 3%.

Table 2.2: A summary of previous studies on the management decision-making (planning and scheduling) of various energy generations retrofitted with CO_2 mitigation strategies (cont.).

Ref.	Plants	Technique	Objective function/ constraint	Planning horizon	Strategy	Outcome
			2.Environmental mode:To minimize the CO_2 emissions while maintaining and enhance power to the grid.		Operation mode: 1.Economic mode 2.Environmental mode 3.Integrated mode	2.The optimal CO_2 mitigation decision are found to be highly sensitive to coal price.
			3.Integrated mode:Combine above objective functions		Under 4 planning scenarios: 1.Base load demand 2.A 0.1% growth rate in demand 3.A 0.5% growth rate in demand 4.A 1.0% growth rate in demand	

2.3 Thesis novelty

The innovative features of this thesis compare to previous literatures are that it offers a temporal multiscalar decision support framework critical for top-down management decision making of coal-fired power plant integrated with PCC system. It focuses on the perspective of the plant manager (enterprise level) to the operator/engineer viewpoint (instrumentation level) by integrating a superstructure optimization-based algorithm (apply to a power plant) with an advanced control strategy embedded into nonlinear empirical PCC model. Whereby, most of the previous studies (as listed in the Table 2.1 and Table 2.2) focused on the management decision (planning and scheduling) at the single level (e.g. enterprise and policy levels respectively) without considering responses arising from the integrated process. Another key distinction of this thesis is that real data is used for electricity and carbon prices based on Australian Energy Market Operator (AEMO) and EU ETS data, respectively. Moreover, futuristic data is forecasted based on historical profile of electricity prices and environmental stability of present level of greenhouse gas emission in Australia (Government estimates of the future carbon price). Even though several studies have employed real electricity prices, the carbon prices have remained fixed in all previous studies, while this thesis incorporates the dynamic profile of electricity and carbon prices. This thesis therefore demonstrates a management tool to support the decision-making in power generation in a carbon-constrained situation. This helps to overcome significant challenges imposed on coal-fired power plants when considering the installation of PCC technology. The decision support framework develops in this thesis accommodates economic, technical, and environmental aspects while indirectly provides futuristic insight in the investment and financial risks of PCC associated with power plant.

Chapter 3

Non-linear system identification of solvent-based PCC plant

This chapter demonstrates the development of PCC dynamic model via black box system identification technique (purely empirical). System identification technique builds mathematical model of dynamical system based on the actual pilot plant or experimental data. In this chapter, the PCC empirical model is developed based on the pilot plant data located at Tarong power station in Queensland. The development of this empirical model requires much less effort and less time consuming, however the model only valid at best for the range of data used in its development.

This chapter contains material published in [48].

3.1 System identification approach

A mathematical model of PCC plant with a 30 wt% MEA solvent is attempted by employing a multivariable non-linear autoregressive with exogenous input (NLARX) model. A standard parametric form of a NLARX discrete time model with one-step-ahead prediction can be described as follows:

$$y_m(t) = f[y_m(t-1), y_m(t-2), ..., y_m(t-n_a), u_r(t), ..., \tag{3.1}$$

$$u_r(t-n_k), ..., u_r(t-n_k-n_b)+1] + e_m(t)$$

where m and r are the output and the input systems respectively. The n_a and n_b are matrices of the past outputs and inputs included in the system, n_k is a matrix of the time delay in each input to output, e_m(t) represents the modelling error, and t the is time step. The function f [ ] represents an unknown nonlinear function where the modelling error generated from this model is neglected.

Since PCC plant is characterized as a multiple input multiple output system (MIMO) and a non-linear process, this black box structure can be an alternative way to develop a robust process model to be substituted with the first principle approach. A simplified PCC process flow diagram consisting of an absorber (ABS), a heat-exchanger (HE) and a desorber (DES) columns is shown schematically in Figure 3.1. Input-output variables for the development of the PCC model via a system identification tool are illustrated in Figure 3.2. The variables were selected according to the literature studies and based of the available data generated from a pilot plant. A comprehensive description of this pilot plant is available elsewhere [49].

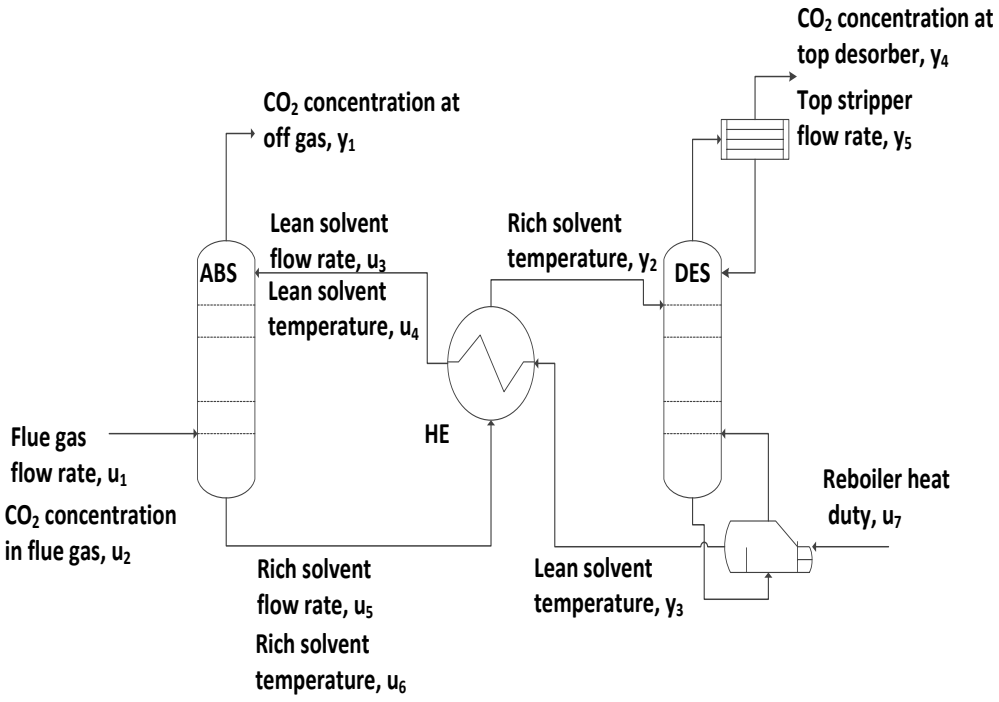

Figure 3.1: A simplified PCC process flow diagram.

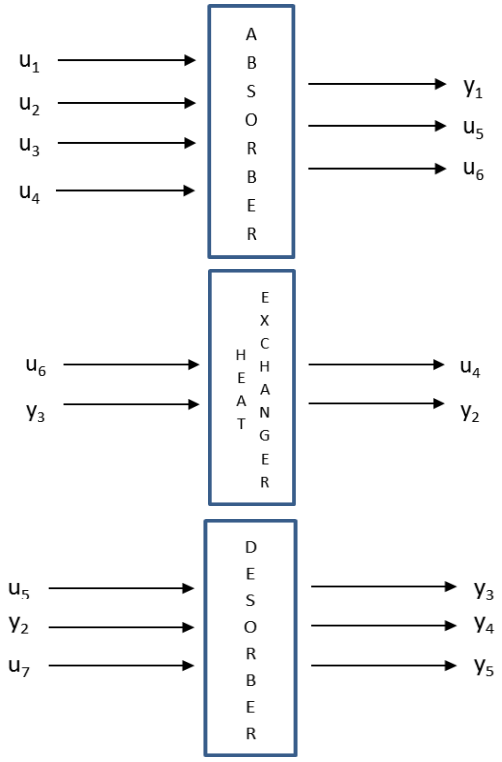

Figure 3.2: Process input output variables for the key PCC process units.

The PCC-NLARX model structure with the input-output model ranges can be described by Equation 3.2.

$$\begin{bmatrix} y_1(t) \\ y_2(t) \\ y_3(t) \\ y_4(t) \\ y_5(t) \end{bmatrix} = \begin{bmatrix} y_1(t-1), ... \\ y_2(t-2), ... \\ y_3(t-3), ... \\ y_4(t-4), ... \\ y_5(t-5), ... \end{bmatrix} \begin{bmatrix} u_1(t), ... \\ u_2(t), ... \\ u_3(t), ... \\ u_4(t), ... \\ u_5(t), ... \\ u_6(t), ... \\ u_7(t), ... \end{bmatrix}$$

$$y_m(t) = \begin{bmatrix} y_1(t) \\ y_2(t) \\ y_3(t) \\ y_4(t) \\ y_5(t) \end{bmatrix}, u_r(t) = \begin{bmatrix} u_1(t) \\ u_2(t) \\ u_3(t) \\ u_4(t) \\ u_5(t) \\ u_6(t) \\ u_7(t) \end{bmatrix} \tag{3.2}$$

where limits for y_m and u_r are as follows:

$$y = \begin{bmatrix} 1 \leq y_1 \leq 99(mass\%) \\ 10 \leq y_2 \leq 120(^oC) \\ 10 \leq y_3 \leq 120(^oC) \\ 85 \leq y_4 \leq 99(mass\%) \\ 30 \leq y_5 \leq 90(kg/hr) \end{bmatrix}$$

$$u = \begin{bmatrix} 400 \leq u_1 \leq 700(kg/hr) \\ 10 \leq u_2 \leq 18(mass\%) \\ 10 \leq u_3 \leq 80(L/min) \\ 20 \leq u_4 \leq 40(^oC) \\ 10 \leq u_5 \leq 60(L/min) \\ 50 \leq u_6 \leq 40(^oC) \\ 50\ 000 \leq u_7 \leq 550\ 000(kJ/hr) \end{bmatrix} \tag{3.3}$$

3.2 PCC plant NLARX model development

The PCC-NLARX model is applied to a set of real data collected from PCC pilot plant located in Tarong power station, Queensland, Australia. A dynamic data subject to the perturbation in steam pressure into reboiler system are used for model development. This PCC model consists of an absorber, a rich/lean heat exchanger and a desorber linked together. The significant contribution of this chapter is an innovative approach to model a PCC plant incorporating a rich/lean heat exchanger unit via input-output measured data. Since the rich/lean heat exchanger unit makes a major contribution to capital and operating costs [50], the involvement of this auxiliary system in the present PCC model development can provide assistance for future research work, for instance in flexible operation with a techno-economic strategy.

To avoid excess computation in the PCC system identification, three unit operation models were developed; the absorber, heat exchanger and desorber models respectively. The dynamic data excluding plant start-up and shut down data were collected from the actual pilot plant where the time interval for each sample was 10 s. Data were then segregated into two subsets, one for model estimation and one for model validation. All data involved in this PCC model development went through the data pre-treatment method which involved removing the biases and outliers. After the validation process, the three models (with best-fit percentage at one-step-ahead prediction output with 95% confidence level) were exported to the Simulink® workspace. Subsequently, each model was linked together to produce a PCC-NLARX dynamic model, combining an absorber, a rich/lean heat exchanger and a desorber. At the end, the Simulink environment was used to run a transient simulation of the PCC system for about ten hours of simulation time.

3.3 Model validation of individual units

Experimental data from the pilot plant and predicted output of the NLARX models for the absorber, heat exchanger and desorber are depicted in Figure 3.3 - Figure 3.5. For the absorber model, the outputs are CO_2 concentration in the off gas (y_1), rich solvent flow rate (u_5) and rich solvent temperature (u_6), while for the desorber model the outputs are lean solvent temperature (y_3), CO_2 concentration in the stripper top (y_4) and top stripper flow rate (y_5). Additionally, the heat exchanger outputs are based on the temperature streams connected between the absorber and the desorber as depicted in Figure 3.2.

From Figure 3.3, it can be observed that the NLARX model and experimental outputs (y_1, u_5 and u_6) match well. Whereas, in Figure 3.4 and Figure 3.5, the model under predicts the value for y_2 and over predicts the value of y_4, though the trend of the model responses are in agreement with the experimental data. The significance of this model validation is to ensure the developed PCC model of each unit can predict and mimic actual responses so as to reduce model error when the individual units are combined in a simplified model as is described in the next section.

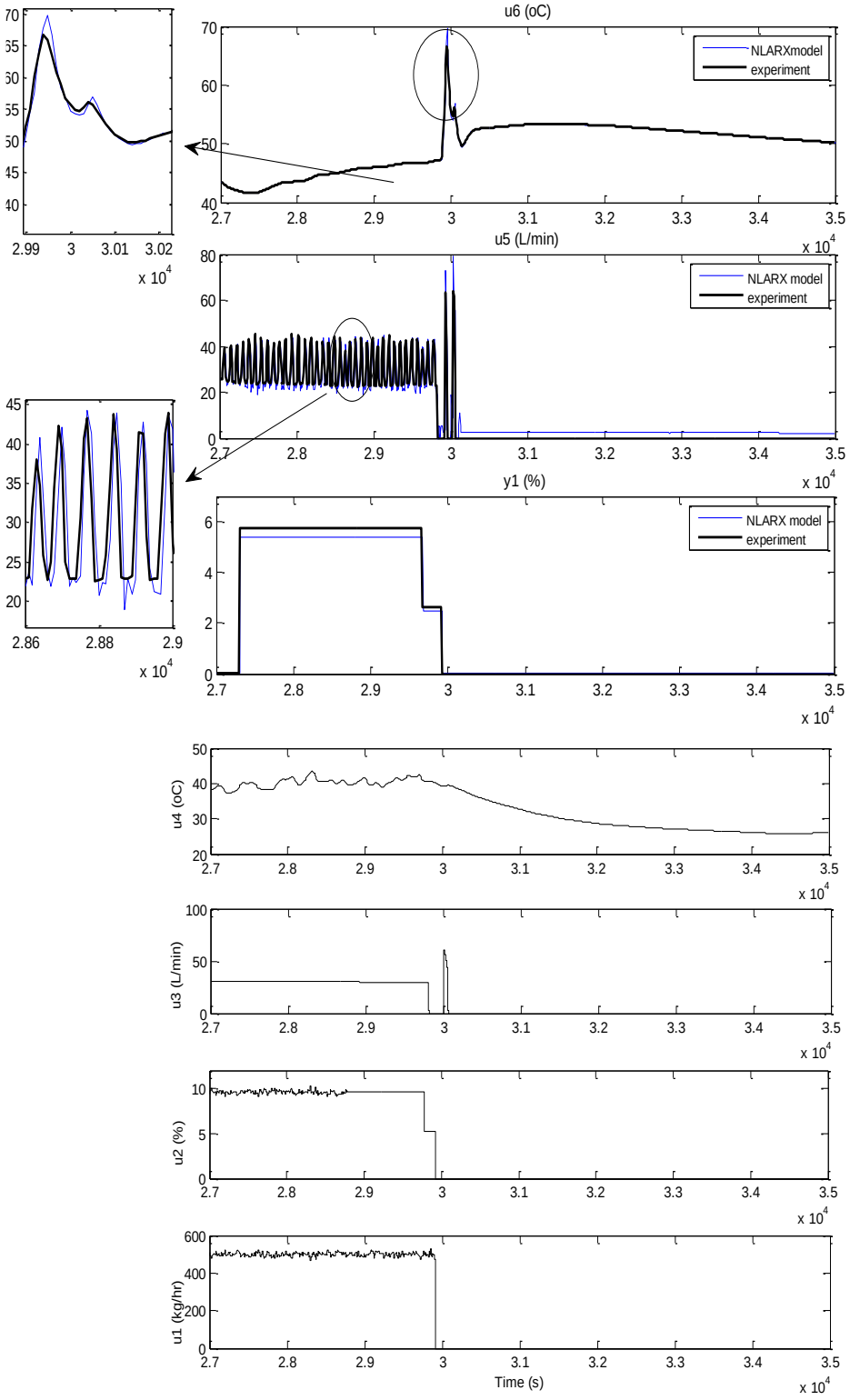

Figure 3.3: Absorber model validation.

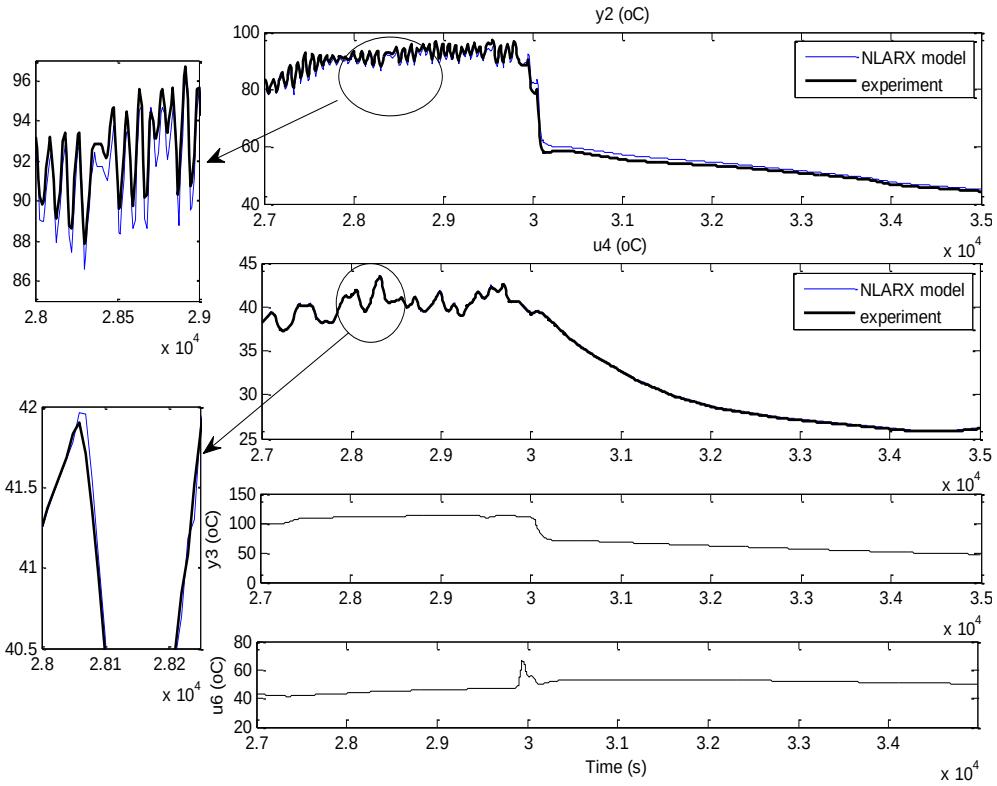

Figure 3.4: Heat exchanger model validation.

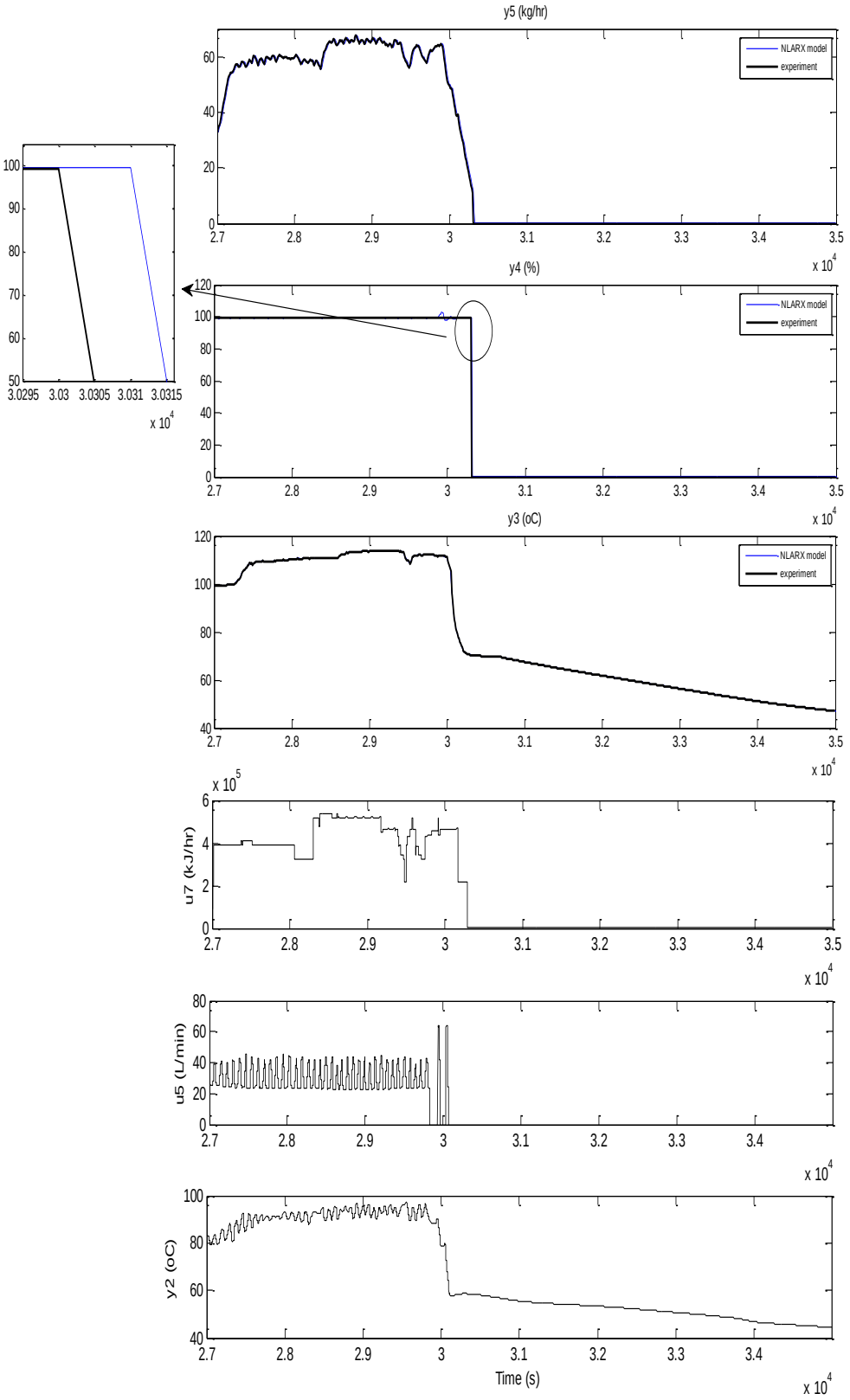

Figure 3.5: Desorber model validation.

3.4 A 4 x 3 system model for PCC plant

A simplified model of the PCC plant can be described by a 4 x 3 system as illustrated in Figure 3.6. A simplified block diagram for this process can be seen in Figure 3.7. A simplified 4 x 3 PCC model structure can be described by Equation 3.4, while the transfer function of the PCC model is delineated Appendix A.

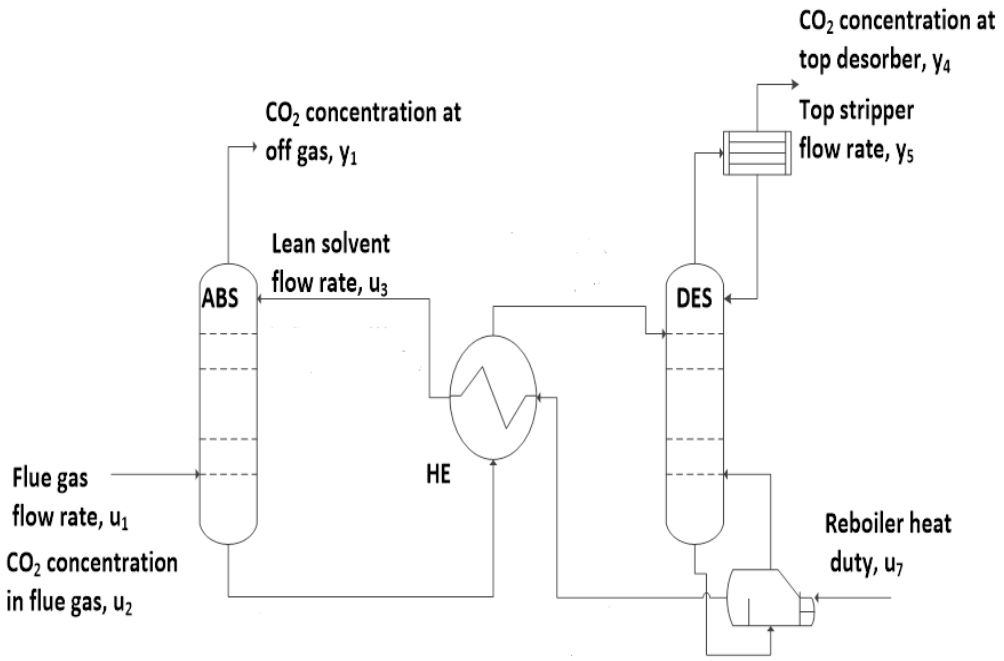

Figure 3.6: A simplified 4 x 3 PCC system.

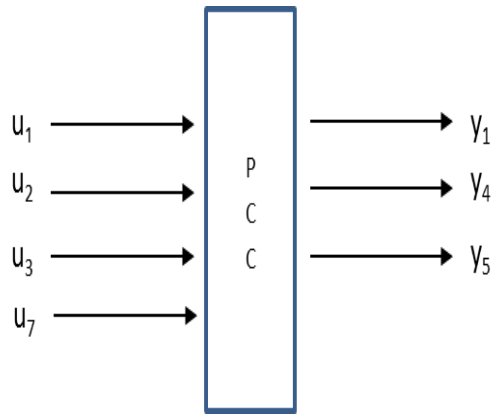

Figure 3.7: PCC model block diagram.

$$\begin{bmatrix} y_1(t) \\ y_4(t) \\ y_5(t) \end{bmatrix} = \begin{bmatrix} y_1(t-1), ... \\ y_4(t-2), ... \\ y_5(t-3), ... \end{bmatrix} \begin{bmatrix} u_1(t), ... \\ u_2(t), ... \\ u_3(t), ... \\ u_7(t), ... \end{bmatrix}$$

$$y_m(t) = \begin{bmatrix} y_1(t) \\ y_4(t) \\ y_5(t) \end{bmatrix}, u_r(t) = \begin{bmatrix} u_1(t) \\ u_2(t) \\ u_3(t) \\ u_7(t) \end{bmatrix} \tag{3.4}$$

3.5 Validation of 4 X 3 system model

Figure 3.8 demonstrates the successful validation of the PCC output variables consist of CO_2 concentration in the off gas (y_1), CO_2 concentration in the desorber top (y_4) and top desorber flow rate (y_5). It can be seen that, the PCC-NLARX model is capable of predicting the dominant dynamics of the PCC experimental measurements which lends credence to the proposed model. Moreover, the development of this dynamic model does not involve a complex model structure

providing a higher execution speed.

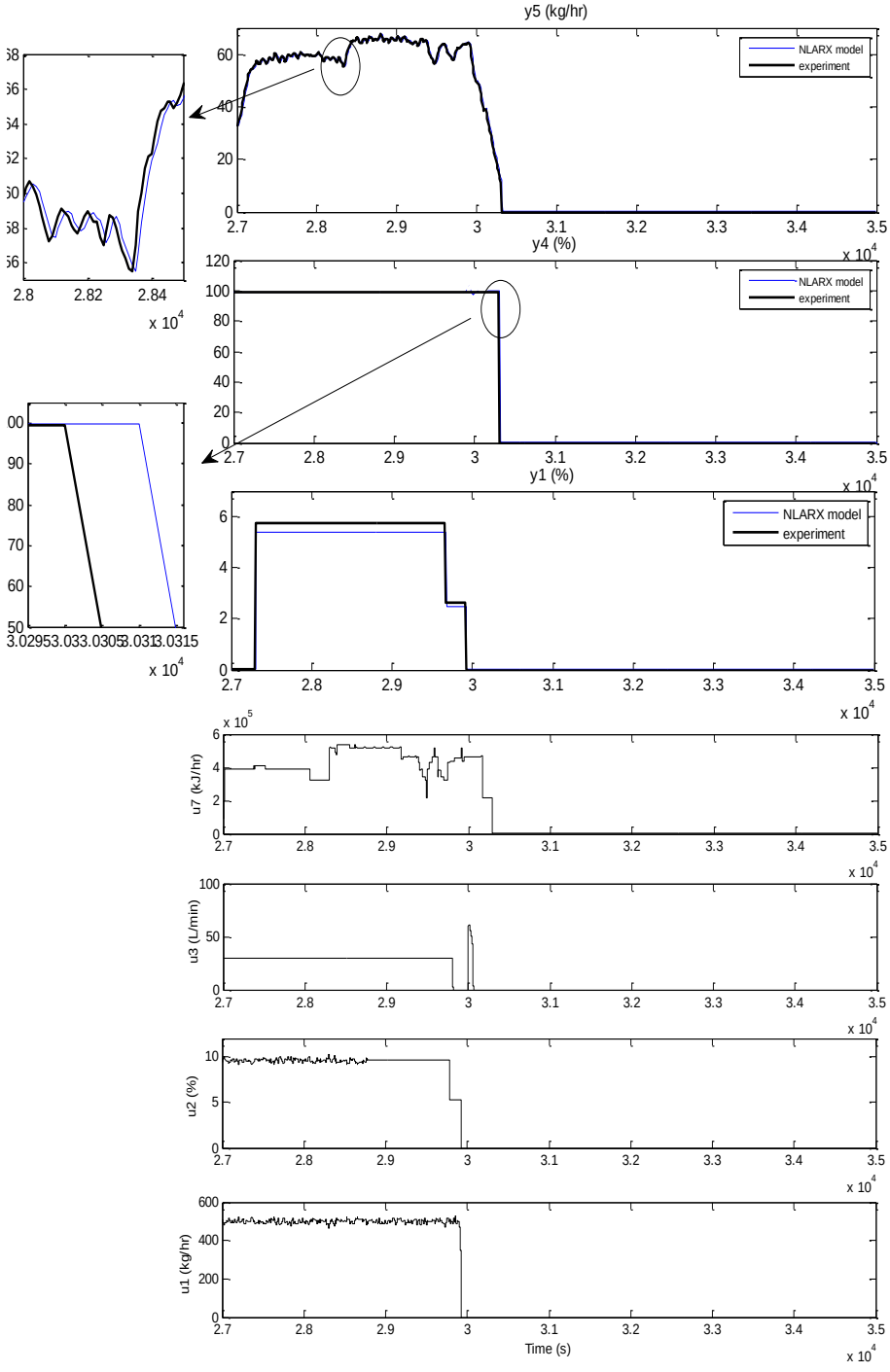

Figure 3.8: Validation of the simplified 4 x 3 PCC model.

3.6 Model solution: Implementation in Simulink

The decisive step in developing a PCC model in the Simulink workspace is to export the NLARX model system identification functions into the Simulink environment. To circumvent the complexity of the Matlab programming language and nonlinear differential equations, a Nonlinear ARX model block function was chosen to imitate the NLARX data driven model. The individual process model (absorber, heat exchanger and desorber) was exported to the Simulink workspace via a Nonlinear ARX model block function. The individual models are then linked together as shown in Figure 3.9. The details of the Simulink PCC model structure with z-functions are illustrated in Figure 3.10. The advantage of the Simulink workspace is its capability to integrate different dynamic models as long as each system has similar input or output variables.

3.7 Open loop dynamic analysis

The objective of this dynamic analysis is to assess the behavior of the PCC process when dealing with process uncertainty such as set-point changes and disturbances. Furthermore, the dynamic analysis can provide an insight into the transient behaviour of the absorption and desorption processes in PCC plant, providing information on dynamic parameters such as time constants which are important for process controllability, start-up and shutdown. The open loop dynamic behaviour of the PCC process is analysed using step changes in the input variables: flue gas flow rate, CO_2 concentration in flue gas, lean solvent flow rate and reboiler heat duty. These step changes reflect the actual operation of a power plant retrofitted with a PCC process. To run the open loop dynamic simulation, the process model was initialized using nominal values referring to Cousins's paper [49] and based on the frequency analysis of pilot plant data.

These include flue gas flow rate at 550 kg/hr, CO_2 concentration in flue gas at 16 mass %, lean solvent flow rate at 26 L/min and reboiler heat duty at 342 000 kJ/hr (100 kW). The perturbations were introduced one at a time during ten hours of simulation time and have been altered independently, where one input is varied and the others remain constant.

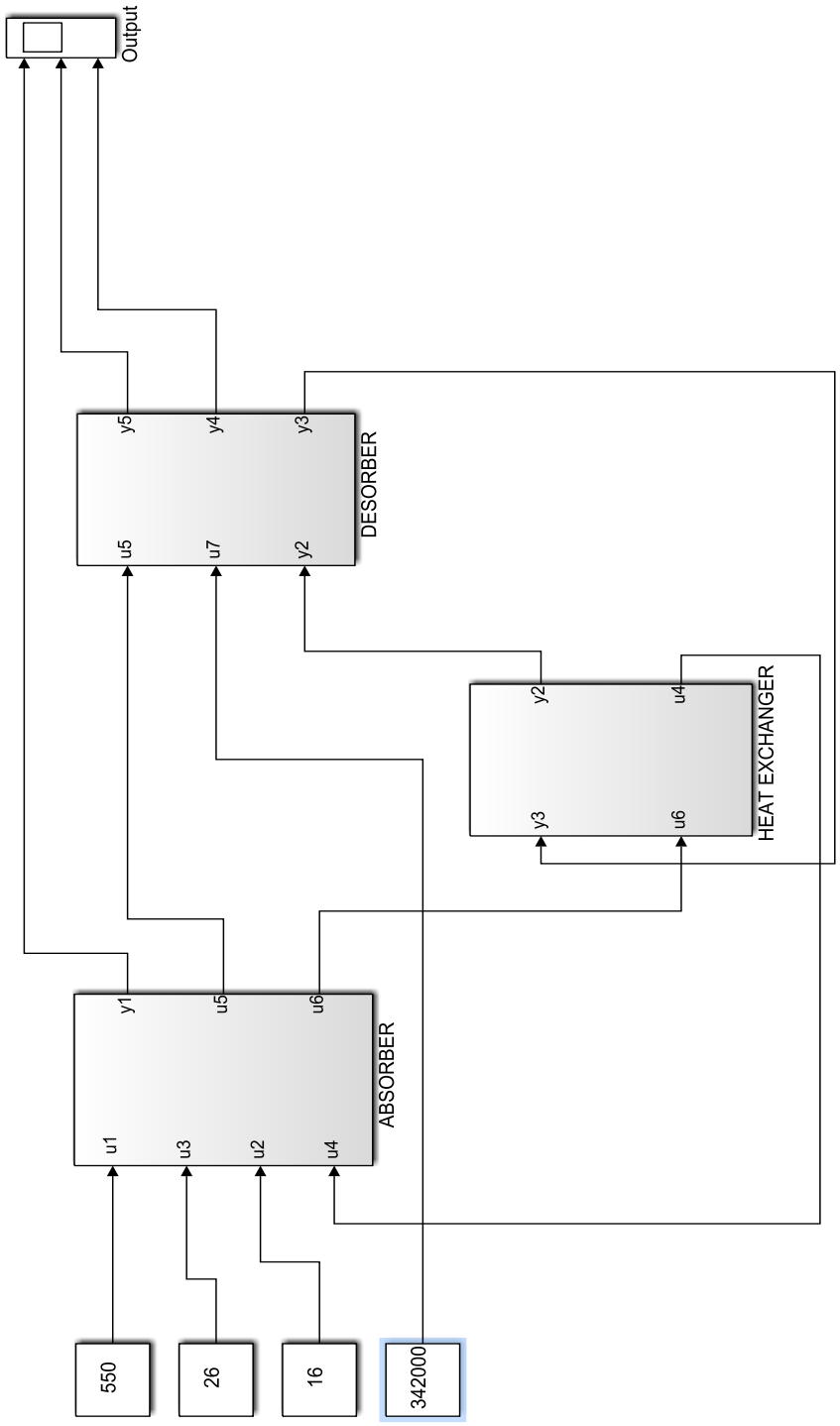

Figure 3.9: Simulink user defined model for dynamic PCC process.

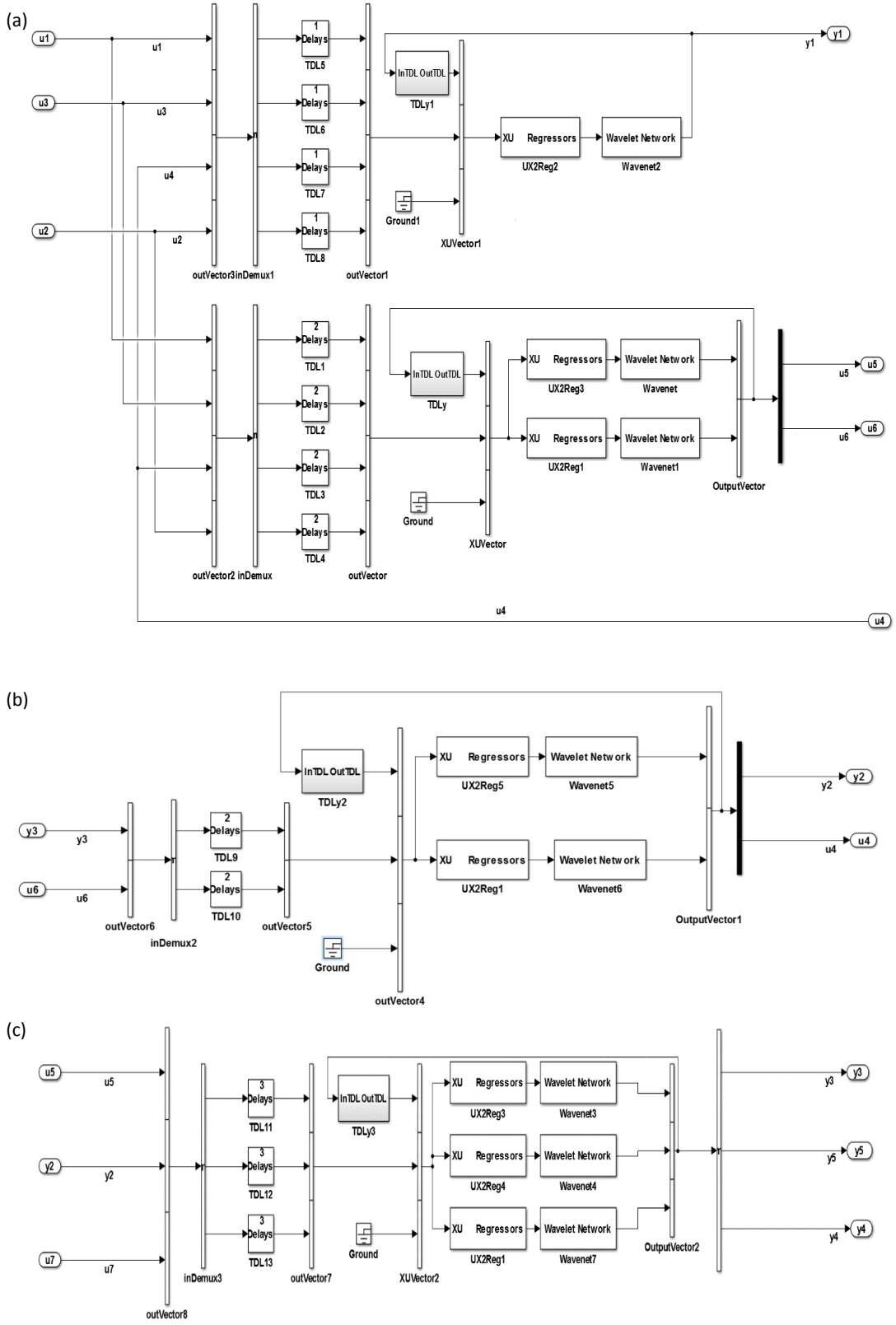

Figure 3.10: The NLARX model structure for (a) absorber, (b) heat exchanger and (c) desorber in Simulink workspace.

3.7.1 Step changes in flue gas flow rate

The variation of flue gas flow rate (u_1) typically associated with the change in power plant load at off-peak and high-peak hours, may contribute to operational challenges for the PCC system. To demonstrate the performance of PCC plant towards upstream operation volatility, independent step tests are introduced to the u_1 with respect to the base case model trajectory as illustrated in Figure 3.11 by assuming CO_2 concentration, lean solvent flow rate and reboiler heat duty are at constant values.

Based on Figure 3.11, the output responses changed rapidly at the onset of the disturbances, revealing an immediate effect from the step change. It can be seen that the output response for CO_2 concentration in the off gas (y_1) increase steeply when subjected to the positive step change. Conversely, CO_2 concentration at the top of the stripper (y_4) and top stripper flow rate (y_5) decreased gradually when the flue gas flow rate (u_1) was increased, which then caused a reduction in total CO_2 gas flow at the top of the desorber column. However, the variation of both variables (y_4, y_5) during increase/decrease flue gas flow rate has only small deviation at approximately 0.03%. This possibly occurred because of the short contact time between vapour and liquid in the desorber column. For a negative step change in flue gas flow rate (u_1), CO_2 concentration in the off gas (y_1) reduced steadily along with a concomitant increase in CO_2 concentration at the top of desorber. Based on this specific analysis, the nonlinearity evident in the three outputs varies as shown by the asymmetric profiles of the responses resulting from the input step changes. This is due to the various ranges of process time constants; 2-3 minutes for the fastest dynamics (u_1-y_1 relationship) to 20-25 minutes for the slowest dynamics (u_1-y_4 relationship).

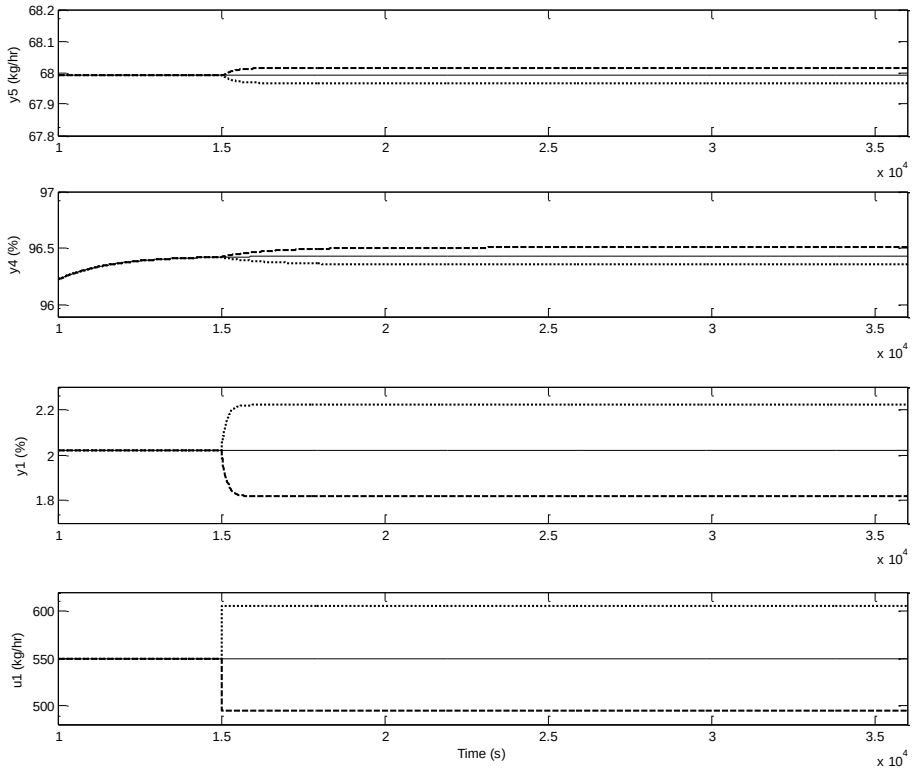

Figure 3.11: Output responses (y_1, y_4, y_5) due to a $\pm$ 10% step change in flue gas flow rate (solid line: base case; dotted line: positive step change; dashed line: negative step change).

3.7.2 Step changes in CO_2 concentration in flue gas

Changes in CO_2 concentration in the flue gas (u_2) commonly occurs due to the complete or incomplete combustion of the fossil fuel. It is also influenced by the composition of coal (i.e. carbon) and the coal usage per unit electricity generated from the power plant. Furthermore, a drop in power plant load may sometimes require plants to 'co-fire' (i.e. with oil) in order to maintain stable operation in the boiler.

As illustrated in Figure 3.12, the step changes did not affect the CO_2 concentra-

tion in the off gas (y_1). This is in contrast to the other two output variables, where significant changes occurred at the onset of the disturbance. For a positive step change of CO_2 concentration in the flue gas (u_2), CO_2 concentration at the top of the stripper (y_4) and the top stripper flow rate (y_5) increased slightly. This consequently elevates the CO_2 gas flow rate at the top of the desorber column. From these results, it appears that only y_4 and y_5 have significant open loop dynamic responses while y_1 does not show a significant response. Different ranges of process time constants were observed; $6-8$ minutes for the fastest dynamics (u_2 -y_5 relationship) to $20-24$ minutes for the slowest (u_2 -y_4 relationship).

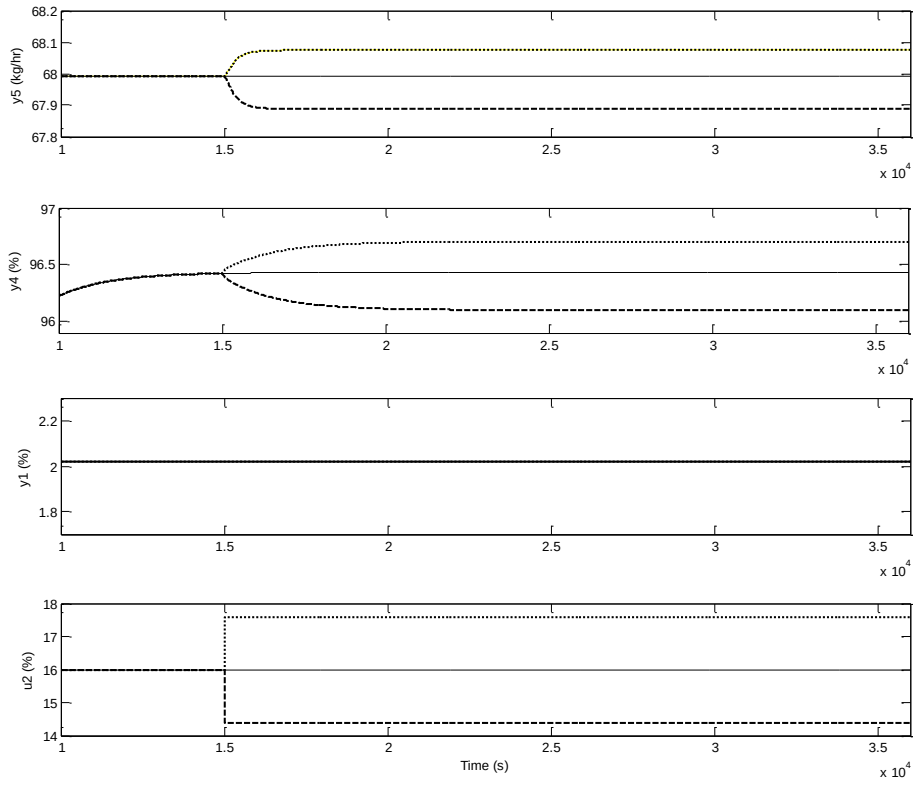

Figure 3.12: Output responses (y_1, y_4, y_5) due to a $\pm$ 10% step change in CO_2 concentration in flue gas (solid line: base case; dotted line: positive step change; dashed line: negative step change).

3.7.3 Step changes in lean solvent flow rate

The third experiment performed was used to determine the effect of lean solvent flow rate on PCC performance. The results of this evaluation are presented in Figure 3.13. It was observed that for a negative step change in lean solvent flow rate (u_3), CO_2 concentration at the top of the stripper column has increased significantly. This possibly occurred because at this specific condition, CO_2 lean loading is also increased which consequently elevates the CO_2 equilibrium partial pressure. Hence, less steam is required for stripping process which then leading to higher CO_2 concentrations at the exit to the stripper column. The nonlinearity of the output responses due to the step changes are similar with the outcome in Section 3.7.2. The process time constants for this dynamic response are $5-7$ minutes for the fastest dynamics (u_3 -y_5 relationship) to $22-24$ minutes for the slowest (u_3 -y_4 relationship).

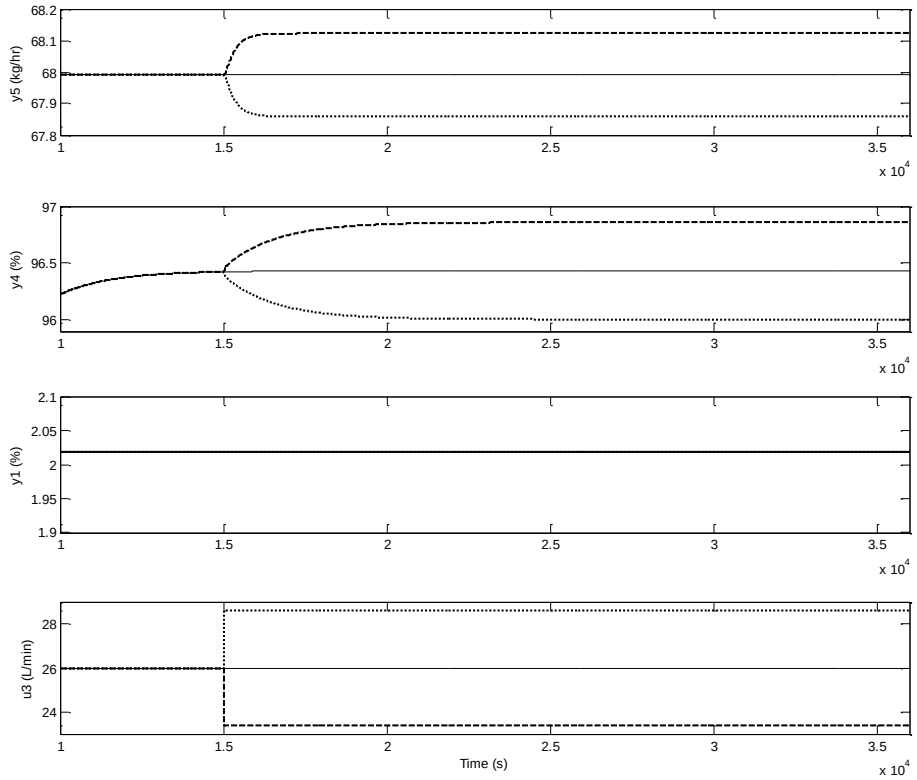

Figure 3.13: Output responses (y_1, y_4, y_5) due to a ± 10% step change in lean solvent flow rate (solid line: base case; dotted line: positive step change; dashed line: negative step change).

3.7.4 Step changes in reboiler heat duty

Reboiler heat duty plays a significant role in the solvent regeneration process which in turn affects the economics (operating cost) of PCC plant. This variable also represents the performance of the desorber column [51]. The changes in reboiler heat duty illustrate the interruption of heat supply from a power plant or external auxiliary system [31]. Fluctuation in steam extraction from the power plant low-pressure steam supply can also contributes to the variation in reboiler heat duty [52, 53]. A positive step change in reboiler duty represents a larger steam flow entering the reboiler system which could happen during off-peak

hours (lower electricity prices). A negative step change imitates a disruption in heat supply from the power plant or a reduction of steam entering the reboiler during peak hours (high electricity prices). The reboiler heat duty (expressed in kJ/hr) was determined by the measurement of the steam flow rate in the reboiler circuit coupled with the heat of condensation of the steam by assuming all steam condensed in the reboiler. However, this computation method may feature a drawback as it will include heat loss to the environment (weather dependant) and reliability of the data itself. Therefore, to improve the desorber model performance, additional data pre-treatment for steam flow rate to the reboiler has been conducted by removing the zero/negative values of flow rate.

As illustrated in Figure 3.14, the perturbations did not affect CO_2 concentration in the off gas (y_1). For a positive step change in reboiler heat duty, the top stripper flow rate increased gradually (y_5). This is in contrast to the decrease observed in the CO_2 concentration in stripper gas flow. At this perturbation, the calculated time constants are approximately $6 - 15$ minutes for the fastest dynamics (u_4-y_5 relationship) to $8 - 27$ minutes for the slowest ($u_3 y_4$ relationship).

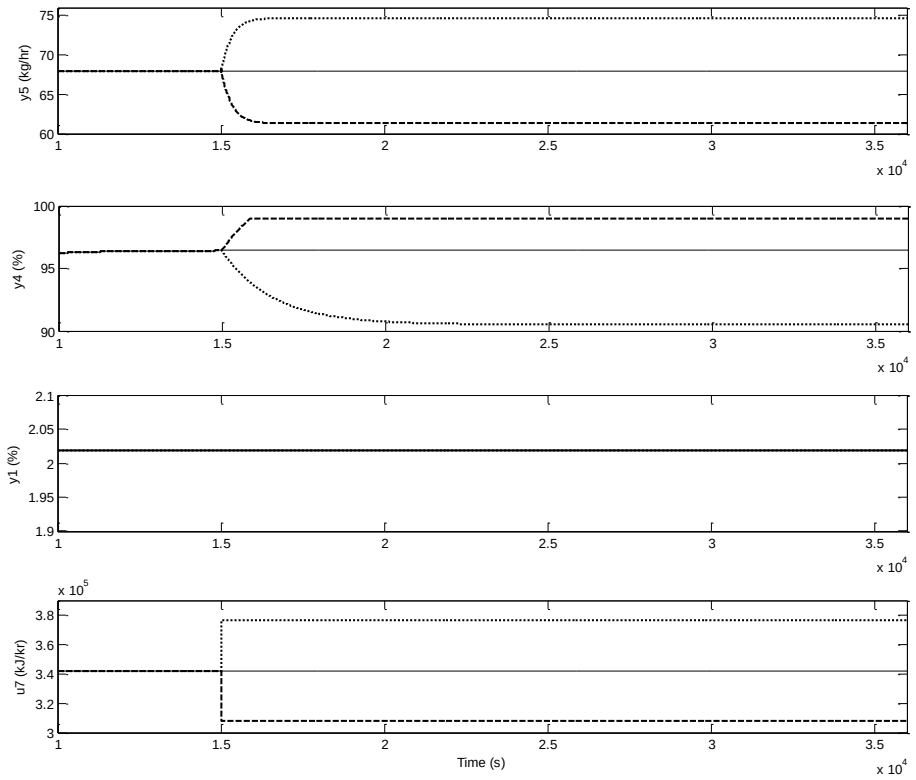

Figure 3.14: Output responses (y_1, y_4, y_5) due to a $\pm$ 10% step change in reboiler heat duty(solid line: base case; dotted line: positive step change; dashed line: negative step change).

3.8 Sensitivity analysis

Local sensitivity analysis via a variable perturbation method was carried out to identify the relative importance of input model parameters on the model output. Information on the sensitivity of the dynamic PCC-NLARX model will aid understanding the model's predictive capability and uncertainty in output corresponding to possible changes in input parameters. Sensitivity analysis also offers information in the dynamics of the process [30]. Positive/negative step changes of input variables have been considered to determine the sensitivity of the output variables towards input changes. In each run of the model, in each step, one of

the inputs is changed and the rest of the inputs were kept constant. The input variables affecting the output are summarized in Table 3.1 along with their sensitivity index (process gain). According to the results, output y_1 is not sensitive to the input variables u_2, u_3 and u_7. While, u_7 is the most influential variable towards outputs y_4 and y_5 followed by the inputs u_3, u_2 and u_1. This supports the open loop dynamic analysis presented in Section 3.7.

Table 3.1: Sensitivity analysis of input-output PCC model.

Input (u_i)	Step change (in u_i)	Sensitivity index ($\triangle y_i/\triangle u_i$) Output ($y_i$)		
		y_1	y_4	y_5
u_1 (kg/hr)	10%	0.99	-0.004	-0.004
	-10%	0.99	-0.015	-0.006
u_2 (mass %)	10%	0.00	0.035	0.019
	-10%	0.00	0.027	0.025
u_3 (L/min)	10%	0.00	-0.037	-0.01
	-10%	0.00	-0.056	-0.019
u_7 (kJ/hr)	10%	0.00	-0.608	0.99
	-10%	0.00	-0.274	0.981

3.9 Key performance metrics of PCC plant

Two key metrics, CO_2 capture efficiency(CC) and energy performance(EP), are evaluated. Both keys are appraised in order to measure the performance of PCC plant. The value of the key metrics at nominal conditions are selected to be around 80% and 4.0 MJ per kg CO_2 captured for the CO_2 capture efficiency and energy performance respectively. The key metrics can be calculated as follows:

$$\text{Carbon capture efficiency, } CC \text{ (mass \%)} = \frac{(y_4/100)y_5}{u_1(u_2/100)}\text{x } 100\% \tag{3.5}$$

$$\text{Energy performance, } EP \text{ (MJ/kg)} = \frac{u_7}{y_5(y_4/100)} \div 1000 \tag{3.6}$$

Previously, Section 3.7 presented validation of the developed PCC model via the predicted outputs profiles. While, here, to ensure the accuracy of the model and its reliability to represent the actual PCC process, experimental and simulation data for *CC* and *EP* are evaluated and compared. Table 3.2 delineates data validation at different operating conditions. It can be seen that the deviations are less than 4% for carbon capture efficiency and less than 7% for energy performance which providing reliability of the developed PCC model.

Figures 3.15 - 3.17 show the dynamic responses of PCC key performance index resulting at ± 10% step tests of respective inputs (u_1, u_2, u_3, u_7). The step changes were introduced one at a time in certain period and have been altered independently, where one input is varied and the others remain constant.

As depicted in Figure 3.15, a decrease in flue gas flow rate causes a sudden increase in *CC*%. An opposite response occurs from an increase in flue gas flow rate. These outcomes are similar to the study conducted by [31, 23, 54, 27]. Concomitantly, *EP* has slightly increased when flue gas flow rate was increased which resulted from the low CO_2 flow rate at the top of the desorber column (Figure 3.11). This is proven by the equation of *EP* (Equation 3.6) where, increasing of CO_2 gas

Table 3.2: Summary of the *CC*% and *EP* at different operating points. The quoted deviations are in comparison with experimental/pilot plant data.

Condition	Operating point	*CC*		*EP*	
		Simulated (%)	Deviation (%)	Simulated (MJ/kg)	Deviation (%)
1	u_1: 489 kg/hr u_2: 10% u_3: 38 L/min u_7: 581 686 kJ/hr	67.3	-3.4	2.18	1.2
2	u_1: 512 kg/hr u_2: 10% u_3: 40 L/min u_7: 550 284 kJ/hr	99	0	3.78	2.2
3	u_1: 505 kg/hr u_2: 10% u_3: 39 L/min u_7: 236 566 kJ/hr	99	0	3.85	6.4
4	u_1: 507 kg/hr u_2: 10% u_3: 39 L/min u_7: 537 822 kJ/hr	99	0	8.56	5.5

flows at the top of the stripper will reduce the amount of *EP*. Similar responses resulted from step changes in CO_2 concentration in flue gas for *CC*% as shown in Figure 3.16. However, the *EP* has reduced significantly at the positive step change of CO_2 concentration as governed by the Gibbs energy of mixing.

Changes in the lean solvent flow rate significantly influence both key metrics as depicted in Figure 3.16. The *CC*% reduced when the lean solvent flow rate was increased and consequently caused an increment in *EP*. Generally, the effect of lean solvent flow rate (increase or decrease) to the PCC output profiles relate to the lean loading range. Based on this specific study, increasing the lean solvent flow rate resulted in a reduction of CO_2 total gas flow rate emitted at the top stripper column (Figure 3.17). This underpinned by the Equation 3.5 where, a reduction in CO_2 total gas at top stripper column ($y_4 * y_5$) caused a decrement

in $CC\%$.

Typically, the desorber column involves complex physical and chemical reactions due to the unstable nature of the heat balance along the column and the reversibility of the CO_2 absorption reaction which consequently affects the performance of the column [55, 56]. Based on Figure 3.18, a reduction in reboiler heat duty contributes to the reduction of $CC\%$ and EP values. Whereas, the opposite performance occurred for a positive step change of reboiler heat duty. For a positive perturbation, it can be seen that at the onset of the disturbance, $CC\%$ and the EP were slightly increased before reducing to new conditions (higher than the nominal condition). These scenarios occur because at the sudden increase of reboiler heat duty, more CO_2 gas flows at the top of the desorber column which then reduces the amount of CO_2 emitted in the off gas stream in the absorber column. However, in this case, the CO_2 concentration in off gas did not change throughout the simulation process (as illustrated in Figure 3.12). Therefore, based on these combined effects, i.e elevation of reboiler heat duty followed by a constant concentration of CO_2 at the absorber's outlet stream produces the corresponding pattern as shown in Figure 3.18. A similar pattern of the energy performance during a negative perturbation of reboiler heat duty was found in [31].

According to the aforementioned responses, the $CC\%$ and EP concurrently changed when there were perturbations in lean solvent flow rate and reboiler heat duty. These can be explained as follows: An amine solvent (lean solvent) flows in the absorber column countercurrent to the flue gas containing CO_2. A chemical absorption reaction takes place between the CO_2 and the amine solvent whereby the lean amine solvent absorbs the CO_2 and enters the desorber column as a CO_2-rich solvent. Essentially, the CO_2 concentration level in the rich solvent is dependent on the solvent circulation rate, contact time and temperature of the

column. This eventually affects the efficiency of CO_2 capture rate at the desorber column. On the other hand, *EP* is defined as the energy required to capture a kg of CO_2 which inherently has a linear relationship with the reboiler heat duty (refer Equation 3.6). These mechanisms suggest why changes in lean solvent flow rate and reboiler heat duty result in significant simultaneous changes to *CC*% and *EP*.

Based on the open loop dynamic analysis, the highest *CC*% can be obtained at a negative step change in flue gas flow rate (u_1) at 83% capture. On the other hand, the lowest *EP* can be obtained for a negative step change in reboiler heat duty, u_7 at 5.07 MJ/kg. However, the aforementioned outcomes are only applicable for an identical operating range of PCC plant and not necessary refer as the optimum conditions. The sensitivity analysis for *CC*% and *EP* is tabulated in Table 3.3. It can be seen that the lean solvent flow rate (u_3) provides significant influence towards *CC*% and *EP*. Therefore, it is suitable to be one of the manipulated variables in the control strategy. Flue gas flow rate and CO_2 concentration in flue gas are inherently behaved as a process disturbance to PCC process and therefore it is impractical to choose them as a manipulated variable. In this work, reboiler heat duty is selected as one of the manipulated variables together with the lean solvent flow rate. Several PCC control literatures have selected reboiler heat duty as one of the manipulated variables [30, 25].

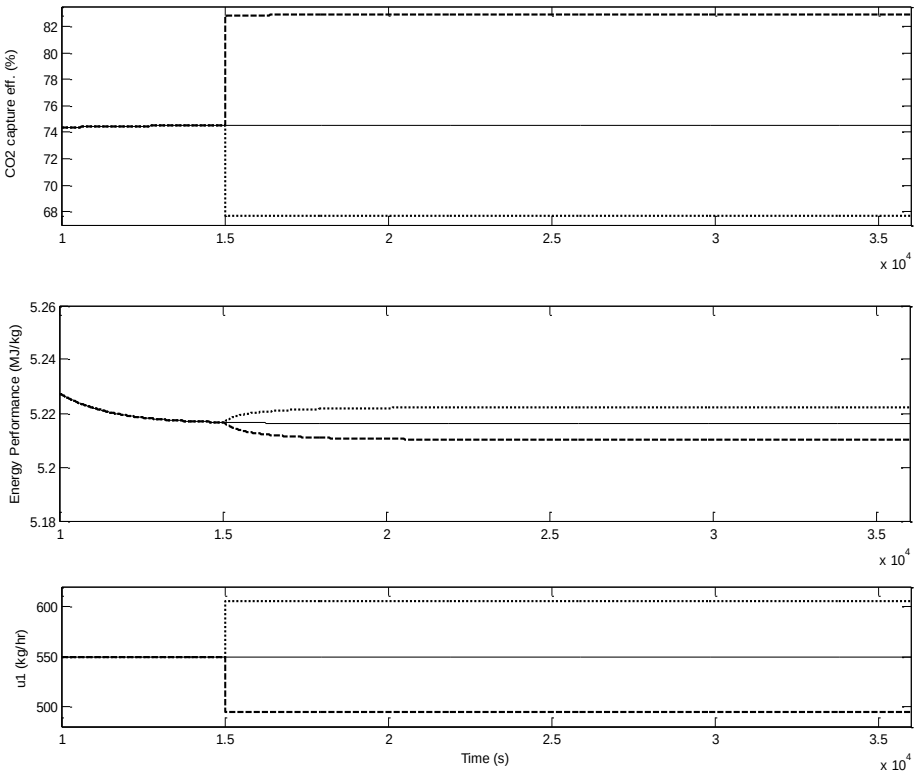

Figure 3.15: Key performance metrics during ±10% step tests in flue gas flow rate (solid line: base case; dotted line: positive step change; dashed line: negative step change).

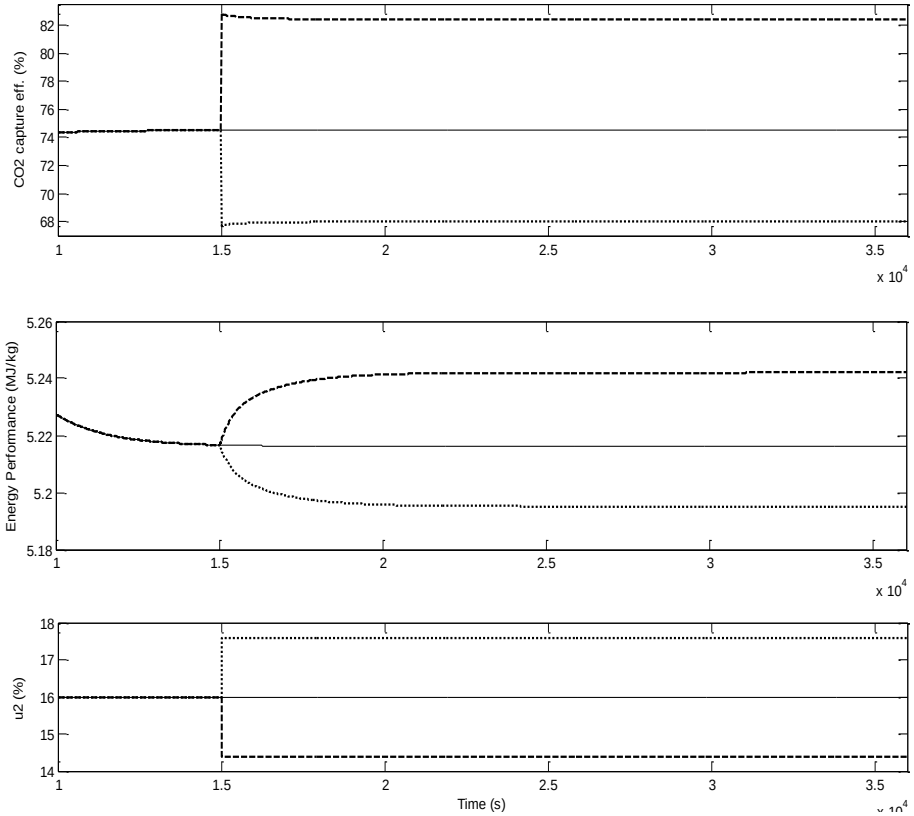

Figure 3.16: Key performance metrics during ±10% step tests in CO_2 concentration in flue gas (solid line: base case; dotted line: positive step change; dashed line: negative step change).

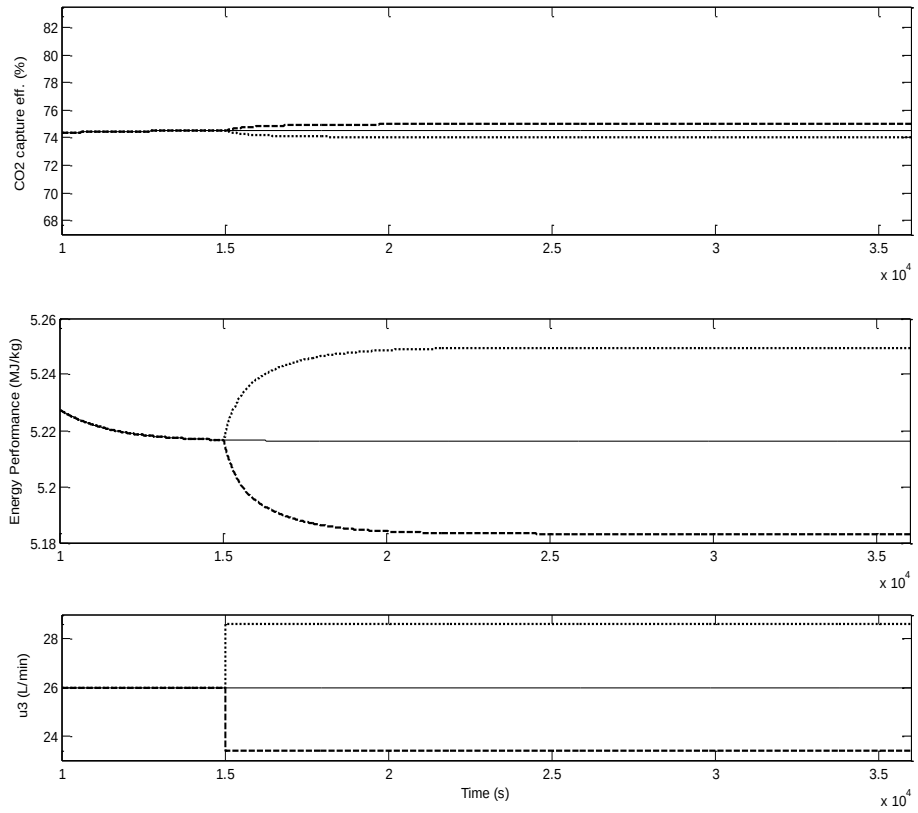

Figure 3.17: Key performance metrics during ±10% step tests in lean solvent flow rate (solid line: base case; dotted line: positive step change; dashed line: negative step change).

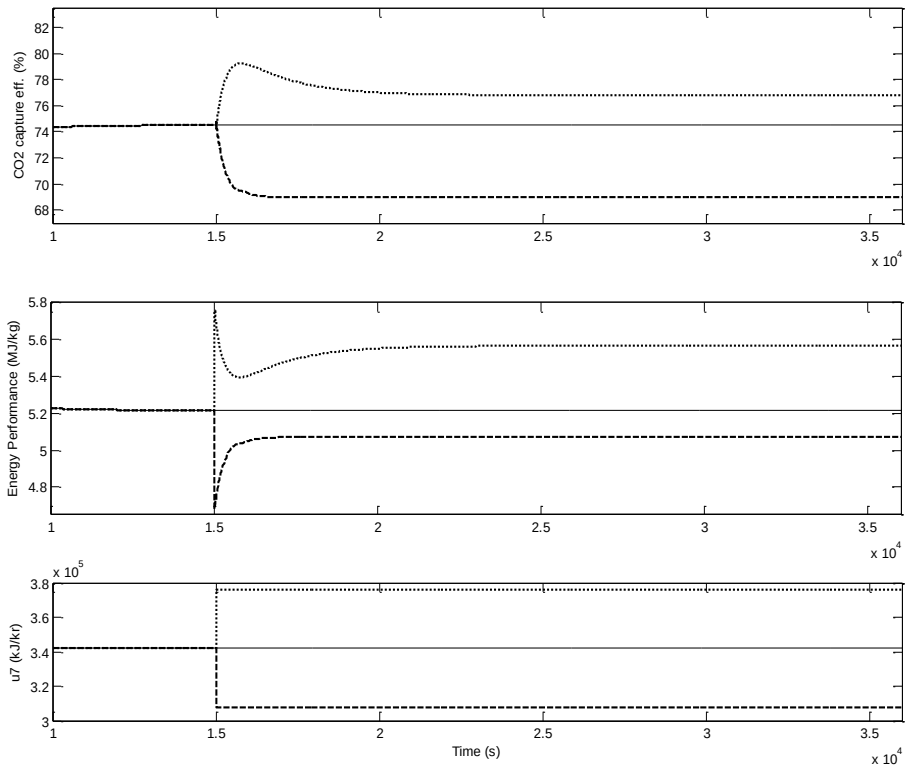

Figure 3.18: Key performance metrics during ±10% step tests in reboiler heat duty (solid line: base case; dotted line: positive step change; dashed line: negative step change).

Table 3.3: Key input-output performance metrics.

Input (u_i)	Step change (in u_i)	Sensitivity index ($\triangle y_i/\triangle u_i$)	
		Output (y_i)	
		EP (MJ/kg)	*CC* (%)
u_1 (kg/hr)	10%	0.004	-0.913
	-10%	0.019	-1.128
u_2 (mass %)	10%	-0.038	-0.872
	-10%	-0.038	-1.06
u_3 (L/min)	10%	0.057	-0.094
	-10%	0.077	-0.04
u_7 (kJ/hr)	10%	0.67	0.309
	-10%	0.287	0.738

3.10 The PCC-NLARX model application range

The developed PCC-NLARX empirical model has limited applicability whereby its validity is for within the range of data used in the model development as delineated in Section 3.1 (limits for y_m and u_r). Where, the operational data used in the development of empirical model are influenced by the design and configuration of the plant. Thus, small discrepancy might apparent if this model is used to predict the response of different size/configuration of PCC plant. Moreover, the quality and quantity of the historical data are of significant importance to ensure the accuracy of the model. Whereby, in many cases, there are limitations in obtaining a good operational data. Based on the open loop dynamic analyses

conducted in this chapter, the PCC-NLARX model predicts responses of a real and specific PCC plant subject to input plant operating conditions. Scale-up of this empirical model is theoretically possible but requires exhaustive information from different sources for instance basic (laboratory) research, mathematical modelling, pilot plant studies and experience gained from commercial PCC unit operations [57]. This empirical model is practical for incorporation with control strategies to assess the potential economic viability of implementation the large scale PCC plant. Nevertheless, careful attention should be made when using this model for scale up or for other PCC plants since the predicted responses may be radically different depending on size and the configuration of any new plant [58].

Chapter 4

Control strategies for flexible operation of solvent-based PCC plant

This chapter demonstrates the development and design of control architecture based on the multivariable control analysis. The objective is to assess the flexibility of the control strategy in PCC control performance that would lead to higher capture rates and enhanced PCC energy performance. At the same time, to accommodate with different PCC constraints for instance environmental, economic and operational constraints. Closed-loop analyses are conducted to assess the controllability performance of the PCC plant with simulated upstream upsets in power plant subject to servo and regulator problems.

This chapter contains material published in [59, 60].

4.1 Controllability analysis: Methodology

This section describes the methodology to develop and implement a conventional PID and an advanced MPC strategies to be embedded into the PCC system. The procedure followed to perform the controllability analysis is presented in Figure 4.1.

Essentially, the objective of the controllability analysis is to develop a flexible control strategy to accommodate with different PCC constraints for instance environmental, economic and operational constraints. Concurrently, to lead, to the enhancement of PCC energy performance and CO_2 capture rate, in response to power plant part-load, electricity and carbon prices. To represent those demands, a specific scenario was created. It includes set point tracking scenario (servo problem) of PCC key performance metrics which are *CC* and *EP*, and disturbance rejection scenario (regulator problem) which are perturbation in flue gas flow rate and CO_2 concentration in flue gas. Here, the environmental constraint is indicated via *CC* and is controlled in a range between 75 - 90 %. While, *EP* is controlled in a range between 3.6 - 4.5 MJ/kg CO_2 to characterize the economic constraint via steam consumptions from power plant intermediate turbine to reboiler system.

4.2 Multivariable control analysis

From the 4 x 3 PCC system, two further output states are defined being *CC* and *EP* (as described in Section 3.9). The 4 x 3 PCC system is then collapsed into a 4 x 2 PCC system as illustrated in Figure 4.2, where, here, the CO_2 concentration at the off-gas (y_1), is defined as a secondary output variable (embedded into the

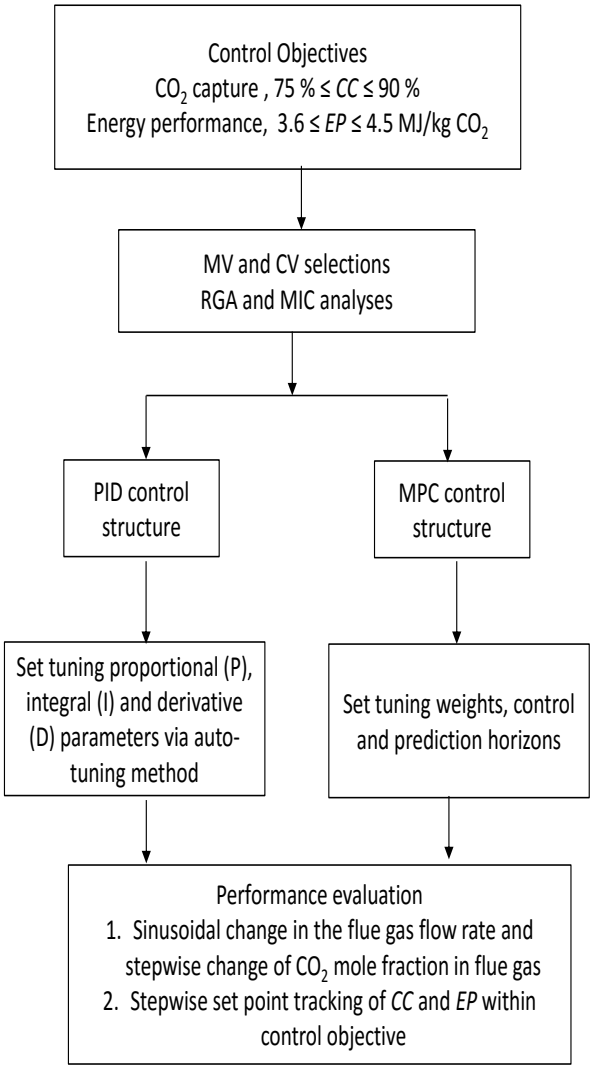

Figure 4.1: Methodology to perform the controllability analysis.

PCC model subsystem in Simulink environment).

As mentioned in the previous chapter, the inputs consist u_1,u_2, u_3 and u_7. The latter two variables (u_3 and u_7) were selected as the manipulated input variables while u_1 and u_2 were indicated as disturbance variables. The multivariable control analyses were then conducted via this reduced 4 x 2 PCC system. Analyses conducted include relative gain array (RGA) and Morari index of integral controllability (MIC). The results are provided in Table 4.1.

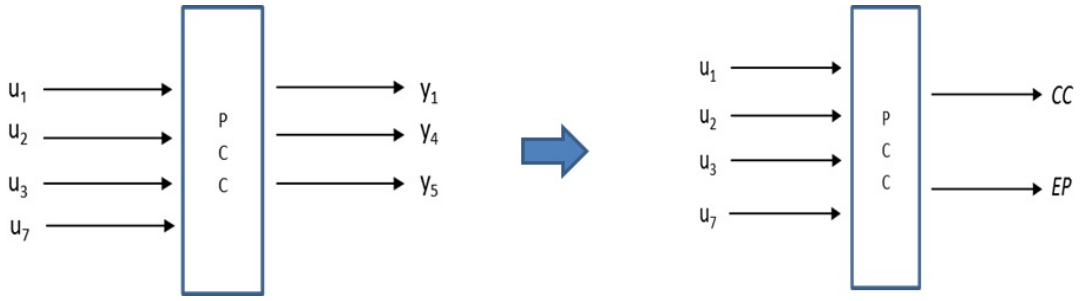

Figure 4.2: A simplified PCC process flow diagram.

Table 4.1: The result of multivariable control analyses of PCC using Simulink model.

Parameter		Result	
		u_3	u_7
RGA	*EP*	[0.2185	0.7815]
	CC	[0.7815	0.2185]
MIC		0.1830	

Based on the RGA analysis, it suggested that *CC* is best controlled using the lean solvent flow rate (*CC*-u_3) and *EP* can be controlled via the reboiler heat duty (*EP*-u_7). Similar findings were presented by others [30, 61, 33, 26]. On the other hand, the MIC calculation revealed positive eigenvalues which shows that the process gains have produced a stable diagonal control structure and therefore the structures are integral controllable, which suggests that the proposed variable pairing can suitability tune without jeopardizing the robustness and stability of existing closed loop system [62, 63]. Figure 4.3 shows a simplified PCC control structure based on the RGA result.

4.2.1 Proportional, integral and derivative (PID) control design

PID controller is a control loop feedback mechanism widely used for industrial application. A PID controller works by minimizing the error between a measured process variable and a desired set point. A typical control law for a PID controller

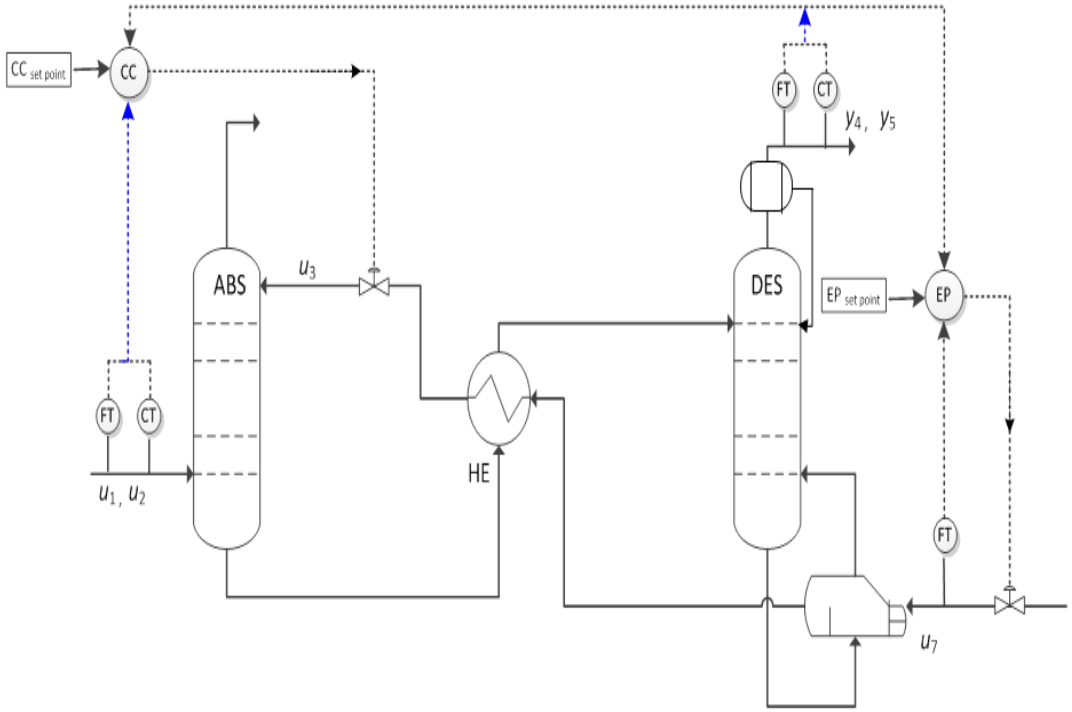

Figure 4.3: A general PCC control structure.

is expressed in Equation 4.1.

$$u(t) = K_p e(t) + \ K_i \int_0^\tau e(\tau)d\tau + K_d \frac{d}{dt} e(t) \tag{4.1}$$

In the above equation, *e(t)* represents the error which is the difference between the current input and the desired set point. The *u(t)* is the output of the algorithm that is attempting to control the input. While, K_p, K_i and K_d are the proportional, integral and derivative gains respectively.

Control architecture of this feedback control system is graphically presented in Figure 4.4. Based on the RGA results, the CC-u_3 control loop is indicated by PID 1 while the EP-u_7 control loop is indicated by PID 2. In this analysis, an advanced PID control based on anti-wind-up scheme is employed to prevent integration wind-up in the controllers. Two anti-windup methods are selected in the controller

design, where PID 1 applies clamping method at respected controller parameters; P = 0.64, I = 0.00014 and D = 521.15. While, for PID 2, back-calculation method is chosen at respected controller paramteres; P = 48.28 and I = 9.65.

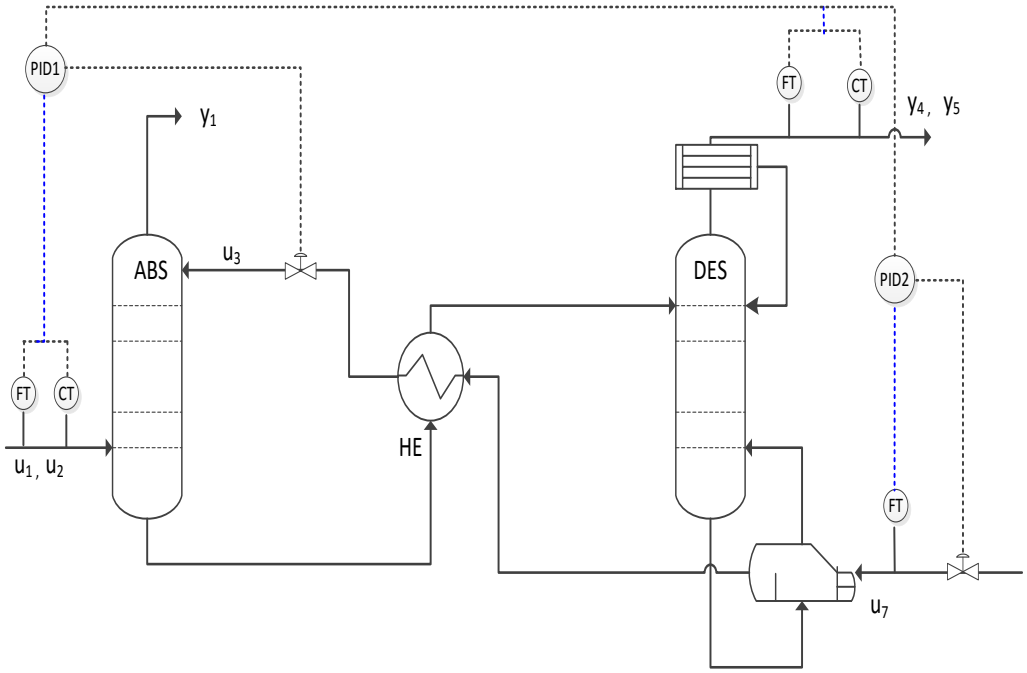

Figure 4.4: A PID control architecture.

4.2.2 Model predictive control (MPC) design

MPC represents a controlled algorithm by explicitly use a process model to forecast the process output at future time instants (horizon). It works by optimizing the future plant behavior (future estimation error) through computing a present control signal (present estimation error) using the process model. Contrary to PID controller, MPC capable to have multiple outputs (multiple control actions) in response to the changes in the input measurements. The advantage of MPC strategy over the conventional feedback control loop (PID) is its capability to handle with multifaceted processes with unstable poles and large time-delays,

such as a PCC process. Another key advantage of MPC is that it can explicitly handle constraints on the inputs and outputs.

In this analysis, MPC scheme is designed and tuned using the controller design toolbox within Simulink® workspace. Both manipulated variables (lean solvent flow rate and reboiler heat duty) are simultaneously manipulated to achieve both control objective; *CC* and *EP*. In the MPC algorithm, a large output weight was set for *EP* compared to *CC*. While, identical input weight was adjusted for lean solvent flow rate and reboiler heat duty. The purpose of tuning the inputs/outputs weights are to predetermine the most influential variable for the closed-loop performance (control analysis). Therefore, based on this control algorithm setting, the MPC will work by prioritizing the *EP* set point control performance rather than the *CC* set point control performance. This is to ensure that no substantial energy will be imposed to the power plant concurrently to optimize the economic operation of the integrated plant (power plant with PCC). The control objectives with manipulated and disturbance variables were incorporated into the MPC architecture as illustrated in Figure 4.5.

4.3 Closed-loop analysis

Fundamentally, integration of PCC plant into coal-fired power plant acquires approximately $10 - 40\%$ extra energy compare to an existing plant without PCC system [64]. To circumvent this energy burden, PCC plant should operate flexibly corresponds with the electricity demand, carbon and electricity market prices. Hence, considering those transient operations and volatile market trends, an intelligent and robust control strategy is required to acclimatize with the dynamic scenarios occurred in PCC operation.

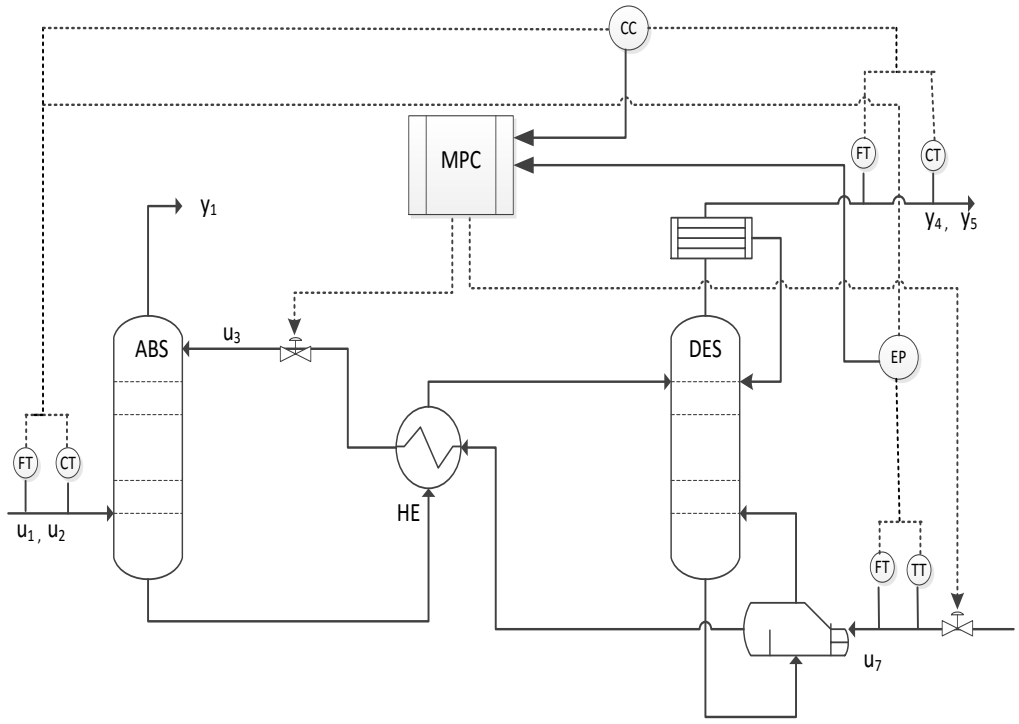

Figure 4.5: The MPC architecture.

Figure 4.6 illustrates the actual 660 MW coal-fired power plant profile data which includes gross power plant load from minimum (200 MW) to maximum capacity (660 MW), flue gas flow rate exhausted from the power plant and CO_2 concentration in flue gas throughout 2 hours operation. It can be seen that the flue gas flow rate increased with the increment of power plant gross load and vice versa. The variation of flue gas flow rate (increase and decrease) represents the high-peak and off-peak hours respectively [60]. While, CO_2 concentration varies randomly based on completeness or incomplete combustion of the fossil fuel. It is also influenced by the composition of the coal (i.e. carbon) and the coal usage per unit electricity generated from the power plant. Furthermore, a drop in power plant load may sometimes require plants to 'co-fire' (i.e. with oil) in order to maintain stable operation in the reboiler system [48, 60]. Based on the actual profile of power plant operation (Figure 4.6), flow rate of flue gas will increase (approximately 20 - 25%) with an increment of power plant gross load (increased

4%) while, the CO_2 concentration are varied between 0.05 - 0.1%.

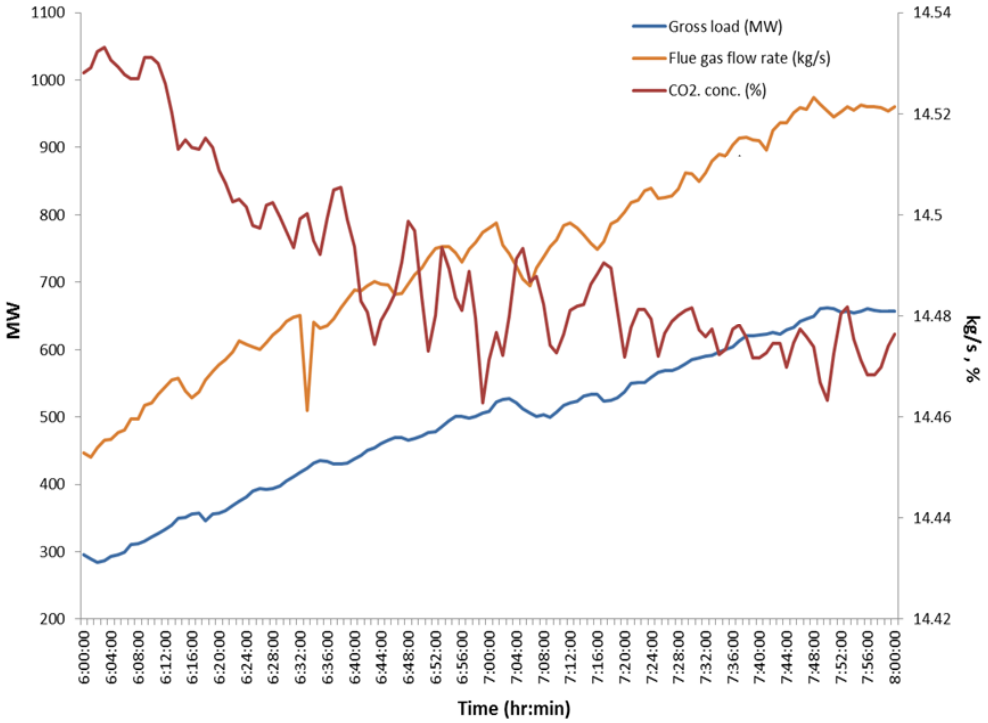

Figure 4.6: Actual profile of power plant gross load, CO_2 concentration in flue gas and flue gas flow rate in the coal-fired power plant.

Figure 4.7 shows a profile of daily electricity prices based on the regional reference price, RRP ($/MWh) and total electricity demand (MW) at NSW on January 2014 for 24 hours duration [65]. Two peaks are spotted throughout the period between 6 to 8 pm (around 10 500 MW) and 7 to 9 am (around 9 500 MW). These two periods are categorized as high-peak hours. On the other hand, off-peak hour is translated by minimum electricity dispatch exhibited between 2 to 5 pm (6 500 MW). Based on these combined profile (in Figure 4.6 and Figure 4.7), a hypothetical control scenario is developed to imitate the actual operation of PCC plant associated with coal-fired power plant. Detail of the scenario is explained in the next section.

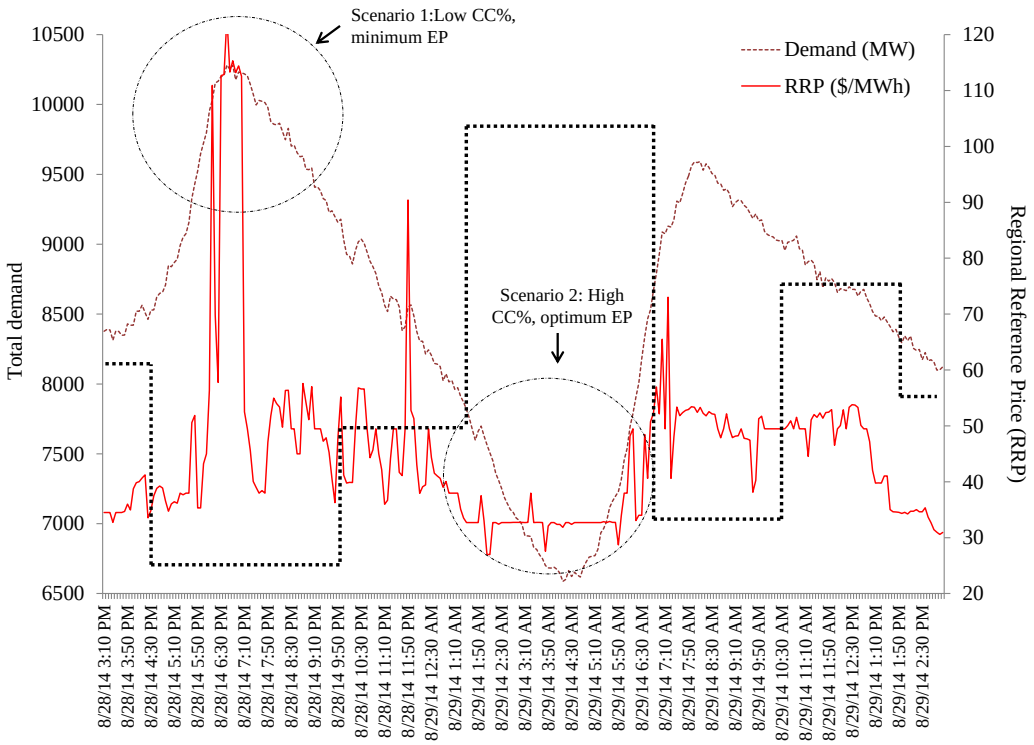

Figure 4.7: Profile of daily electricity price and dispatch in NSW on 28 August 2014 obtained from AEMO.

4.4 Control implementation strategy

To evaluate controller robustness and its capability to adapt with the dynamic operation of PCC plant retrofitted into coal-fired power plant, two control scenarios were developed by combining actual trends in Figures 4.6 - 4.7. The control scenarios were designed to simulate approximately 24 hours of PCC operation which starts from 3 pm and ends at 3 pm of the following day.

Scenario 1 (in Figure 4.7) represents high-peak period illustrated by the elevation of electricity demand (increased in power plant load and electricity price). At this condition, PCC plant may necessary to launch a transitory decrement of $CC\%$. This can be done by reducing the amount of steam delivering to the reboiler system (at PCC plant) since this steam can be used in the high/intermediate

turbine to meet the increased in power demand. Therefore, for this scenario, a controller is responsible to reduce the capture rate concurrently minimizing the *EP* at 3.6 MJ/kg CO_2.

Scenario 2 (in Figure 4.7) features off-peak period demonstrated by low electricity demand which usually translated by the low electricity prices (cheap). At this condition, more low-pressure steam from the steam turbines can be dedicated for the PCC plant. Under this scenario, a control algorithm should be able to capture CO_2 at the maximum rate but at the same time maintaining optimal energy performance of PCC plant at 4 MJ/kg CO_2.

To illustrate the actual operation of integrated power plant and PCC facility, the sinusoidal changes of flue gas flow rate and random stepwise of CO_2 concentration in flue gas were introduced to PCC plant (Figure 4.8). Essentially, flue gas flowrate increases during high-peak period and vice versa during off-peak period. In this analysis, the sinusoidal pattern is chosen to imitate an extreme operation of power plant under the unprecedented situation. Where, the sinusoidal perturbation of flue gas flowrate will demonstrate a combination of normal and irregular operations of power plant. This is to challenge the robustness of proposed controllers not only at anticipated operation (off-high peak hours) but also under the unprecedented operation. On the other hand, set point changes for *CC* and *EP* are elucidated by combining Scenarios 1 and 2 (Figure 4.7) as projected in Figure 4.9.

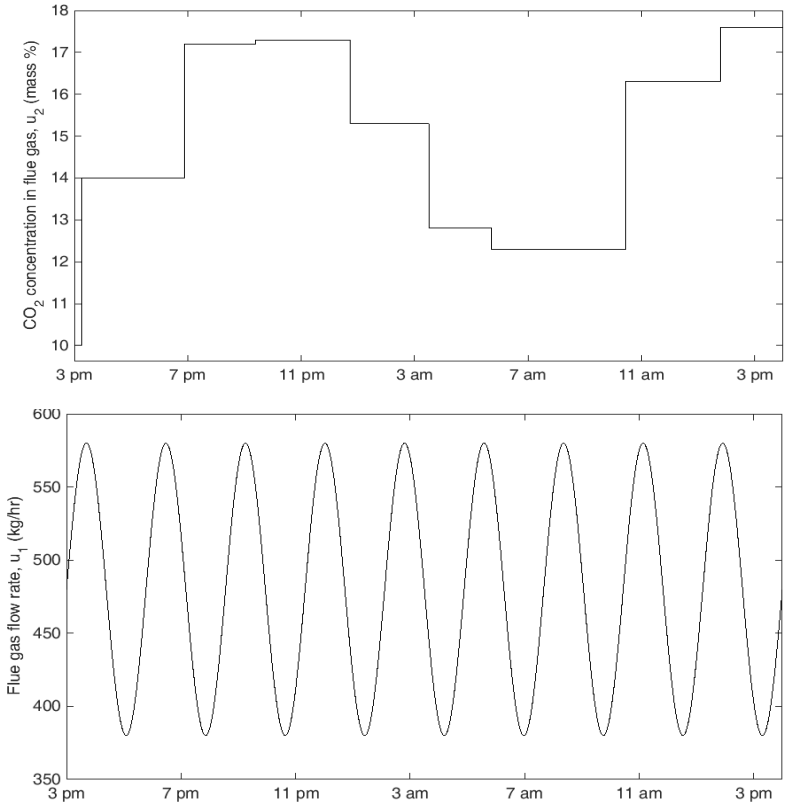

Figure 4.8: Perturbation profile for flue gas flow rate (u_1) and CO_2 concentration in flue gas (u_2.)

4.5 Control performance evaluation

To evaluate the limitation and capability of the proposed control strategies (PID and MPC), simultaneous extreme perturbations were introduced into the flue gas flow rate and CO_2 concentration in flue gas as illustrated in Figure 4.8, concurrent with the set point changes of *CC* and *EP* (depicted in Figure 4.9).

The simulation results for control performance evaluation are shown in Figures 4.10 - 4.11. Figure 4.10 represents the controller performance for *CC* and *EP*, while Figure 4.11 features the responses from the manipulated variables (reboiler heat duty and lean solvent flow rate) towards the set point tracking and disturbance rejection cases over the simulation horizon. It can be seen that, the MPC strategy exhibits satisfactory set point tracking and disturbance rejection for *CC*

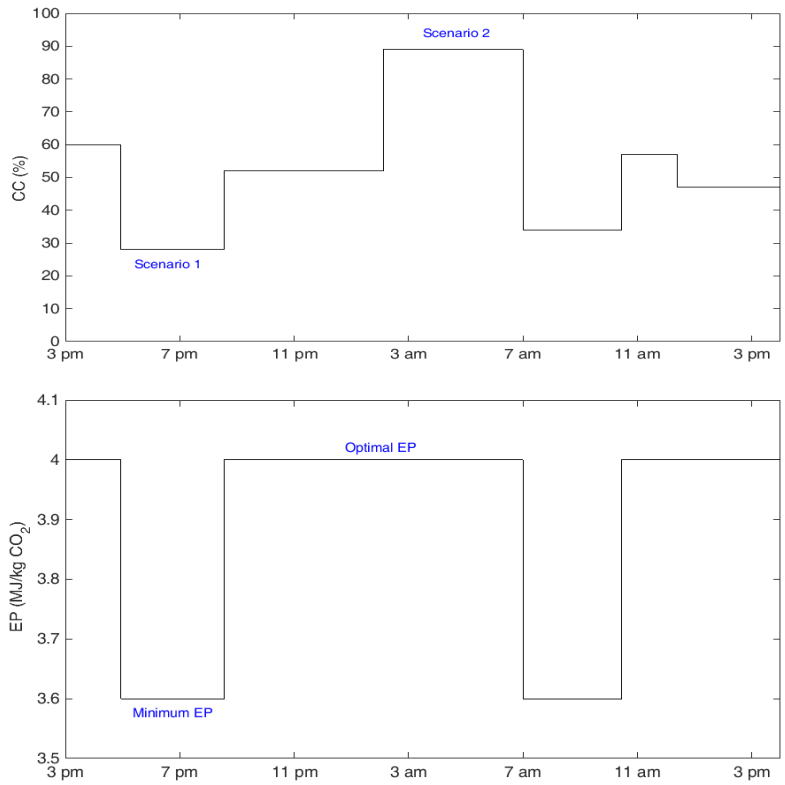

Figure 4.9: Set point changing profile for CO_2 capture efficiency (CC) and energy performance (EP).

compared to PID controller. This can be demonstrated by the response of lean solvent flowrate. Where, sudden and large transitions of lean solvent flow rate were appeared at every 3 to 4 hours in order to ensure the best CC performance. This scenario evident the robustness of MPC scheme in handling with the extreme set point tracking and disturbance rejection scenarios. Nevertheless, an instant reaction of lean solvent flowrate could jeopardize the overall performance of PCC process. Since practically, PCC system will take some time to react with any changes/perturbations in the process. This condition could be one of the biggest challenges if MPC scheme is to be considered for large-scale installation/deployment. Similarly, for EP, MPC outperformed the PID control strategy by providing excellent set point tracking and disturbances rejection throughout the simulation period.

As shown in Figure 4.10, under the extreme perturbations, PID controller is incapable to reach the *CC* and *EP* set points efficiently. For instance, in *CC* performance, PID controller unable to track each set point changes throughout the simulation horizon (under-resumed the set point changes). This performance can be translated with the response of lean solvent flow rate. Where, under the extreme perturbations and unprecedented set point changes, PID 1 unable to maximize the lean solvent flow rate (depicted in Figure 4.10) in order to capture high amount of CO_2. Similar responses exhibited in reboiler heat duty. Interestingly, satisfactory control performance was showed in *EP* between 4 pm to 9 pm and between 9 pm to 3 am. This possibility occurs because under the Scenario 1, both *CC* and *EP* are at minimum level therefore it is easy for PID 2 to manipulate reboiler heat duty in order to attain the *EP* set point. It is noticeable that both PID controllers started to violating the set point target (reach it capability's limit - after 3 am) under the extreme changes of *CC*, u_1 and u_2. Moreover, the spikes evident in the *CC* and *EP* PID control signals at time between 7 am to 11 pm were caused by aggressive proportional and derivative response towards the disturbances and abrupt changes in set points.

MPC controller has shown satisfactory and excellent control performances for *CC* and *EP* respectively. Based on Figure 4.10, it can be seen that there are slight deviations at the time when the PCC plant launched a transitory increment of *CC* where it took approximately one hour for *CC* to reach it new set point. This can be explained by the fact that the reaction in amine-based PCC process is not instantaneous [21] and therefore it requires some time for the reaction to complete. Random fluctuations of lean solvent flow rate and reboiler heat duty were resulted from the extreme perturbations and unprecedented pattern of set points introduced to the PCC system. Where, as *CC* increased, more CO_2 needed to be recovered, therefore the lean solvent flow rate was increased accordingly in order

to attain the respective *CC* new set points. It can also be observed, throughout the simulation period, optimal reboiler heat duty has been utilized. Which characterized the economic and technical (operation) benefits of PCC system embedded with MPC strategy. The fluctuations of manipulated variables evident an active/progressive responses of manipulated variables towards those conditions in handling with the set point tracking and disturbance rejection problems. On the other hand, an excellent control performance of *EP* was featured by the capability of MPC to track the *EP* set points consistently throughout the simulation horizon.

Based on these analyses, PID controller reaches its control limitations where it fails to perform efficiently under the extreme and unprecedented operations of power plant retrofitted with PCC facility. Contrariwise, MPC provides highly reputable performance by its ability to capture maximum CO_2 without much consumption of reboiler heat duty (PCC plant operated at the optimal energy performance). Thus characterizes the flexibility of the PCC plant when embedded with suitable control strategy such as MPC. Since, the response represent 24 hours of plant operation, thus careful attention should be taken into consideration while interpret this control responses.

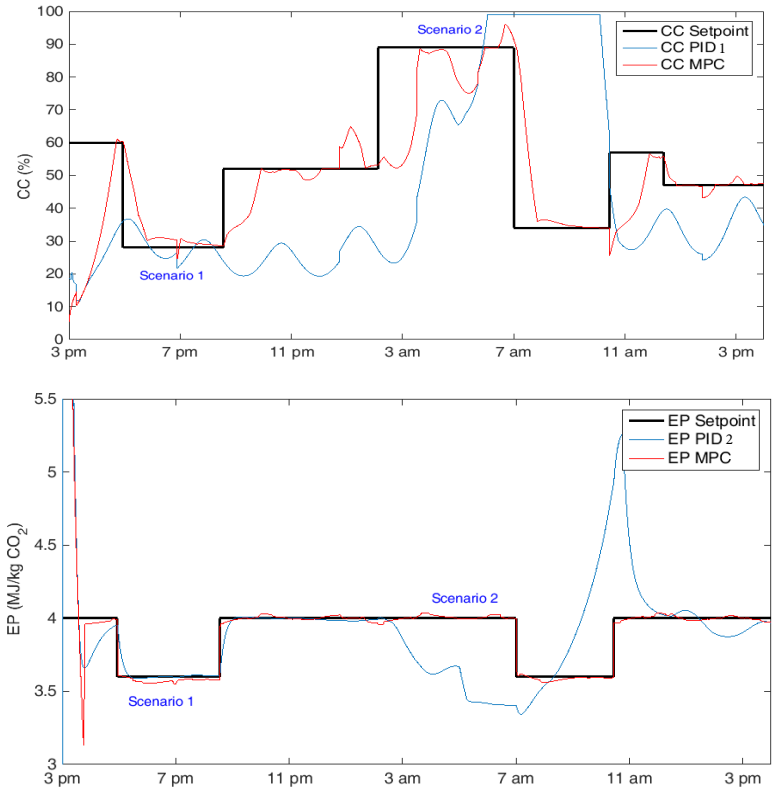

Figure 4.10: The controller performance (PID controller and MPC) for CO_2 capture efficiency (CC) and energy performance (EP) under set point tracking and disturbance rejection cases.

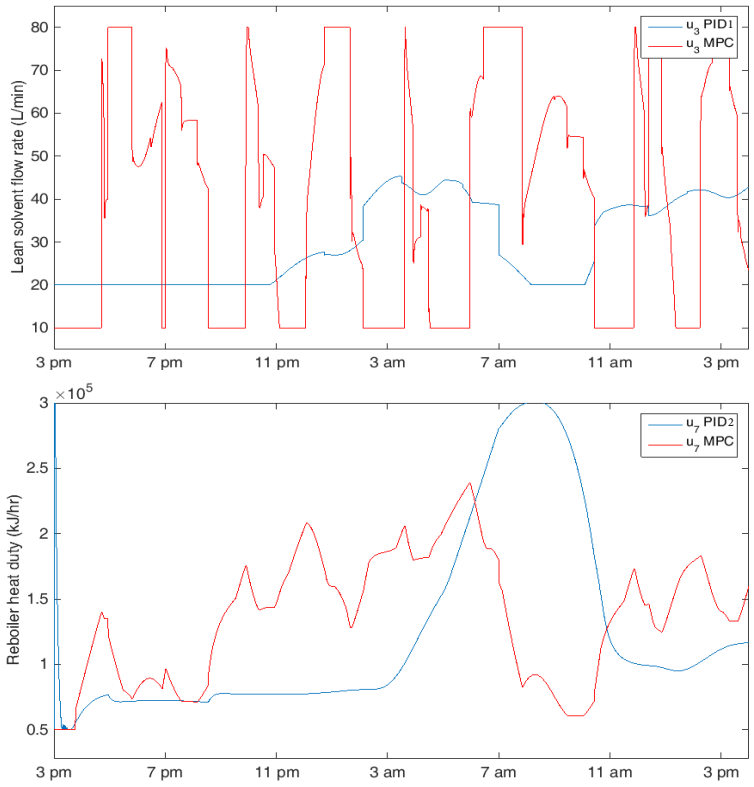

Figure 4.11: Response of lean solvent flow rate and reboiler heat duty from PID controller and MPC.

Chapter 5

Techno-economic analysis of PCC system associated with coal-fired power plant

This chapter presents an algorithm that combines MINLP (optimization algorithm) with MPC (control algorithm) and demonstrates its application for coal-fired power plant retrofitted with PCC plant. The objective of the optimization algorithm is to maximize net operating revenue of the plant by forecasting optimal power plant load and CO_2 capture rate. While, the MPC algorithm is used to control the performance of PCC plant by ensuring the robustness of PCC control strategy under real-time perturbation pattern from the upstream process. This chapter focuses on the development, capability and application of the control-optimization algorithm in the operation of power plant retrofitted with PCC system. The advantage of this integrated algorithm is its capability to capture financial benefits hidden in the dynamics of electricity and carbon price trends, and does so applicable for a real-time carbon trading.

This chapter contains material published in [66, 67].

5.1 Development of the hybrid MPC-MINLP algorithm (control-optimization algorithm)

Two independent algorithms are integrated to perform a control-optimization study of PCC retrofitted to the coal-fired power plant which incorporates four levels; regulatory/policy, enterprise, plant and instrumentation levels. Briefly, the algorithm interfaces multiple time scales (temporal) from seconds represented by instrumentation level to years represented by regulation/policy level, while considering size scales (multiscalar) transcending across from control actuators to equipment all the way to multi-plant superstructure (the power plant and capture plant are effectively described by integrated dynamic models).

At the top level, the optimization process uses a genetic algorithm (GA) function for mixed integer non-linear programming (MINLP) problems. In this analysis, GA is selected as a solver because of its capability to handle large number of parameters, easily distributed and suitable for nonlinear integer. Moreover, GA searches in parallel from the population points thus it can prevent being trapped in local minima solution like conventional solvers. It optimizes the dynamic model superstructure encompassing of a 660 MW coal-fired power plant and PCC plant. Both models were constructed via reduced model and were validated against real power plant data. This superstructure models were employed and adopted from [68] while the optimization formulation was adopted from [41]. Here, the net load matching mode has been chosen as the optimization formulation. Both works [68, 41], were conducted by fellow colleagues in my research group and thus not a genuine contribution of this thesis. On the other hand, the bottom algorithm involves an advanced control strategy of the PCC plant employing the MPC control law. The development of PCC dynamic model at the instrumentation level has been explained in Chapter 3. While, the MPC control strategy (at the

plant level) was designed based on the controllability study elucidated in Chapter 4. The two algorithms (control and optimization algorithms) are then integrated to demonstrate a control-optimization algorithm (the hybrid MPC-MINLP) as illustrated in Figure 5.1.

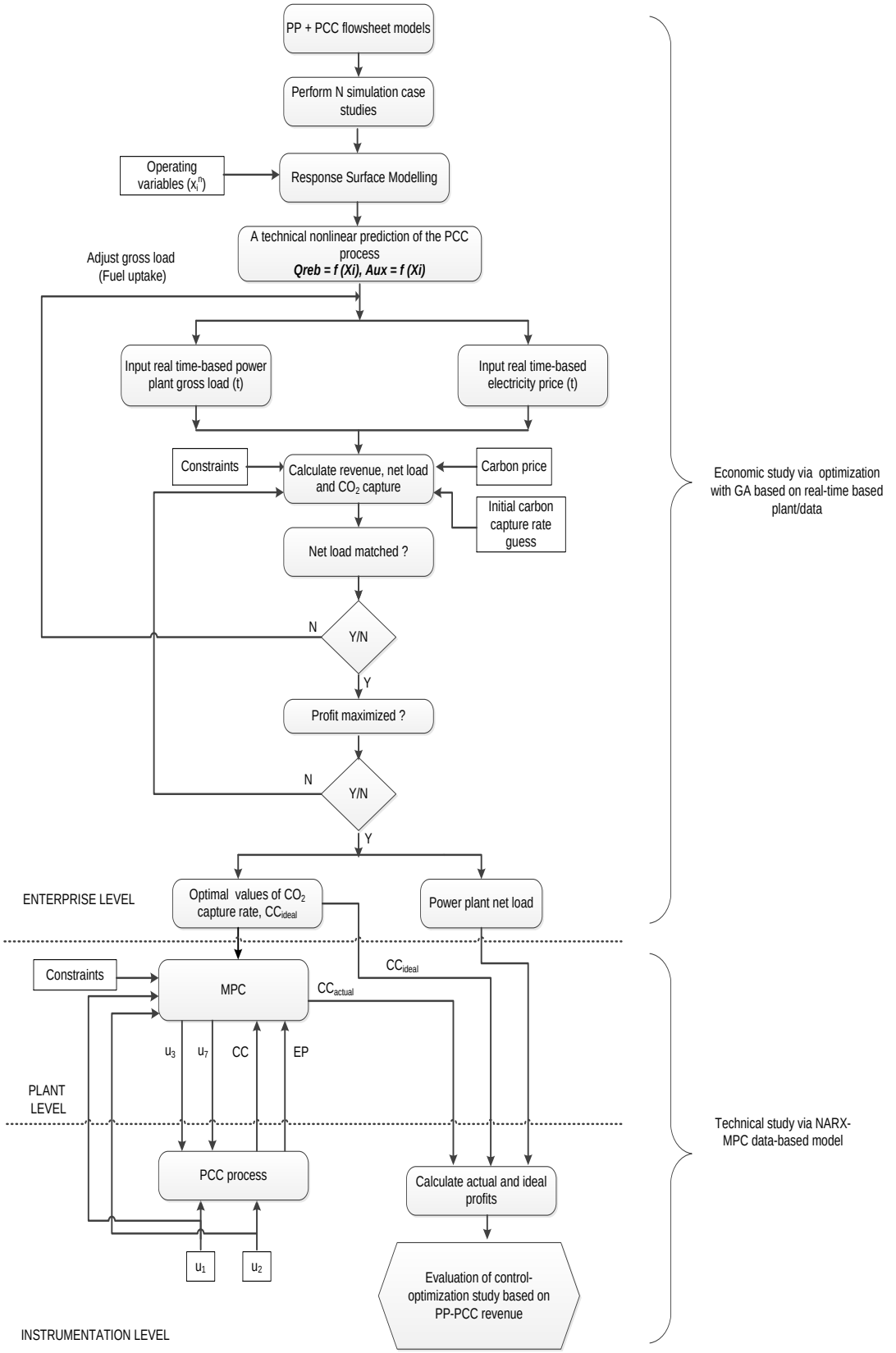

Figure 5.1: The control-optimization algorithm (the hybrid MPC-MINLP) for power plant integrated with PCC plant.

According to Figure 5.1, at the enterprise level, the optimization algorithm is used to assist decision making of a power plant retrofitted with PCC system. The main objective and concern at this level is to ensure maximum net operating revenue at optimal power plant load and CO_2 capture rate (CC). The objective function of the optimization algorithm is to feature the system net operating revenue as described in Equation 5.1.

$$Max_{Revenue} = \int P_e * (Power\ plant\ net\ load - PCC\ penalty) * dt - \tag{5.1}$$

$$- \int C_t * CO_2\ emitted * dt - P_{PP} - P_{PCC}$$

Where P_e is the price of electricity and C_t is the carbon price. The net operating revenue composite consists of three individual costs which include P_{PP} as the power plant operational cost, P_{PCC} as the PCC operational cost and finally, the cost of CO_2 emission (indicated in the second integration term). The first integration term in the above equation represents the revenue generated through selling of electricity. The capital costs for the power plant and PCC plant are not considered by assuming the size of both have been fixed for all cases. The operating cost are evaluated through Equations 5.2 - 5.3 and magnitude of the cost terms are tabulated in Table 5.1.

$$P_{PP} = O\&M_{PP,coal} * size_{PP}/8760 \tag{5.2}$$

$$P_{PCC} = (FCI_{PCC} * 0.12) + (sol_{loss} * sol_{cost}) \tag{5.3}$$

Where, $O\&M_{PP,coal}$ is operation and maintenance costs of power plant ($/MW), $size_{PP}$ is size of power plant, FCI_{PCC} is fixed capital investment, sol_{loss} is solvent lost (kg/tonne-CO_2 captured) and sol_{cost} is cost of solution ($AUD /kg).

Table 5.1: Operating and maintenance costs assumptions for the power plant and PCC system.

Variable	Assumption
$O\&M_{PP,coal}$	$AUD 50 000/MW/year [69]
Coal specific cost	$AUD 1.5/GJ
Power plant capacity/size	660 MW
$O\&M_{PCC}$	Eq. 2 from Li et al. [70]
Solvent loss	1.5 kg MEA/ tonne-CO_2 captured
Solvent cost	$AUD 2/kg MEA
Sequestration cost	$7/tonne-$CO_2$ captured

At the enterprise level, the optimization algorithm generates three inputs and two outputs. The inputs are power plant gross load*(t)*, electricity price*(t)* and carbon price*(t)*, where the inputs are in a function of time, t. While the outputs are optimal CO_2 capture rate (CC_{ideal}) and net power plant load. The optimization algorithm observes the prevailing situation in the plant based on the real-time inputs to make timely decisions of the outputs. The optimization algorithm then dispatches the outputs to the bottom layer. This level exhibits process optimization under dynamic operation with 30 minutes time intervals.

Subsequently, at the plant level, a control algorithm is implemented in conjunction with the data-based PCC dynamic model to control the PCC plant performance. Here, the control algorithm receives a signal (CC_{ideal}) from the optimization algorithm. At the same time, MPC scheme regulates u_3 and u_7 (act as manipulated

variables) to ensure that the plant meets the control objective by tracking the set point of CC_{ideal}. Here, the output response of the MPC scheme is actual CO_2 capture rate (CC_{actual}). Where, the CC_{actual} represents the actual output of CO_2 capture based on the response from the MPC algorithm.

At the instrumentation level, a 4 x 2 PCC system is employed. The inputs consist of u_1, u_2, u_3 and u_7, while the outputs are *CC* and *EP*. As mentioned before, the u_3 and u_7 are played as the manipulated variables while the u_1 and u_2 are constant at 500 kg/hr and 14 mass% respectively. Here, the *EP* represents the amount of energy required to capture a kg of CO_2, which then being controlled at 4 MJ/kg. The values for those two inputs (u_1, u_2) are selected based on the nominal operating conditions of actual pilot plant. While, the value of energy performance is set at 4 MJ/kg in order to ensure the PCC plant is operated within the optimal energy requirement. Both levels (plant and instrumentation levels) exhibit plant wide control operation under dynamic operation with 10 seconds time intervals.

Since both algorithms (optimization and control algorithms) have difference sample time, a rate transition block function was used as a medium to transfer the output signal from the MINLP algorithm (enterprise level) to MPC controller (plant level) to ensure the sample time is coordinated as shown in Figure 5.2. In this case, a rate transition will transmit the optimization output signal from 30-minute interval time to 10-second interval time. Another advantage of this block function is its capability to ensure integrity of the traded data and to guarantee deterministic data transfer. Figure 5.2 depicts the simulation model for control algorithm executed in Simulink workspace.

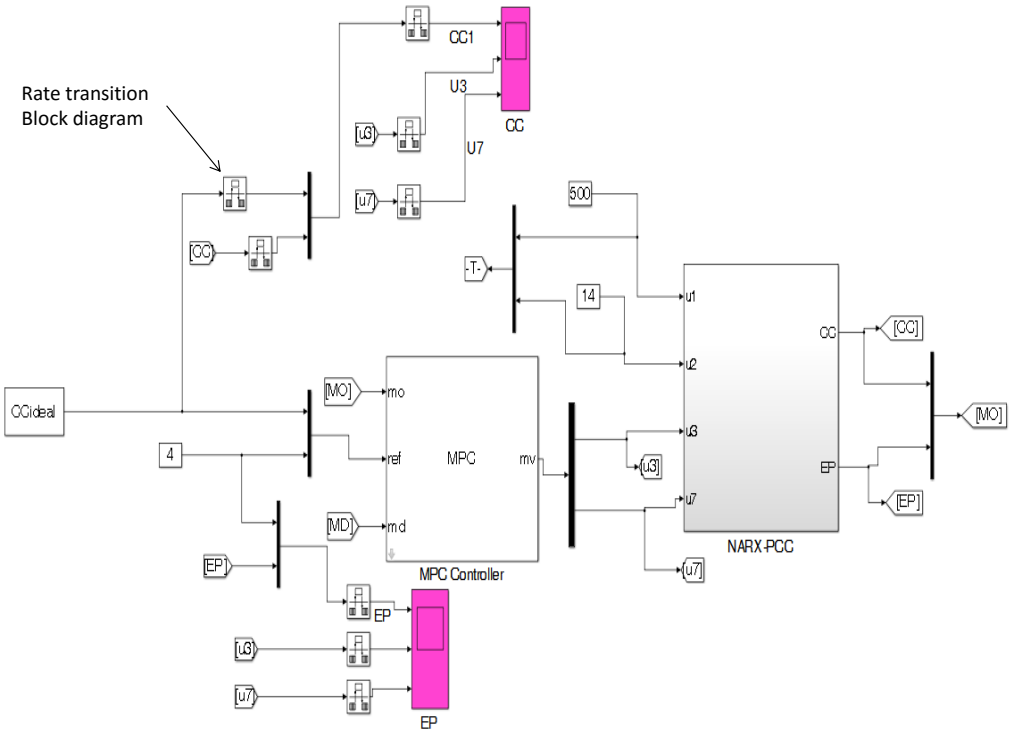

Figure 5.2: A rate transition block function connected between control and optimization algorithms in PCC model in Simulink workspace.

5.2 Capability and applicability of the hybrid MPC-MINLP algorithm

The capability (in term of sensitivity and best-response algorithm) of the developed control-optimization algorithm (hybrid MPC-MINLP) is evaluated based on the 24-hour operation of integrated plant. While, the application of developed algorithm is demonstrated based on the yearly operation of integrated plant. Both are evaluated based on the historical and future scenarios in Australia.

Two techno-economic scenarios represent by fixed operation mode and flexible operation mode were developed. The fixed operation mode was initiated by constraining the lower and upper bounds of CO_2 capture rate at 90% while maintaining the objective function (maximize plant net operating revenue) at correspond-

ing power plant loads. Whereas, in the flexible operation mode, CO_2 capture rate was allowed to vary along with the power plant loads in order to maximize plant net operating revenue. The general optimization formulation for fixed and flexible operation modes is given in Table 5.2.

Table 5.2: Operation modes for power plant retrofitted with PCC system.

	Fixed operation mode	Flexible operation mode
Objective function:	Maximize revenue (t, P_e, $x_1 = 90\%$, x_2, C_t) s.t.	Maximize revenue (t, P_e, x_1, x_2, C_t) s.t.
Process model:	Q_{reb} (x_1,x_2), E_{Aux} (x_1,x_2)	
Initial conditions:	$x_1 = CR^I$, $x_2 = PPL^I$,	
Process variables bounds:	$CR^{Min} < x_1 < CR^{Max}$ $PPL^{Min} < x_2, < PPL^{Max}$	
Constraints:	$h(x_1,x_2) < 0$	

Where x_1 and x_2 are the capture rate (%) and power plant load (MW Gross) respectively. The CR^I, CR^{Min} and CR^{Max} are the initial, lower bound and upper bound carbon capture rates and PPL^I, PPL^{Min} and PPL^{Max} are the initial, minimum and maximum power plant loads. The h denotes the process inequality constraints that means the net electricity output of the power plant does not exceed the historical net load of the power plant at any particular time. While, the Q_{reb} and E_{Aux} represent the reboiler heat duty and auxiliary electrical energy requirement respectively as presented in Equations 5.4 and 5.5. These non-linear reduced models were developed via response surface methodology to the data obtained from the sensitivity analyses using the commercial software MODDE (Umetrics, Sweden). The models were created by first performing a sensitivity analysis (model simulation) of the independent variables and recording the resultant response variable values. The response variable results were then used in the regression process, and all data were scaled into the interval of [-1, 1] in order to provide a universal tolerance of error to all the factors in the regression

process. For comprehensive explanation on these reduced model development, one can refer to [68].

$$Q_{reb} = 168.4 + 117x_1' + 78.12x_2' + 20.64x_1'^2 + 43.4x_1x_2 + 3.53x_2'^2 \tag{5.4}$$

$$E_{aux} = 28.97 + 16.06x_1' + 2.392x_2' - 1.85x_1'^2 + 1.87x_1x_2 - 0.75x_2'^2 \tag{5.5}$$

The hybrid MPC-MINLP algorithm was implemented in Matlab (Mathworks, USA) and solved using a PC with a dual core i7 processor and 16 GB RAM. For each scenario, the optimization algorithm was executed three times to ensure the reliability and consistency of the generated outputs (ideal CO_2 capture rate and power plant net load). Table 5.3 lists the average deviation for each simulation cycle for flexible operation mode (24-hour operation). It can be seen that the average deviations for all scenarios are relatively small and can therefore be ignored. Therefore, for this work, the last generated outputs were reported (third simulation cycle) as the final optimization outputs.

Table 5.3: The average deviations of triplicate optimizations in CC_{ideal} and power plant net load for flexible operation mode.

	CO_2 capture rate, CC_{ideal}	Power plant net load
\$AUD 5/tonne CO_2	0.01%	0.001%
\$AUD 25/tonne CO_2	0.06%	0.004%
\$AUD 50/tonne CO_2	0.03%	0.021%

Initial conditions optimization variable bounds for minimum and maximum power plant loads and carbon capture rates for running the power plant associated with PCC plant were taken to be:

$\mathrm{CR}^{Min} = 25\%$

$\mathrm{CR}^{Max} = 90\%$

$\mathrm{CR}^{I} = 50\%$

$\mathrm{PPL}^{Min} = 0$ MW

$\mathrm{PPL}^{Max} = 700$ MW

$\mathrm{PPL}^{I} = 500$ MW

Here, the algorithm consists of two conditions which are ideal and actual conditions. The top-down section (enterprise level) represents the ideal operation of power plant associated with PCC facility (integrated plant) by demonstrating a slow-time scale to attain a close to optimal economic operation. While, the bottom-up section (plant and instrumentation levels) illustrates the actual operation of integrated plant corresponding to the inputs/responses despatch from the ideal operation. This section (plant and instrumentation levels) illustrates a robust fast-time scale regulatory control subject to all uncertain condition imposed by the enterprise level.

5.2.1 A 24-hour operation analysis based on carbon pricing mechanism (fixed carbon price)

In a 24-hour scenario, two techno-economic scenarios were developed based on the historical (year 2011) and futuristic electricity prices (year 2020) at three different rate of carbon prices ($AUD 5, 25, 50/tonne-$CO_2$). The electricity prices for both scenarios are illustrated in Figures 5.3 - 5.4 respectively. The

computation time required for execution of MINLP algorithm for one scenario (24-hour) was approximately 5 hours. While, at the plant level, the computation time required for MPC controller was about 10 minutes.

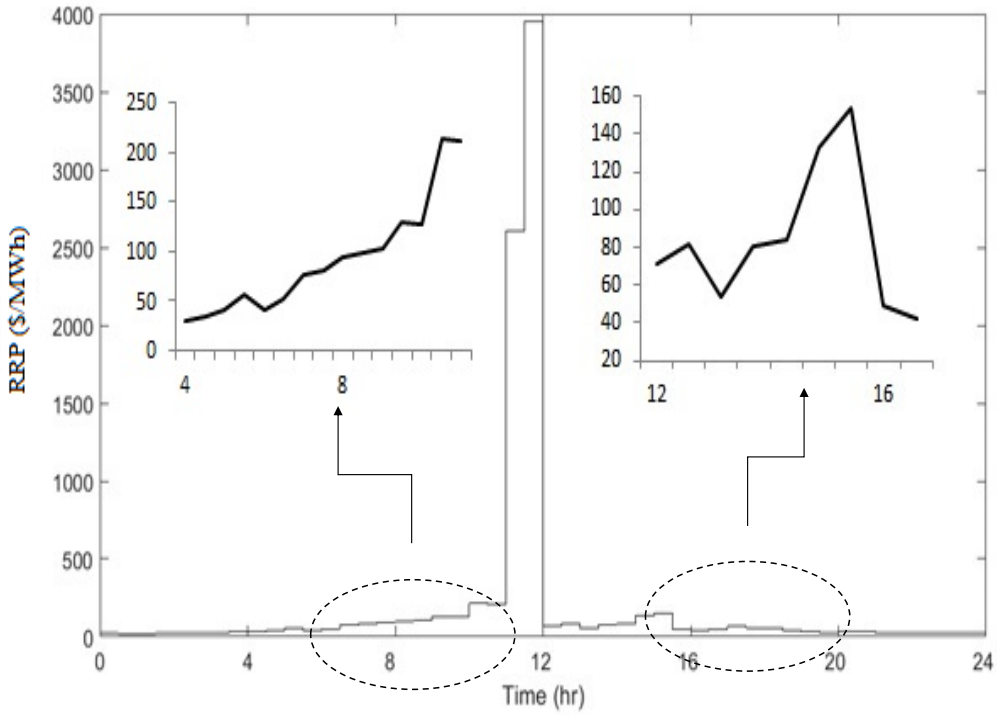

Figure 5.3: The electricity prices (regional reference price, RRP) for 2011.

5.2.1.1 Fixed operation mode: Year 2011 and 2020

Figure 5.5 shows power plant net loads generated from the MINLP algorithm for year 2011 and 2020 for fixed and flexible operation modes. The results were combined to illustrate a comparative study between both modes. During fixed operation mode, at corresponding electricity and carbon prices, optimizer forced power plant to generate more energy at each time interval compared to the flexible operation mode as depicted in Figure 5.5. For instance, in year 2011 and 2020, at \$AUD 5/tonne-CO_2 of carbon price, fixed operation required additional 60 MW (from the loads generated via flexible mode) at every half hour in order for

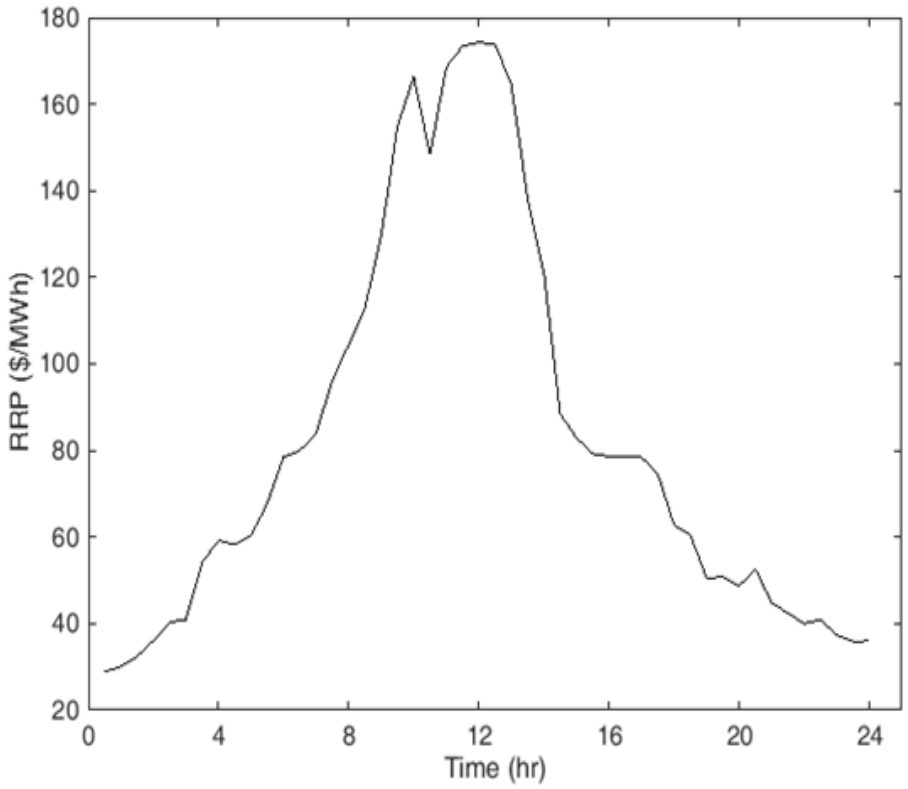

Figure 5.4: The electricity prices (regional reference price, RRP) for 2020.

plant to obtain maximum net operating revenue. Contrary, an initial ramp up was generated for flexible operation mode in year 2011 (at carbon price of $AUD 25/tonne CO_2 and $AUD 50/tonne CO_2) in order for plant to gain maximum operating revenue. Interestingly, for flexible operation mode, a positive spike featured at all rates of carbon prices between hour of 22 and 24. The spike featured due to the sudden change (increase) of power plant gross loads that have been fed to the optimization algorithm (MINLP algorithm) as illustrated in Figure 5.6 (dashed circles). This response evident that the MINLP algorithm is well performed by trying to imitating the historical gross loads of power plant subject to maximum net operating revenue.

The output responses from the controller are depicted in Figure 5.7 and appeared to be identical under three different carbon price rates. Here, only control performance for year 2011 is illustrated, since similar performance appeared in year

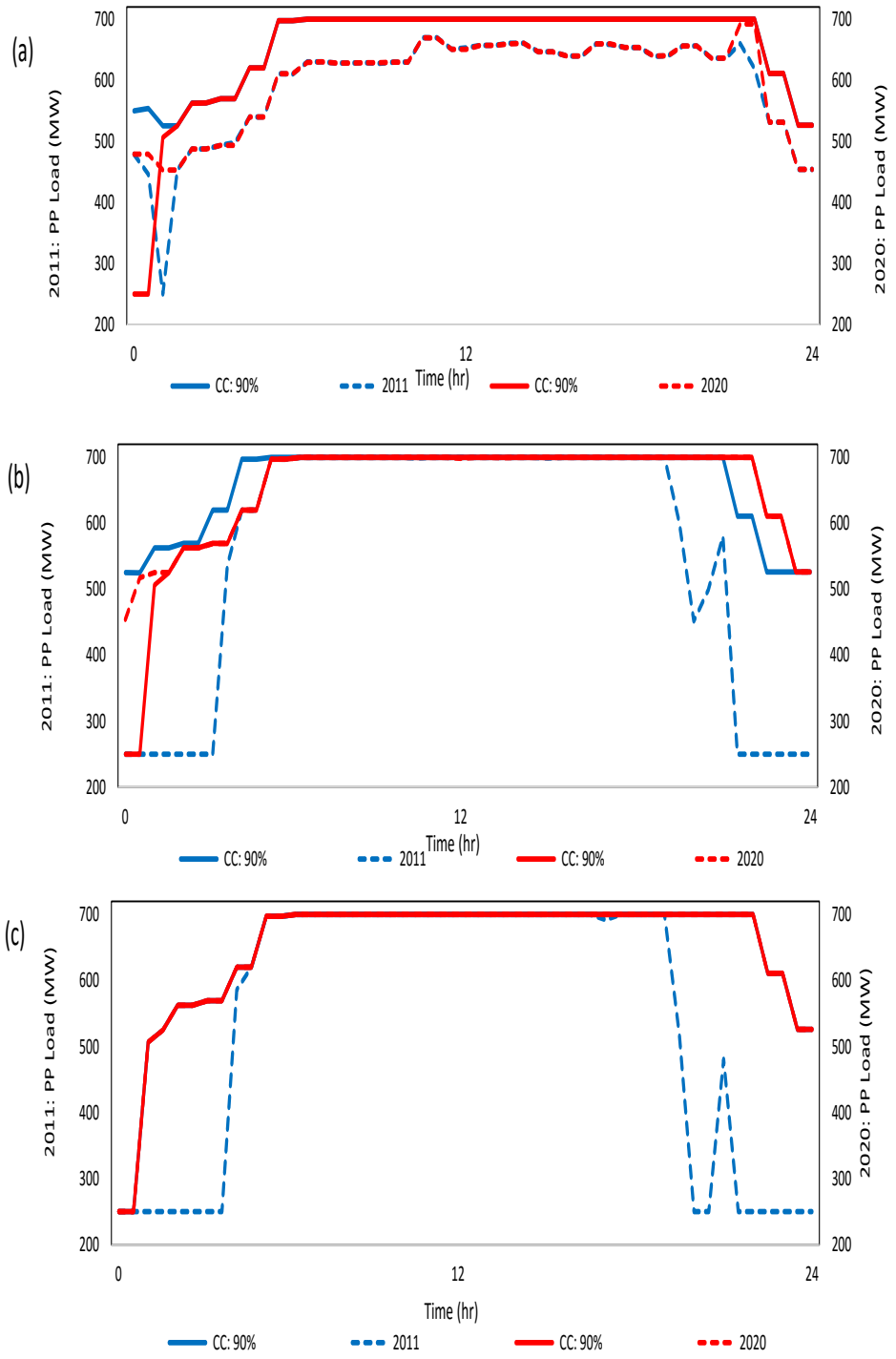

Figure 5.5: Power plant load generations at respective carbon price rates. (a) \$AUD 5/tonne-CO_2 (b) \$AUD 25/tonne-CO_2 and (c) \$AUD 50/tonne-CO_2 (dashed line: fixed mode operation (constant CO_2 capture rate, CC at variable power plant loads); continuous line: flexible mode operation (variable in CO_2 capture rate, CC and power plant loads)) for 2011.

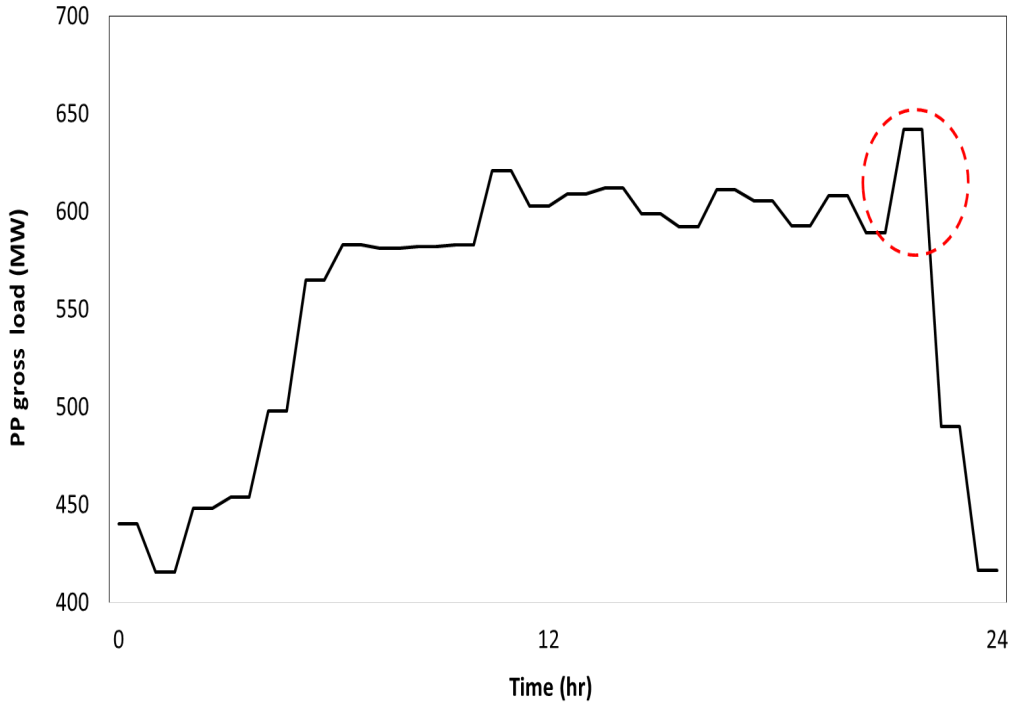

Figure 5.6: Real time-based power plant gross load profile inputted to the optimization algorithm.

2020. In Figure 5.7, the black line indicates the CC_{ideal} which was calculated from the economic optimization algorithm, while the red bar is the actual CO_2 captured based on responses from the MPC controller in the PCC process. Since the MPC controller is capable to track the CC_{ideal} perfectly, there is no deviation in ideal and actual revenues for this specific operation mode.

5.2.1.2 Flexible operation mode: Year 2011

Figure 5.8 shows that the techno-economic analysis based on year 2011 with the aims to generate maximum plant revenue for a given duration. Figure 5.8 (a-i, b-i, c-i) illustrate the power plant loads generated from the optimization algorithm in conjunction with the optimal CO_2 capture in Figure 5.8 (a-ii, b-ii, c-ii). It can be seen, at the highest carbon price ($AUD 50/tonne-$CO_2$), CO_2

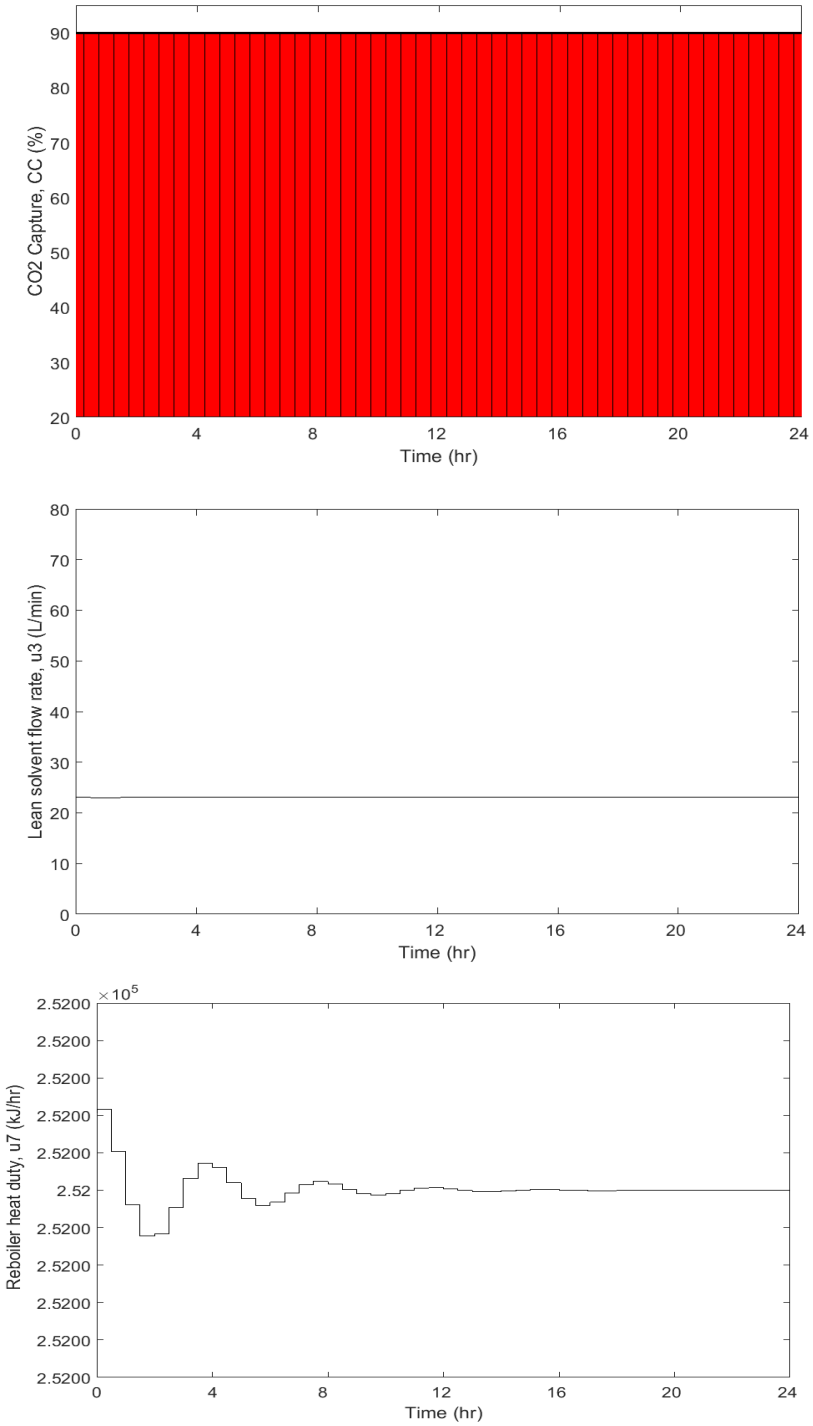

Figure 5.7: Control responses for fixed operation mode under three carbon prices (($AUD 5, 25, 50 tonne-$CO_2$) (black line: CC_{ideal}; red bar: CC_{actual})) for 2011.

was captured at almost maximum plant capacity, 90% and opposite performance occurred at low carbon price. Where, PCC plant operated at minimum capacity between 20% - 30%. Moreover, during high-peak demand where high electricity prices were induced $AUD (2500 - 4000/MWh$_e$), the capture rate was observed to decrease and at low electricity prices $AUD (100 - 200/MWh$_e$, the capture rate appeared to increase as illustrated in Figure 5.8 (b-ii) and (c-ii) respectively. These behaviours are comparable to the study conducted by [41, 71]. It is evident that there are trade-offs between the power plant load and CO_2 capture rate in order to obtain maximum plant revenue.

At the plant level (Figure 5.8(a-ii, b-ii, c-ii)), the control responses are represented by the black line and red bar respectively. It can be seen in Figure 5.8 (b-ii) and (c-ii), there is a slight deviation at the time when the PCC plant launched a transitory increment (hours 4 - 8). This is explained by the fact that in the PCC process, the reaction of CO_2 absorption in amine solvent is fast, but not instantaneous [21], and therefore it affects the performance of CC_{actual} to track the CC_{ideal} consistently. Furthermore, the dynamic nature of PCC plant itself caused a process to take some time to attain a new steady state point [71].

Besides that, two spikes have been spotted in the CC_{ideal} at 13 hours and 14 hours (Figure 5.8 b(ii)). The spike at both times is due to the abrupt reduction of electricity prices (refer Figure 5.3). Since the optimization aims at achieving maximum net operating revenue, an ideal carbon capture rate is calculated every half hour based on the power plant load and electricity price. Therefore, drops in electricity price, coupled with moderate to high carbon prices lead to spikes in the carbon capture rate in order to maximize net operating revenue. Conversely, a sudden drop in the ideal carbon capture rate is observed in Figure 5.8 c(ii) at 10 hours, which can be attributed to sudden jump in electricity price at that time.

It can be observed, based on these two circumstances, the optimization algorithm is sensitive to rapid and high magnitude changes in electricity prices.

On the other hand, Figure 5.8(a-iii-iv, b-iii-iv, c-iii-iv) illustrates the response of PCC manipulated variables, which are u_3 and u_7. The responses show that the u_3 was compensating with the u_7 in order to tracking the CO_2 capture set point (CC_{ideal}). In other words, both manipulated variables showed proactive reactions in handling unprecedented changes of the PCC plant. This performance featured the robustness of MPC scheme where at the same time can substantially enhance the efficiency and flexibility of the PCC process. It can also be observed that the reboiler heat duty decreased when maximum power plant load was imposed. This condition elucidates that less steam is provided to the stripper column of PCC plant due to more steam use in the power plant to generate more electricity. This inverse correlation between the power plant load and reboiler heat duty (steam) has been deeply explained by Van der Wijk et al. [72] in their study.

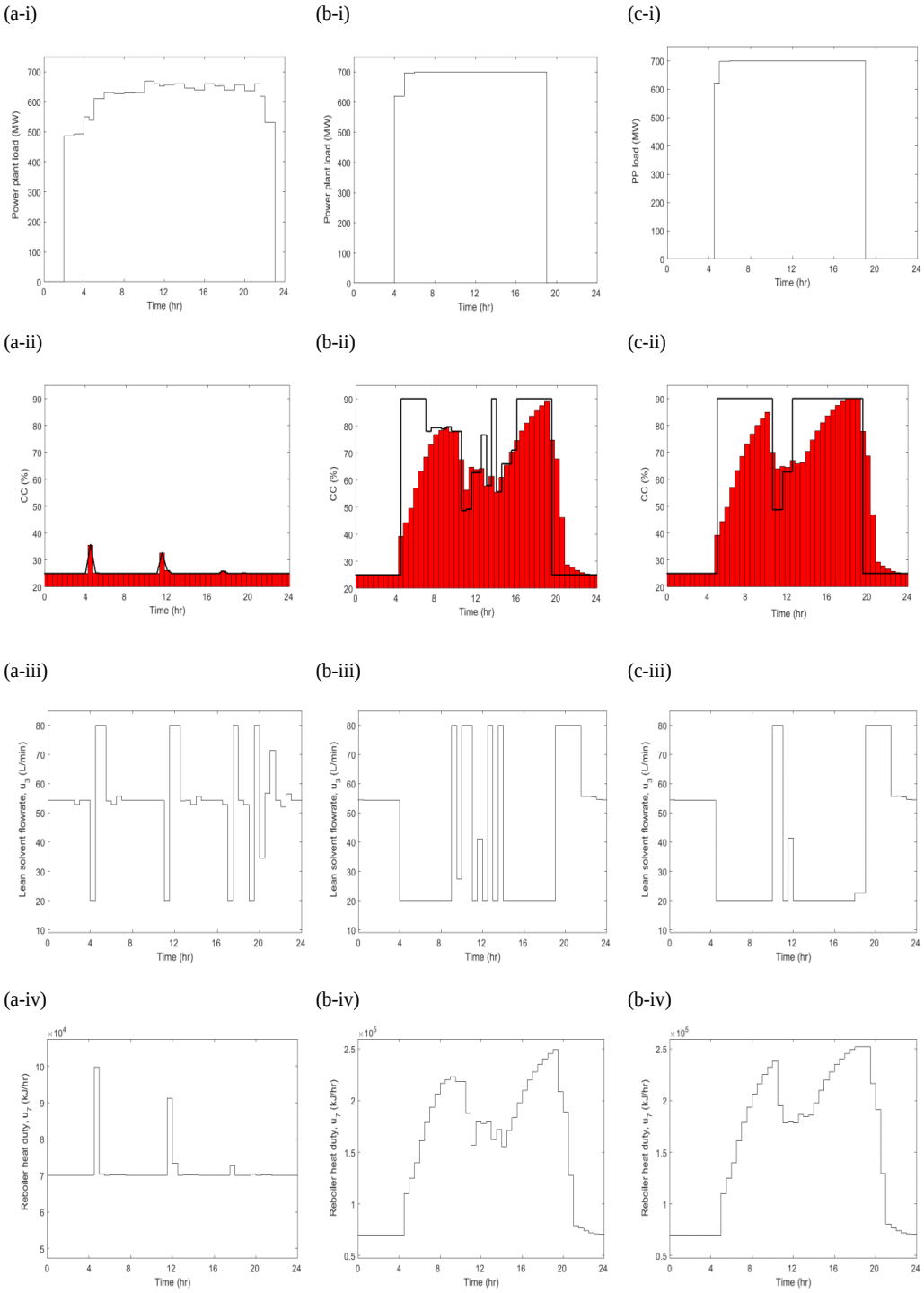

Figure 5.8: A techno-economic analysis for year 2011 at carbon price (a) \$AUD 5/tonne-CO_2 (b) \$AUD 25/tonne-CO_2 and (c) \$AUD 50/tonne-CO_2 (black line: CC_{ideal}; red bar: CC_{actual}).

5.2.1.3 Flexible operation mode: Year 2020

The forecast techno-economic analysis for year 2020 is illustrated in Figure 5.9. Figure 5.9(a-i, b-i, c-i) shows the power plant loads generated from the optimization algorithm corresponds with the optimal CO_2 capture in Figure 5.9 (a-ii, b-ii, c-ii). While, Figure 5.9(a-iii-iv, b-iii-iv, c-iii-iv) features the control algorithm responses which are u_3 and u_7. It can be seen under high carbon price ($AUD 50/tonne-$CO_2$) scenario, the optimizer has suggested to capture high percentage of CO_2 (90%) throughout the day even during high electricity prices (hours 8 - 12). Same outcome was indicated in Qadir's work [41] under same trial year (2020) when solar repowering technology was injected to the power plant associated with PCC. This is showed that in case of intermittently of solar sources and seasonal changes, the integration of power plant with PCC alone is still yet capable to capture maximum rate of CO_2. Furthermore, even at a stagnant CO_2 capture rate (90%), imposing a fix carbon rate ($AUD 50/tonne-$CO_2$) may give significant impact to the total net revenue as illustrated in the next section (Financial benefit). This is commensurate with the study conducted by [42].

Identical control performance occurred when PCC plant launched a transitory increment from low to high capture rate (hours 18 - 23) as illustrated in Figure 5.9(c-ii). Where, it took approximately 4 hours for actual CO_2 capture rate (CC_{actual}) to reach the set point (CC_{ideal}). Interestingly, this relatively longer settling time able to reduce the operational burden of PCC process, since a rapid set point tracking of CO_2 capture in response to dynamic operation of power plant entails operational distress to the process [42]. As expected, MPC performed an excellent set point tracking of CO_2 capture under carbon price rate, $AUD 50/tonne-$CO_2$ and satisfactory tracking performance at $AUD 5/tonne-$CO_2$ and $AUD 25/tonne-$CO_2$ of carbon tax respectively. These reflect by the diminutive deviation between ideal and actual total revenues generated from the

system (less than 1% error per day) as tabulated in Table 5.4 in the next section. Moreover, MPC capable to reduce the utilization of reboiler heat duty consequently minimizing the amount of energy penalty associated with the solvent regeneration.

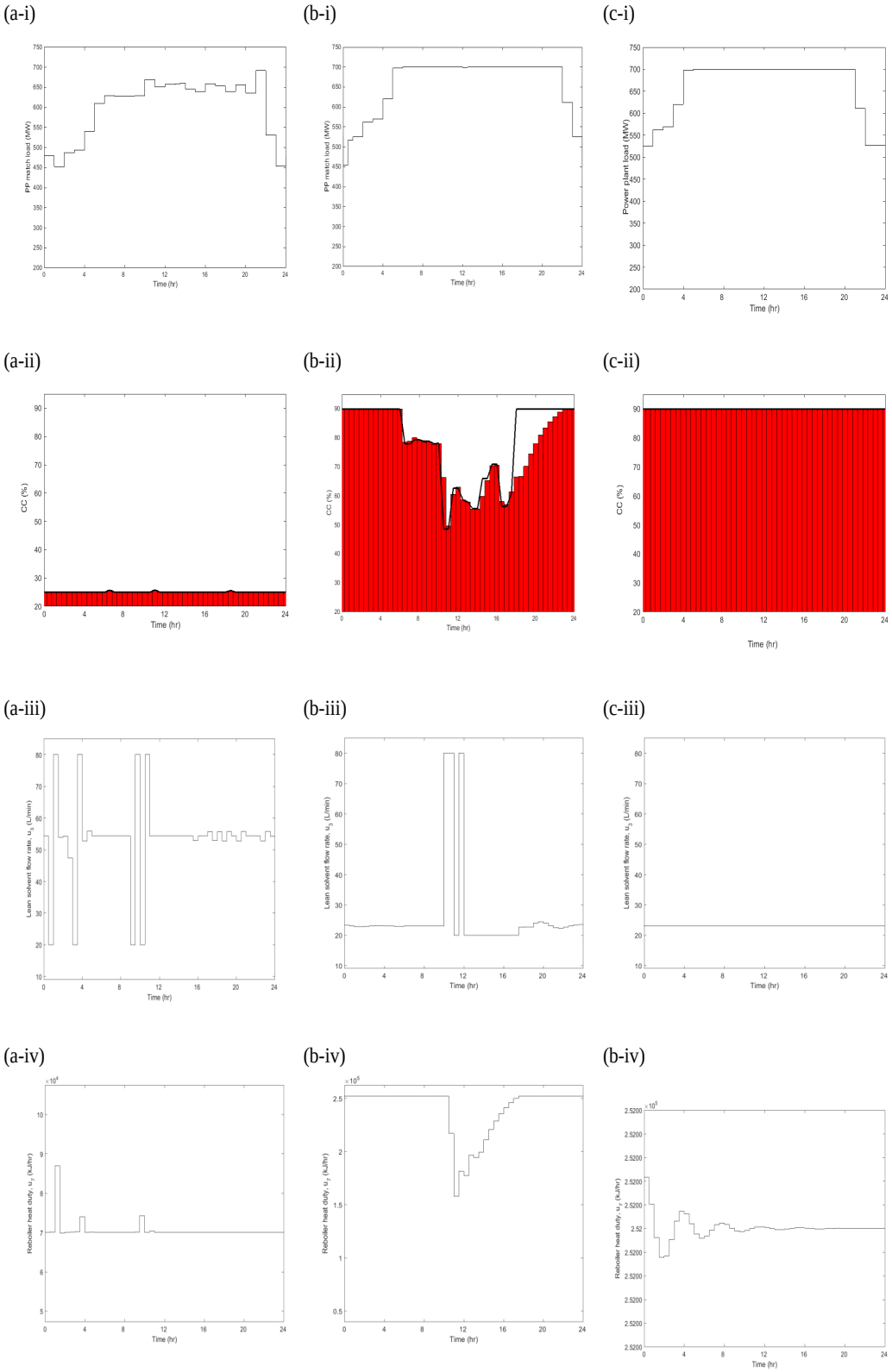

Figure 5.9: A techno-economic analysis for year 2020 at carbon price (a) $AUD 5/tonne-$CO_2$ (b) $ 25/tonne-CO_2 and (c) $AUD 50/tonne-$CO_2$ (black line: CC_{ideal}; red bar: CC_{actual}).

5.2.1.4 Financial benefit: Revenue comparison

Normalised ideal and actual total net operating revenues are illustrated in Figure 5.10. Normalising was carried out via a ratio of revenue in the range 0 to 1, by dividing revenue of each scenario by the maximum revenue among all the scenarios (fixed and flexible operation modes). Here, '1' illustrates the highest/-maximum cost incurred while '0' indicates minimum/lowest cost incurred. The key reason of this 0 to 1 scale is to provide reference to the investor/plant manager on the potential plant revenue possible when installation of PCC system is taken into consideration. Due to the extensive demand in the implementation of large-scale PCC plants (in the present and future), this scalable plant (power plant integrated with PCC system) revenue can provide a quick and practical guide-line/reference to the investor/plant manager. The right hand side of Equation 5.1 was segregated into four individual terms as given in Equation 5.6.

$$(PP+PCC)_{Rev} = A - B - C - D \tag{5.6}$$

Where A represents the plant revenue generated through selling of electricity, B is cost of CO_2 emission (carbon price paid), C and D are the power plant and PCC operational costs respectively. Table 5.4 tabulates the net operating revenue deviation for each operation mode at three different carbon prices. As expected, net operating revenue generated from fixed operation mode is much lower compared to that in flexible operation (actual) with an average difference of 7% for three different rates of carbon price for year 2011 and 2020 as illustrated in Figure 5.10.

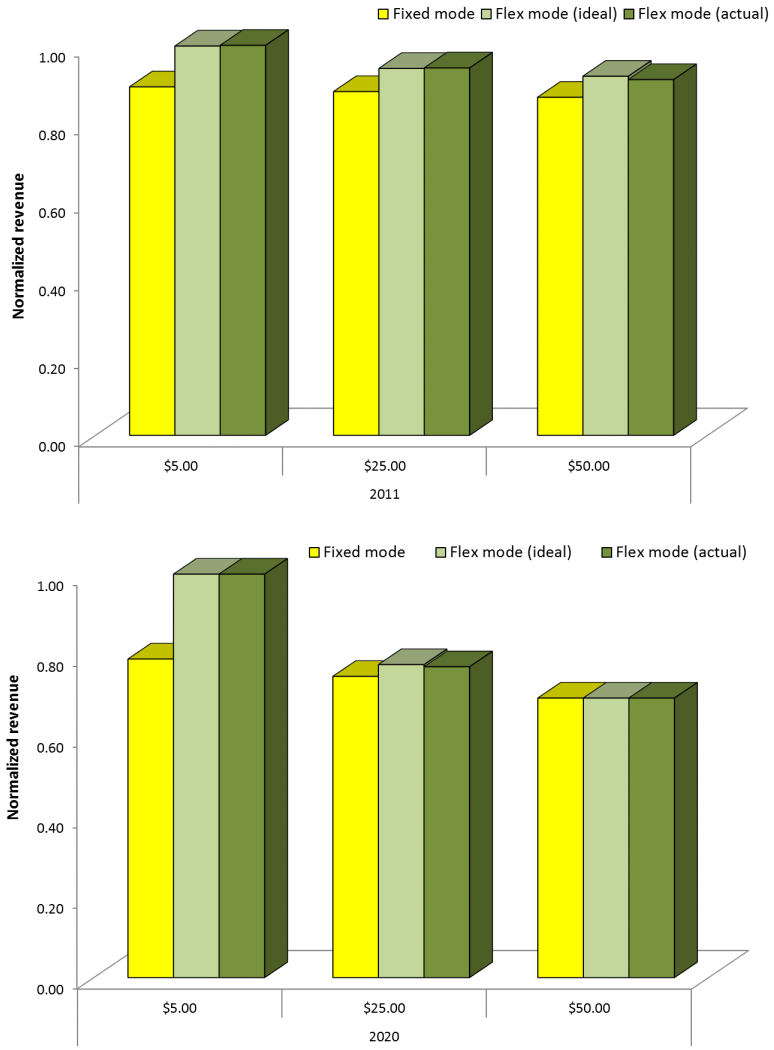

Figure 5.10: Comparison between ideal/actual net operating revenue for fixed operation mode, ideal revenue for flexible operation mode and actual revenue for flexible operation for year 2011 and 2020.

Table 5.4: Net operating revenue deviation for fixed and flexible operation (actual) modes at respective carbon prices ($AUD 5/tonne-$CO_2$, $AUD 25/tonne-$CO_2$, $AUD 50/tonne-$CO_2$).

Plant mode	Plant net operating revenue ($)		
Deviation (%)	$AUD 5/tonne-$CO_2$	$AUD 25/tonne-$CO_2$	$AUD 50/tonne-$CO_2$
2011	10.7	5.1	3.5
2020	21.0	3.1	0.0

This outcome occurs because, during fixed operation mode, when maximum capture rate is required, the PCC plant is forced to increase its operational capacity,

thus affecting the power plant operation. To clarify this result, net operating revenue breakdown is illustrated for both operation modes ($AUD 25/tonne CO_2) in year 2011 as showed in Figure 5.11. It can be seen, for fixed operation mode, a huge cost is imposed on the integrated plant due to the substantial amount of power plant and PCC operating costs (C and D), resulting in reduction of revenue for fixed operation mode. Moreover, this type of operation mode (fixed mode) can be an operational burden on the integrated plant, and thus reduce plant performance in the long term. It is anticipated that only a small total cost of CO_2 emission (B) needs to be paid for fixed operation mode compared to flexible mode.

On the other hand, the surplus revenue generation is caused by a small decrement in actual PCC operating cost, as illustrated in Figure 5.11 (for case at carbon price of $AUD 25/tonne CO_2). This surplus revenue is influenced by the flexibility of integrated plant where consequently generate optimal plant operation and optimal plant operating costs. To illustrate the impact of individual cost towards plant net operating revenue, the actual net operating revenue composite for flexible operation mode for three different carbon prices is illustrated in Figure 5.12.

5.2.2 Yearly operation analysis based on emission trading scheme (ETS)

In a yearly scenario, similar two techno-economic scenarios were developed based on the historical (year 2011) and futuristic electricity prices (year 2020). This section extends the scope of previous section by imposing real-time carbon prices (carbon-trading scheme, EU ETS) and evaluating maximum revenue for an entire year. The forgoing section focused on the development and capability of the

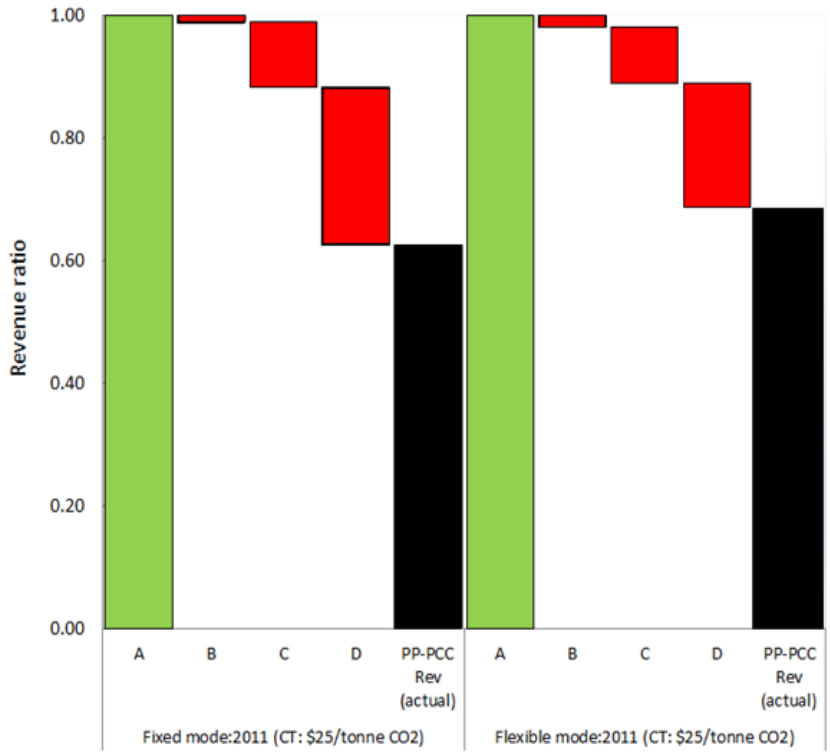

Figure 5.11: Breakdown of actual plant net operating revenue for flexible operation mode for scenario under carbon prices of $AUD 5, $AUD 25 and $AUD 50 per tonne CO_2 (A: plant revenue generated through selling of electricity, B: cost of CO_2 emission (carbon price paid), C: power plant operational cost and D: PCC operational cost).

hybrid MPC-MINLP algorithm in the operation of power plant retrofitted with PCC process with an objective function to maximize plant revenue for a 24-hour planning horizon. While, the current section presents a low-carbon management framework founded on the hybrid MPC-MINLP algorithm and employing real-time electricity load and price trends (representing Australian energy market) as well as variable carbon price trends for the duration of an entire year in 2011. This section also extends to the use forecast electricity and carbon price trends for the entire year of 2020. Significant learning is gained for the role of optimal operation of PCC processes in enhancing the efficiency of the PCC technology and in enhancing its economics towards full-scale commercial implementations.

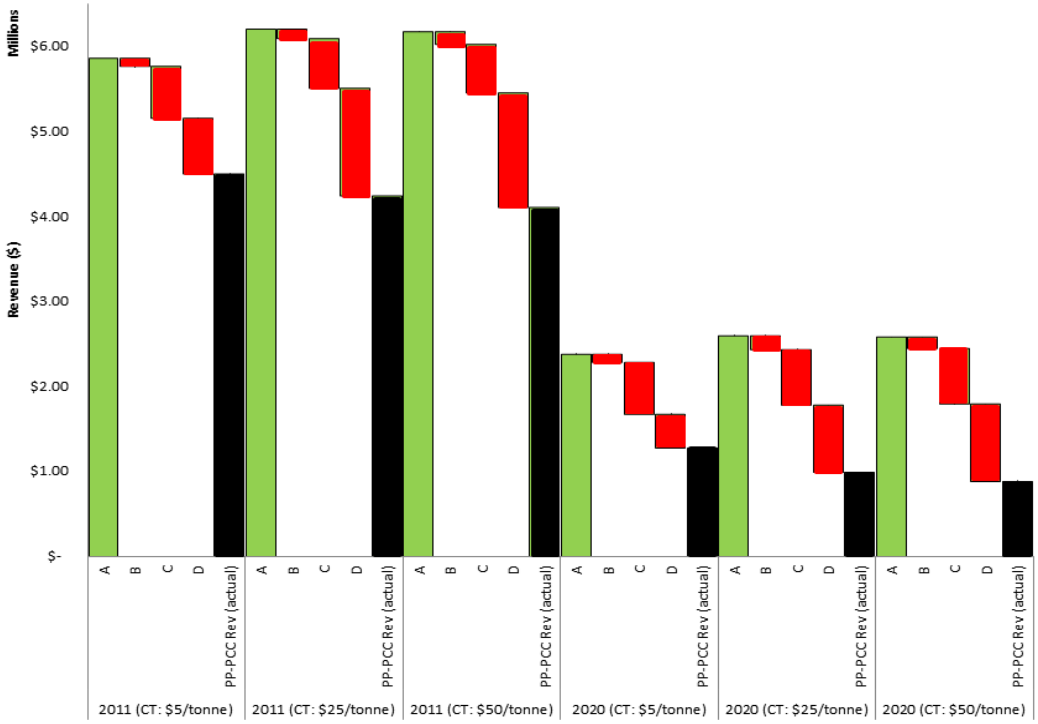

Figure 5.12: Actual revenue composite of power plant retrofitted with PCC system.

The innovative features of this work are that it offers a temporal multiscalar decision support framework critical for top-down management decision making of coal-fired power plant integrated with PCC system. Another key distinction of this analysis is that real data is used for electricity and carbon prices (for the full year 2011) based on AEMO and EU ETS data, respectively. Moreover, futuristic data (for the full duration of the year 2020) forecast based on historical profile of electricity prices and environmental stability of present level of greenhouse gas emission in Australia (Government estimates of the future carbon price).

Figure 5.13 shows the profile of electricity and carbon prices for both years. For 2011, electricity prices (RRP) were obtained from [73] for one whole year with data points for every 30 minutes. Whereas, for year 2020, the projected electricity prices were calculated by assuming 5% yearly increment from the base

year 2008 with an identical time interval as 2011. In year 2011, negative wholesale electricity prices were observed between the month of May and June. This fall occurred during the time where electricity prices in Queensland were higher than in NSW, which caused electricity to flow counter-price (flow from higher-priced region across interconnector into lower-priced region) into NSW. These counter-price flows were influenced by the disorderly bidding associated with network congestion [74].

To provide some relevance and realism to this study, carbon price trend have been adapted and extracted based on EUA historical data [75]. For year 2020, a hypothetical carbon price trend was calculated by assuming 5% yearly increment and 3% inflation rate induced yearly from the base year 2008. This estimation is based on the core policy scenario proposed by the Treasury Department, Australia [76]. Besides that, the carbon prices for 2011 were adapted and normalized from the EUA historical data. Here, we consider carbon prices as one of the significant variables in the optimization study since it can influence the profitability of power plant integrated with PCC [77].

As depicted in Figure 5.1, the first step involves execution of an optimization algorithm via a parallel computational technique. The computation time required for one scenario (one year) via parallel computations were approximately 4 - 6 days. While, the computation time required for MPC controller to perform one scenario (one year) is about one hour.

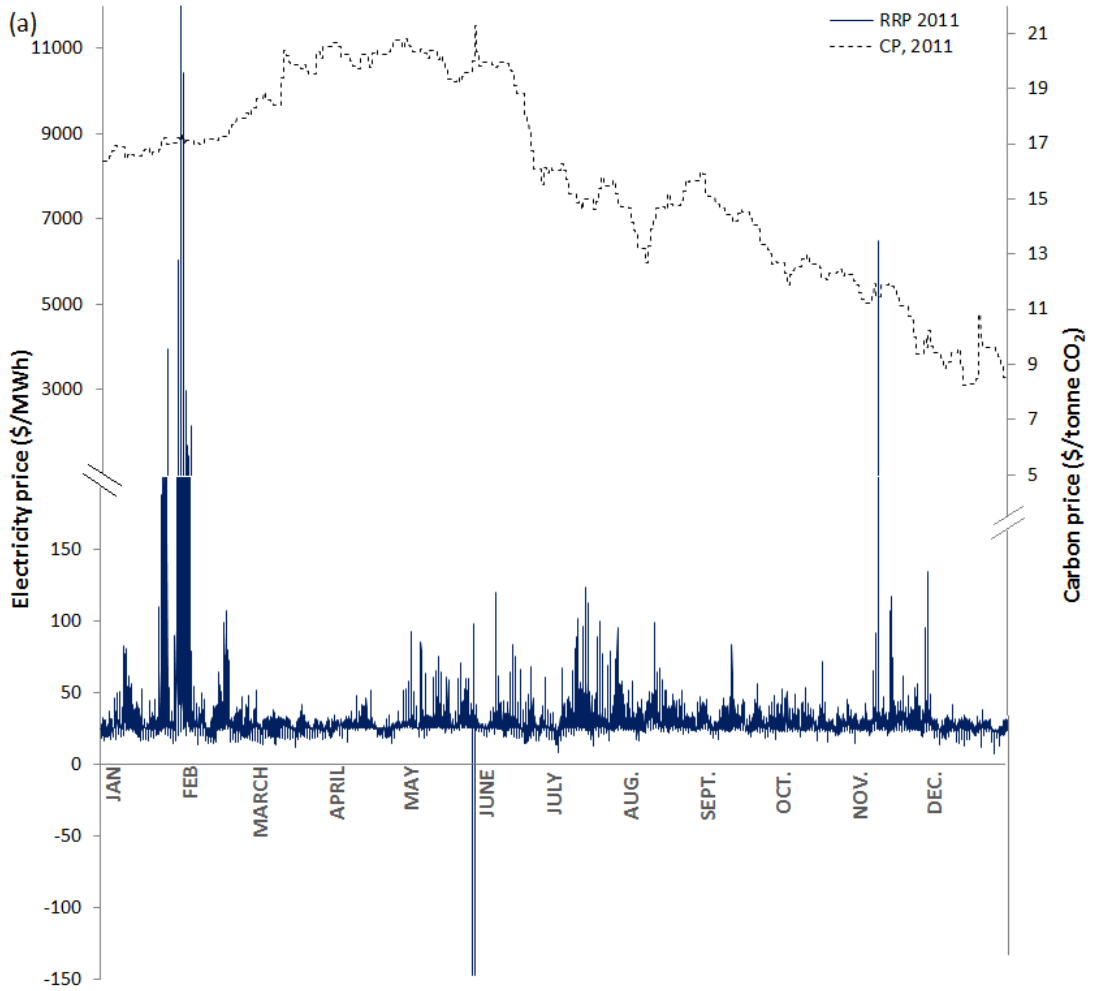
(a)
RRP 2011
CP, 2011
Electricity price ($/MWh)
Carbon price ($/tonne CO2)
11000
9000
7000
5000
3000
150
100
50
0
-50
-100
-150
21
19
17
15
13
11
9
7
5
JAN
FEB
MARCH
APRIL
MAY
JUNE
JULY
AUG.
SEPT.
OCT.
NOV.
DEC.

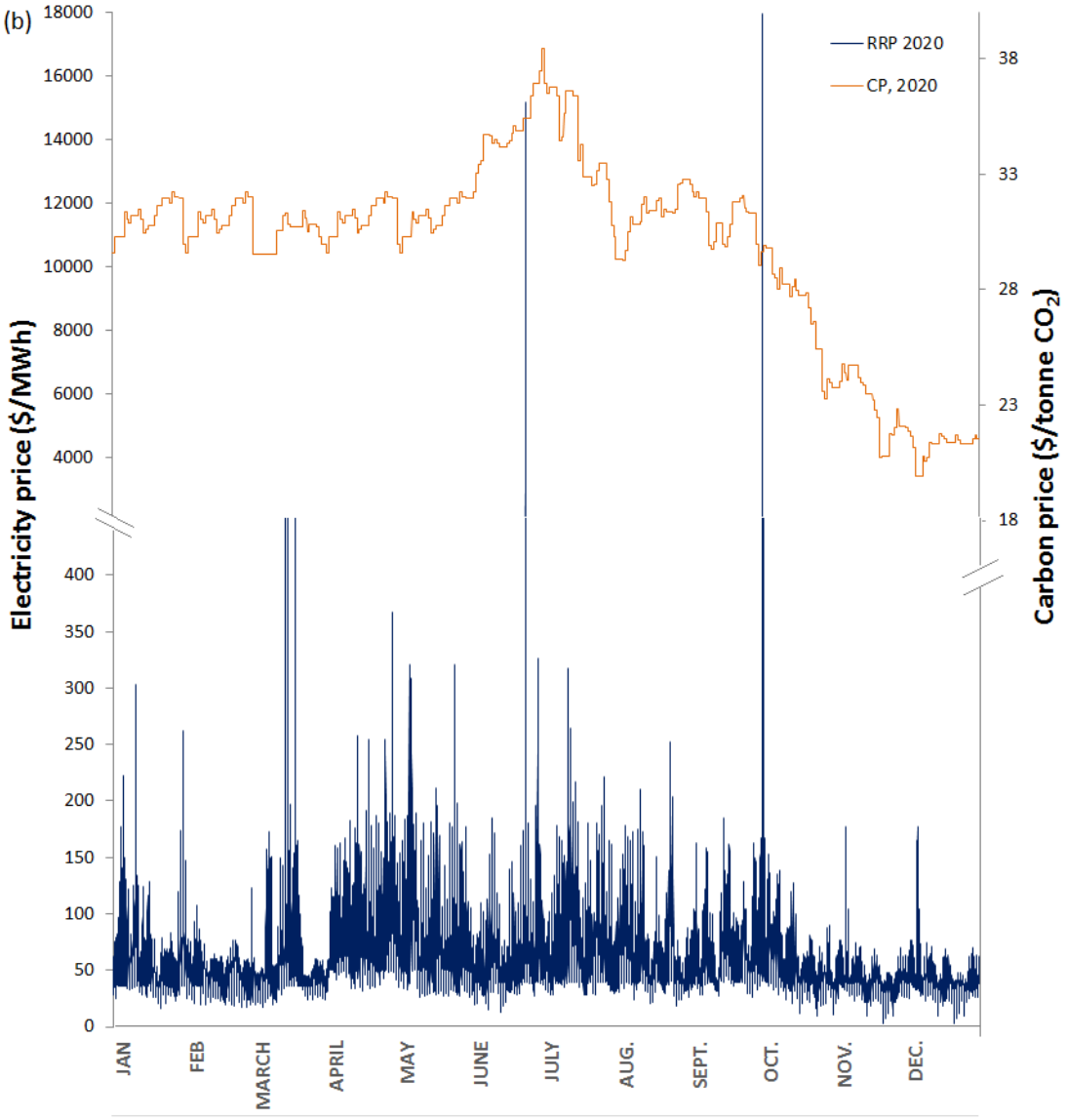

Figure 5.13: The electricity and carbon prices for one year at every 30 minute time intervals, (a) 2011 and (b) 2020.

5.2.2.1 Possible operation modes for coal-fired power plant

Integration of coal-fired power plant with PCC involves three general operating modes; load following, base load and unit turndown [78] as illustrated in Figure 5.14. The flexibility of output corresponds with the seasonal and diurnal fluctuations in electricity demand (electricity prices) and is also based on the

prevailing environmental policy regulated by the responsible authorities. Load following mode requires the ability to accommodate different ramp rates that are reflected in changes in flue gas flow rate and composition [78], while baseload is the minimum amount of energy produced (usually at constant outputs) at a low cost during all hours of the year [79]. In contrast, unit turndown occurs due to thermal transience in boiler and turbine components resulting in decrease of thermal efficiency at low load (high turndown) [79]. In this study, we consider these three operation modes based on the nameplate capacity of power plant load without considering the actual load factor exhibited by the plant for a given period. This study is more to predict plausible power plant operation modes when retrofitted with PCC plant with the objective to attain maximum plant net operating revenue and provide information for making future investment decisions.

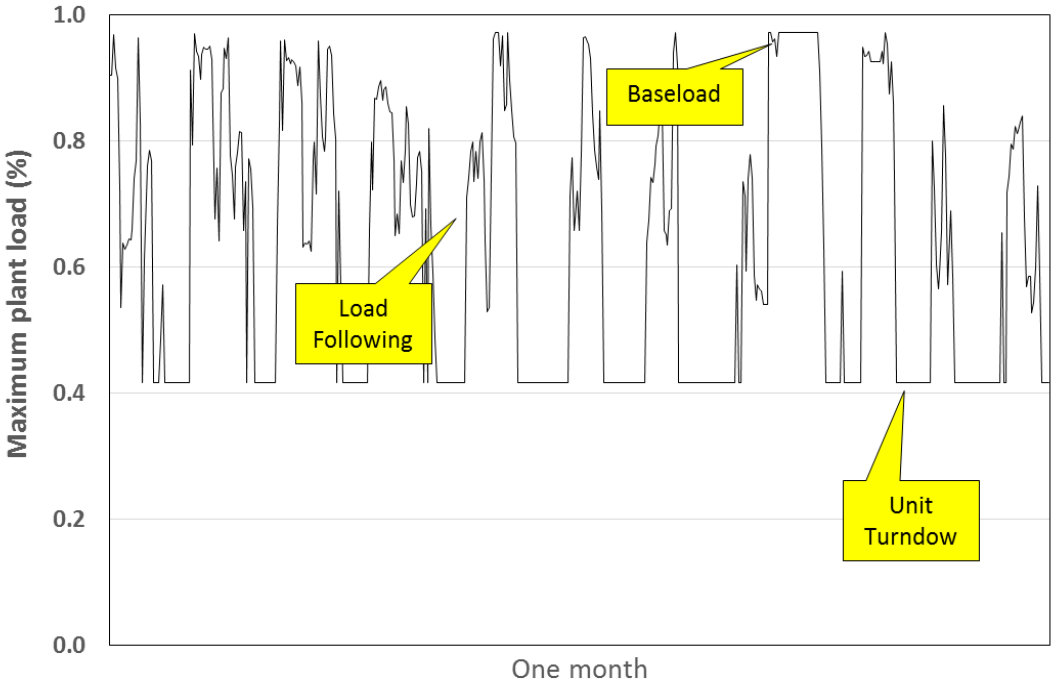

Figure 5.14: Three possible generation modes for coal-fired power plant.

5.2.2.2 Fixed operation mode: Year 2011 and 2020

Figure 5.15 shows the hybrid MPC-MINLP algorithm output for fixed operation mode for the years 2011 and 2020. Based on year 2011, the optimization output suggests power plant to operate at unit turndown in order to obtain maximum plant net operating revenue. To improve the visibility, the trend of power plant load (2011) under the prevailing electricity prices at a selected period in January were magnified as illustrated in Figure 5.16. It can be seen that unit turndowns are frequently implemented during the period of low electricity prices (low demand). Whilst, at the same time, load following mode is operated throughout the year to balance the overall annual energy production and consumption. Contrarily, for year 2020, power plant operated at irregular alternation of generation modes with chaotic dynamics (an abrupt change) of unit turndown and load following in order to attain maximum plant net operating revenue. Apparently, in both years, periodic plant shutdowns for maintenance execution were proposed by the optimizer to imitate/match with the actual operation of coal-fired power plant based on the gross loads inputted to the algorithm.

At the control level, the output responses from the controller (u_3 and u_7) appeared to be constant throughout the planning horizon for years 2011 and 2020. Based on Figure 5.15, the black line indicates the CC_{ideal} which was calculated from the optimization algorithm (at enterprise level), while the red bar is the actual CO_2 captured through responses from the MPC controller in the PCC process (at the plant level). The benefit of employing MPC algorithm in terms of achieving ideal net operating revenue is explained in the next section. Since the MPC controller is capable to track the CC_{ideal} perfectly, there is no deviation in ideal and actual net operating revenues for this specific mode.

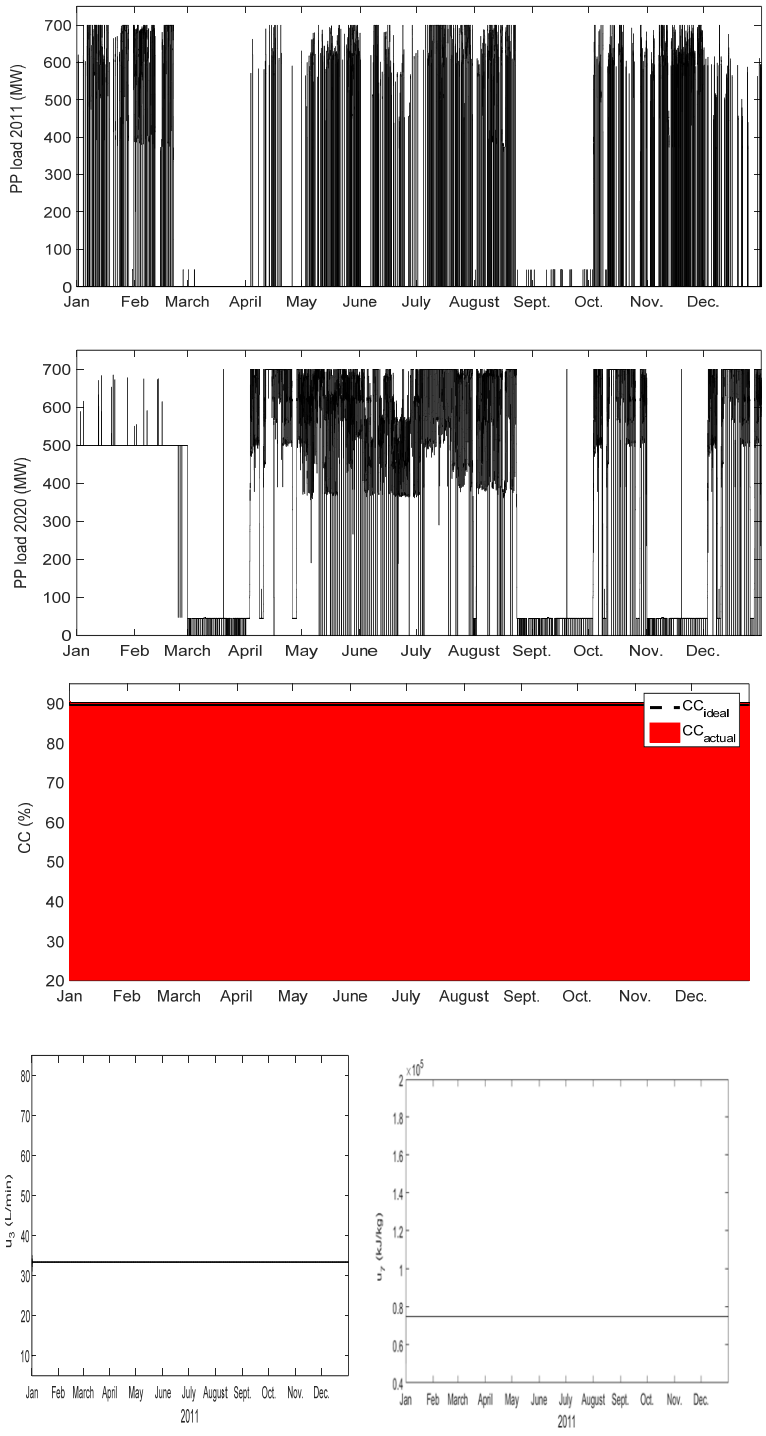

Figure 5.15: Control-optimization responses from fixed operation mode for year 2011 and 2020.

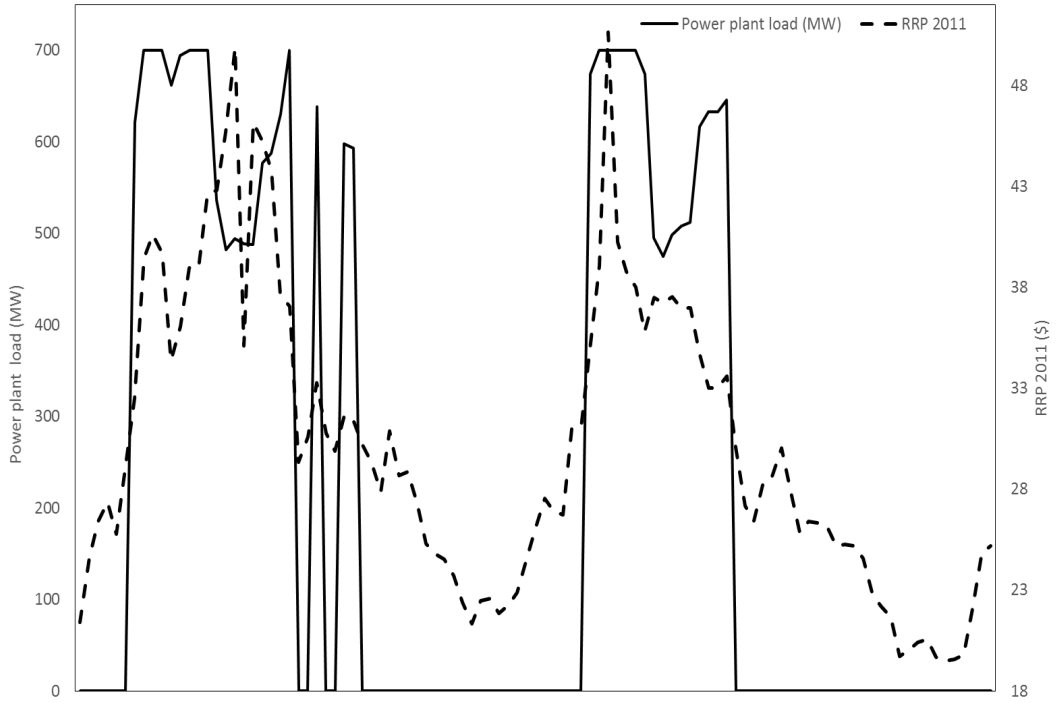

Figure 5.16: Unit turndown operation of power plant for year 2011 at selected period in January.

5.2.2.3 Flexible operation mode: Year 2011

Figure 5.17 shows results obtained with hybrid MPC-MINLP algorithm. Figure 5.17(a-b) illustrates the power plant load and ideal CC_{ideal} generated by running the MINLP algorithm at the corresponding electricity and carbon prices. Whereas, Figure 5.17(b-d) displays the CC_{actua1}, u_3 and u_7 responses produced from the action of MPC algorithm.

As can be observed in Figure 5.17(a), the power plant operated in load following for a high proportion of the time throughout the year. This reflects that during load following operation, power plant combined with PCC generated low cost generation corresponding to its prevailing electricity and carbon prices. The

power plant unit turndown mode is implemented as per the real power plant operation as shown in Figure 5.17(a). Short-term maintenance (shutdown) plans were observed in the months of May, June, July and December. This decision is due to the low electricity prices observed during those four months (Figure 5.13). This meant that the extended shutdown periods (March and September) imparted influence on the optimizer output as the optimizer algorithm attempted to match the actual power plant loads as per constraint equation in Table 5.2. With such a high occurrence of the mixed operation modes, it is evident that in the future, uninterrupted operation of coal-fired power plant in baseload will not be feasible and will virtually disappear from the market [78].

At the plant level, the MPC controller has shown satisfactory control performance in tracking the CC_{ideal}. It can be seen from Figure 5.17(b) that the optimizer suggests regular minimum capture rate from September to December, which is due to relatively high electricity prices. On the other hand, it can be observed that the u_3 and u_7 were compensating each other in responses to set point change of CO_2 capture rate. The responses show that the lean solvent flow rate is relatively more sensitive compared to the reboiler heat duty in its reaction to the fluctuation of CC_{ideal}. In other words, lean solvent flow rate gives a faster/ahead response than the reboiler heat duty. This performance showed that the MPC was able to reduce reboiler heat duty (economic wise) while achieving capture set point which characterize the flexibility of the PCC process. It can also be observed that the reboiler heat duty decreased when maximum power plant load was imposed. This condition elucidates that less steam is provided to the stripper column of PCC plant due to more steam use in the power plant to generate more electricity. The benefit of employing MPC algorithm in terms of achieving ideal net operating revenue is explained in the next section.

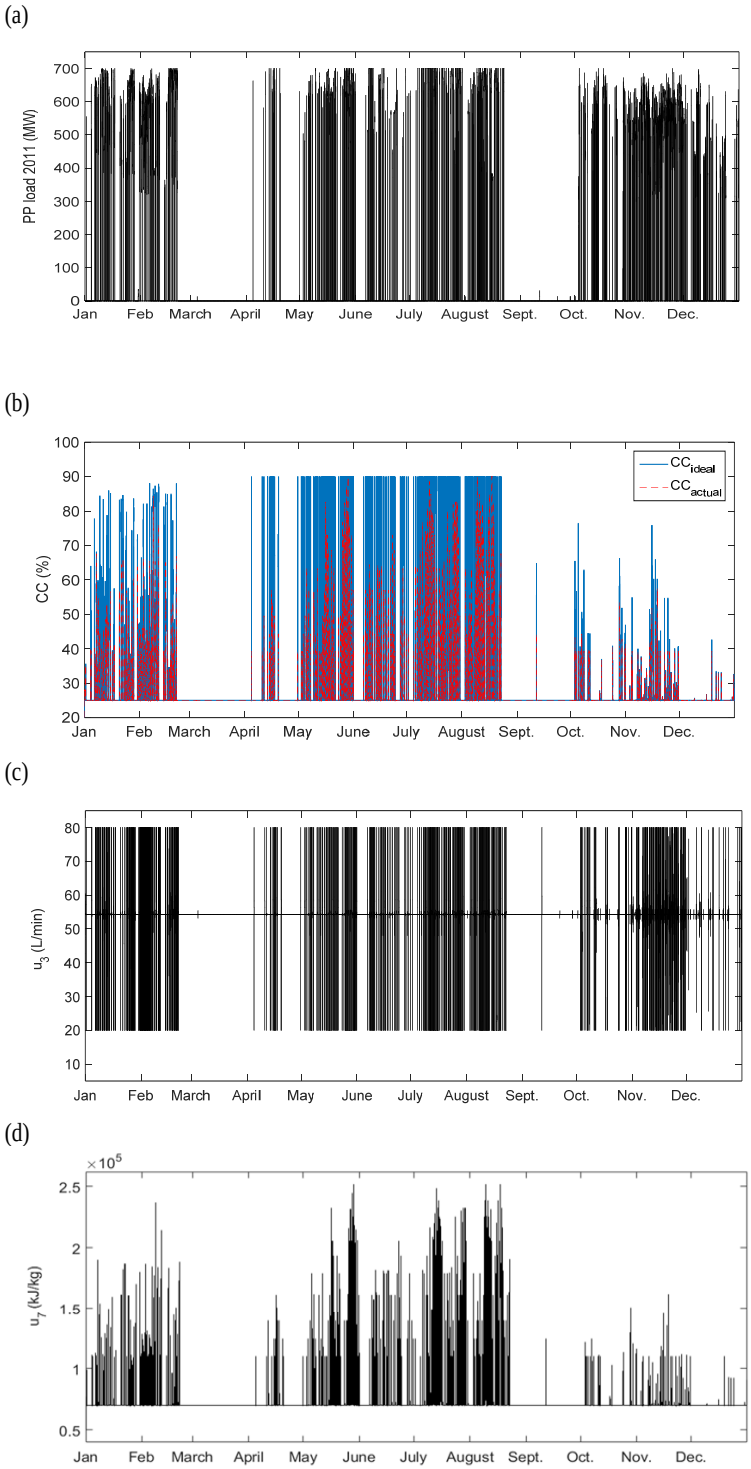

Figure 5.17: Control-optimization responses from flexible operation mode for year 2011.

5.2.2.4 Flexible operation mode: Year 2020

Baseload operation mode suggested a high proportion of the time for operation of coal-fired power plant retrofitted with PCC for year 2020 as illustrated in Figure 5.18. Where, baseload operation was run between month of January and March. Additionally, the power plant is operated in recurrent maximum load with intermittent narrow unit turndown and load following. This result is particularly relevant to power plant operation since energy systems do not all operate in the same way [77]. Moreover, these mixed operation modes of power plant in line with scheduled shutdowns are actually assisting to reduce the running cost of both power plant and PCC.

At the plant level, the MPC controller has shown satisfactory control performance in tracking the ideal CO_2 capture rate. It can be observed that there are slight deviations at the time when PCC plant launched a transitory increment as illustrated in Figure 5.18(b). This is explained by the fact that the reaction in amine-based PCC process is not instantaneous [21] and requires a few minutes for the reaction to complete. This consequently affects the performance of CC_{actual} to track the CC_{ideal} consistently. Furthermore, the dynamic nature of PCC plant itself causes a process to take some time to attain a new steady state point [71]. For clarification, we magnified the response of power plant load and CC% as illustrated in Figure 5.19. The benefit of employing MPC algorithm in terms of plant net operating revenue is explained in the next section.

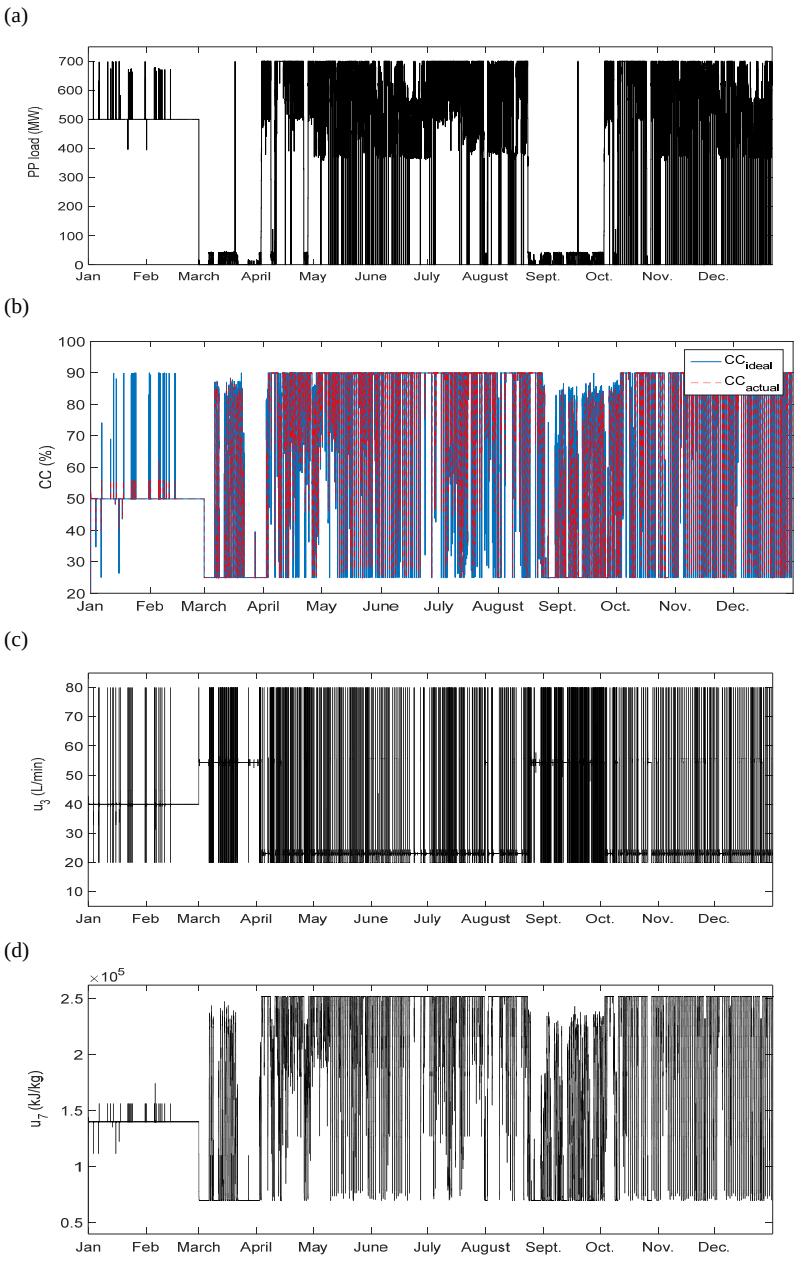

Figure 5.18: Control-optimization responses from flexible operation mode for year 2020.

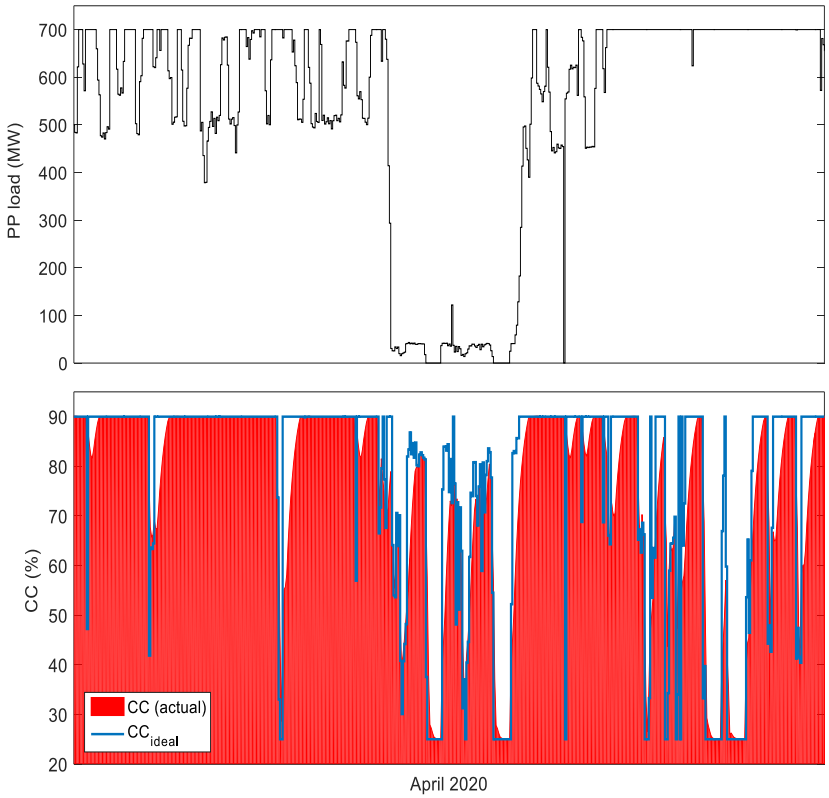

Figure 5.19: Power plant load and CO_2 capture rate for year 2020 at selected month (April).

5.2.2.5 Financial benefit: Revenue comparison

Gross revenue costs of operation and the resultant net operating revenue of the system are graphically illustrated in Figure 5.20 and Figure 5.21 for years 2011 and 2020 respectively by scaling the revenues from 0 to 1 which indicated by normalized revenue. Based on year 2011, for the year profiles, fixed operation mode incurred operation costs approximately 18% higher than the operation costs under flexible operation (actual) mode. Whereas, in year 2020, flexible operation (actual) mode attained 14% higher net operating revenue compared to fixed operation mode. The aforementioned results illustrate that the application of flexible operation mode enhances plant net operating revenue and provides significant

cost saving. This corroborates with the study conducted by [71].

In the flexible operation mode, the system subject to 2020 electricity and carbon prices generated annual net operating revenue of approximately 12% of the gross revenue. On the other hand, the system with 2011 electricity and carbon prices incurred a net operating revenue loss roughly 13% of the gross revenue. This negative net operating revenue occurred possibly because of the lower bound set for the power plant output (0 MW) and CO_2 capture rate (25%). For instance, during times of very low electricity prices (possibly even negative), the cost of operation of the power plant and PCC plant would exceed the revenue generated from selling the electricity generated. Based on this outcome, it can be perceived that the electricity prices have a significant impact on the net operating revenue generated from the integrated plant, which consequently influences the power plant loads projected from the algorithm as explained earlier. The individual cost for net operating revenue for year 2011 and 2020 under fixed and flexible operation modes are tabulated in Table 5.5.

The performance of MPC controller was evaluated based on the deviation in ideal and actual net operating revenue (controller error). According to the calculated net operating revenue (Figure 5.20 and Figure 5.21), MPC algorithm exhibited superior control performance by minimizing the controller error to an average of 4%. From the results of this study, it can be concluded that, from an operational perspective, it would be beneficial to invest in this optimization framework and its control systems which could allow for a PCC plant retrofitted to a coal-fired power plant to operate flexibly in the year 2020. Caution must be taken in making investment decisions on investing in control systems to ensure that the cost does not exceed any potential benefits of flexible operation. Contrariwise, under 2011 electricity prices, the operation costs of PCC plant retrofitted to a coal power

plant exceed the gross revenue of the power system.

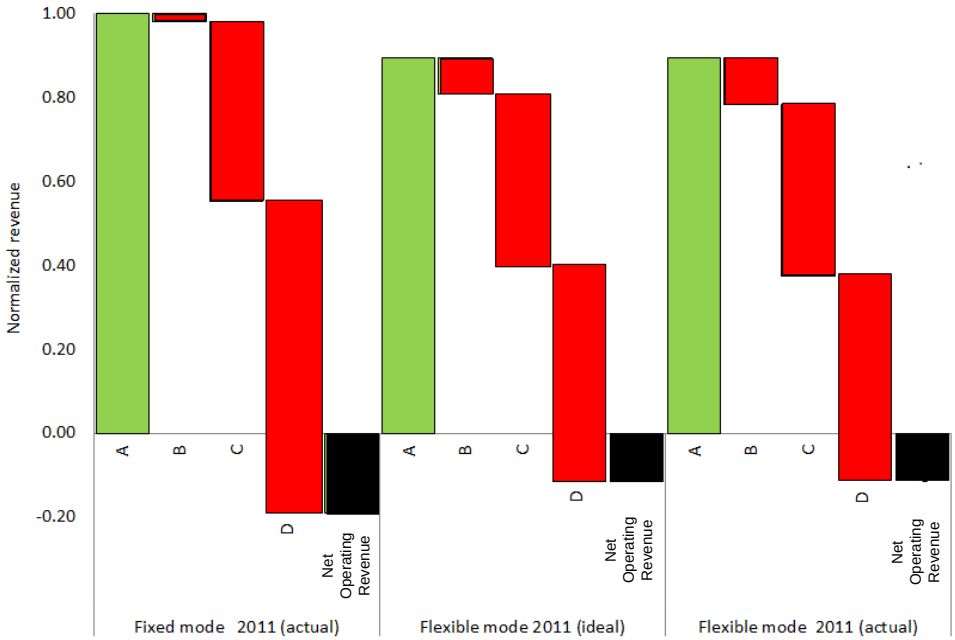

Figure 5.20: Revenue breakdown for power plant retrofitted with PCC for year 2011.

Table 5.5: Net operating revenue and its individual costs for year 2011 and 2020 subject to fixed and flexible operation modes.

	2011		2020	
	Fixed operation mode (Millions $/year)	Flexible operation mode (actual) (Millions $/year)	Fixed operation mode (Millions $/year)	Flexible operation mode (actual) (Millions $/year)
Net operating revenue	-31	-18	48	56
Gross revenue generated through selling of electricity	162	145	436	461
Cost of CO_2 emission	3	18	18	49
Power plant operational cost	70	66	156	164
PCC operational cost	120	78	214	191

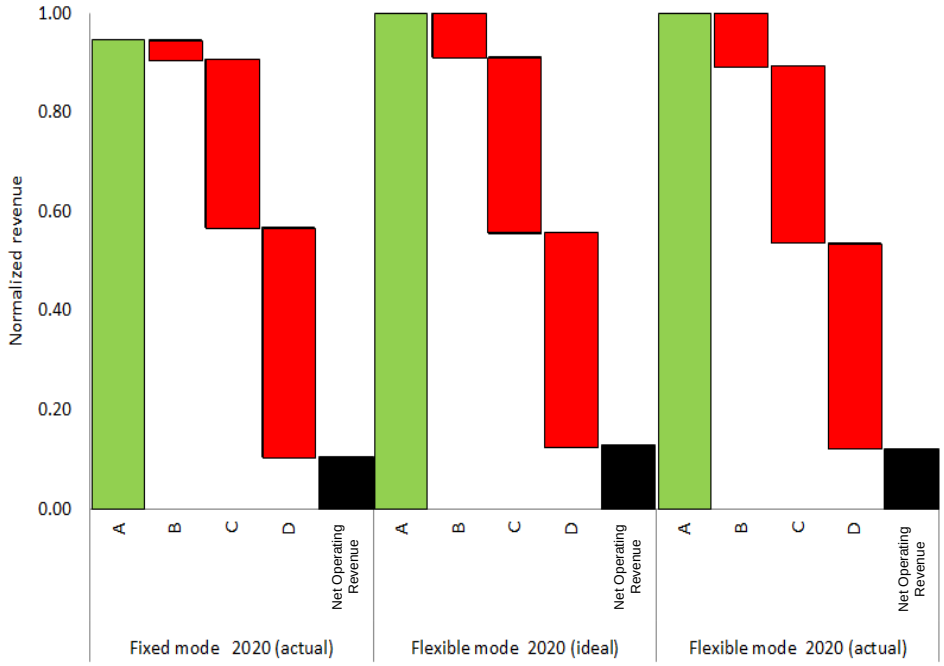

Figure 5.21: Revenue breakdown for power plant retrofitted with PCC for year 2020.

5.3 Contribution of the techno-economic analysis

The outcomes from these analyses present original contributions in the area of low-carbon management for future power plant emissions by providing a dataset/profile of power plant loads (baseload, unit turndown and load following) and $CC\%$ (which are the outputs from the developed optimization-based control algorithm) for integrated power plant with PCC facility. Where, the actual scale of PCC pilot plant has been employed for this analysis. Both data are beneficial for future insight if 'carbon capture ready' power plants are to become a reality. As such, a new 'carbon capture ready' power plant can be built and operated based on the technical data obtained from this study. For instance, modern coal-fired power plants are relatively flexible [80] and require dynamic operation modes

(traditionally only operated in baseload mode) in sensible timescale in response to external uncertainties, which include electricity prices, carbon market prices and electricity demand. Therefore, these analyses/data may serve as a baseline or reference information to the contractor, engineer and plant operator. Thus, this will shorten the design, commissioning and troubleshooting stages, concurrently increasing the technical lifetime of the plant by adapting with future economic, technological, environmental and safety concerns. Furthermore, those uncertainties provide vital impact on the power plant output and net profit, marginal cost of generation and the emission profile [78, 80]. Nevertheless, careful attention should be made for this techno-economic analysis since the exclusion of capital cost might radically change the forecast decision of the developed hybrid MPC-MINLP algorithm. As such, at high capital cost, implementation of carbon prices might not be effective for integrated plant. Consequently, it provides negative implication to the prevailing climate policy [81]. This scenario might influence the accuracy in investment decision making of PCC plant with control technology especially for countries which have different economic and political status. Whereby, high capital cost tends to be higher in rich countries compare to developing countries.

Chapter 6

Optimization strategy for large-scale deployment of PCC technology in black coal-fired power plant under ERF scheme

This chapter employs a previously developed management decision support tool (the hybrid MPC-MINLP algorithm) for a real implementation in the emission abatement activity of black coal-fired power plant in Australia. In this chapter, future operational and financial uncertainties of power plant operation under the ERF scheme are evaluated. This is performed by estimating a feasible price for a tonne of ACCU that can provide financial benefit to the power plant throughout the crediting period. This analysis accommodates economic, technical, policy and environmental aspects while indirectly offers futuristic insight in the relevance of commercial deployment of the PCC system at black coal-fired power plants in Australia.

6.1 ERF project: Integration of PCC technology into existing black coal-fired power plant

Post combustion CO_2 capture technology (PCC) is the most mature and feasible technology that can be employed by the power generation sector to reduce emissions from the existing fleet of coal-fired power plants. This chapter evaluates the feasibility of using financial support offered by policy mechanisms such as the ERF to facilitate a PCC project at a coal-fired power plant (the ERF project). The evaluation must account for multiple plant objectives while at the same time considering numerous constraints, including those emerging from the regulations associated with the funding program (i.e. the ERF). A comprehensive explanation pertaining to the ERF scheme and its project requirement has been explained in Section 1.3. However, it should be noted that additional requirement and amendment in the ERF scheme may occur with time due to the political transition and electoral changes. Thus, the ERF-related information available in this thesis may only pertinent at the time of completion this analysis. An updated information pertaining to the ERF scheme is available in [11].

As a preliminary study, a contract period (crediting period) of 7-year is demonstrated to determine the relevance of ERF policy towards black coal-fired power plant in NSW, Australia. This is analysed by predicting the financial and operational uncertainties of the proposed ERF project. The actual contract period for ERF project can be varied between 7 to 25 years depending on the project scale. However, the implementation of longer period (more than 7 years) requires substantially higher computational power (supercomputer) and thus for this specific analysis, a 7-year of planning horizon and emission baseline of 7 100 000 tonne/year are assumed to be able to replicate a minimal period of coal-fired power plant ERF project. Several assumptions have been made as below.

1. The ACCUs are valued at $AUD 50/tonne CO_2., and this value is applied whether the ACCUs are purchased by the ERF, by a business seeking to reduce its libility under the SGM or if used by the power station to acquit its own liability under the Safeguard Mechanism. This figure was obtained by conducting a breakeven analysis of plant net operating revenue using developed temporal multiscalar decision support framework (hybrid MPC-MINLP algorithm) available in Chapter 5. Scenario for year 2020 under flexible operation mode has been chosen for this breakeven analysis as shown in Figure 6.1. While the figure of $50/tonne CO_2 is significantly higher than prices seen in the first few ERF auctions [11], it is not inconsistent with the cost of some of the more expensive abatement measures that will be required if Australian is to meet its emissions reduction target [82].
2. Applying a Safeguard Meachnism baseline of 7.1 $MTCO_2$.
3. Assuming Government purchases 100% of the emission offered.

6.2 Objective and contribution

This analysis can be considered as a feasibility study for the proposed ERF project as it assesses the financial viability of the project. This analysis also explores different strategies for operating the PCC plant, and so could aid in the design of an advanced control system that manages the operation of the power plant and the PCC unit. This analysis also assess the suitability of financial instruments such as the ERF for driving the uptake of retrofitted PCC on the existing fleet of power stations.

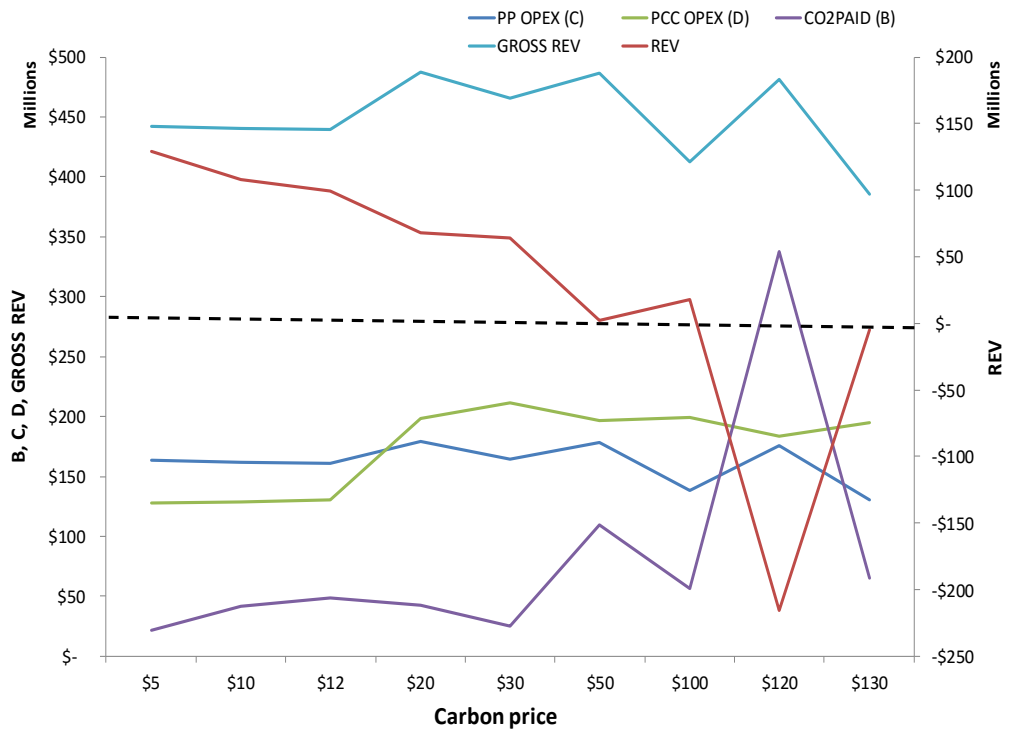

Figure 6.1: Breakeven analysis to determine the feasibility of ACCU price.

6.3 Multi-objective constrained optimization algorithm (an improved hybrid MPC-MINLP algorithm)

In this study, a multi-objective constrained optimization algorithm encompasses of a 660 MW black coal-fired power plant with PCC (integrated plant) models are simulated to determine a relevance of ERF project (PCC technology) in term of political, financial, social and environmental perspectives and the effect of climate change policy (ERF scheme) towards Australia's sustainable energy and climate neutrality. The multi-objective constrained optimization algorithm was improved and improvised to accommodate with the ERF project requirement based on the developed hybrid MPC-MINLP algorithm available in Chapter 5. Where, a new level namely policy level was linked with the prior three levels as depicted in

Figure 6.2. The description of each level is briefly explained below:

1. Policy level: To evaluate the implication of ERF scheme towards Australia emission reduction and financial outcome specifically for coal-based power generations. At this level, the environmental constraint (emission baseline) is introduced to establish a linkage between economic and emission abatement activities. Furthermore, it is imperative for technical decision-making of electricity generation. With the emission constraint, the NSW's future emissions cannot exceed the regulated emission baseline. Where, here, the future emission from coal-fired power plant cannot surpass the designated emission constraint (CO_2 emission baseline) as given in Equations 6.1 and 6.2. Both equations represent the path and end-point constraints respectively.

$$CO_2\ emitted \leq E_{baseline} \tag{6.1}$$

Where, the $E_{baseline}$ is the emission baseline (environmental constraint) for the black coal-fired power plant at each time instant/time interval.

$$\sum_{t_i=1}^{t_f} CO_2\ emitted \leq E_{baseline} \tag{6.2}$$

Where t_i is the initial time of the contract period and t_f is the final time of the contract period. While, the $E_{baseline}$ is emission baseline (environmental constraint) for the black coal-fired power plant retrofitted with PCC system over the contract period.

2. Enterprise level: To determine the optimal operation of coal-fired power plant retrofitted with PCC system under ERF scheme by considering economic benefit (maximum net operating revenue) of the integrated plant

which involves increasing the revenue of selling electricity and incentive from ERF project as delineated in Equation 6.3.

$$Max_{Revenue} = \int P_e * (Power\ plant\ net\ load - PCC\ penalty) * dt\ +\ P_{ERF} - P_{PP} - P_{PCC} \quad (6.3)$$

Subject to:

$Q_{reb}(x_1,x_2)$, $E_{Aux}(x_1,x_2)$

$x_1 = CR^I$, $x_2 = PPL^I$

$CR^{Min} < x_1 < CR^{Max}$

$PPL^{Min} < x_2 < PPL^{Max}$

$h_1\ (x_1,x_2) < 0$

$h_2\ (x_1,x_2) < 0$

Where, P_{ERF} features the incentive obtained from the emission reduction in ERF project. While, h_2 illustrates the environmental constraint (CO_2 emission from power plant does not exceed the emission baseline over the planning horizon (each time instant/contract period)) as delineated in Equations 6.1 and 6.2. Unless stated, all the parameters have similar definition as available in Table 5.2. Initial conditions optimization variable bounds for minimum and maximum power plant loads and carbon capture rates for running the power plant associated with PCC plant were taken to be:

$CR^{Min} = 5\%$

$CR^{Max} = 90\%$

$CR^I = 10\%$

$PPL^{Min} = 10$ MW

$\text{PPL}^{Max} = 700$ MW

$\text{PPL}^{I} = 200$ MW

3. Plant and instrumentation levels: To evaluate actual operation of the PCC plant embedded with advanced control strategy (MPC) retrofitted into black coal-fired power plant by considering emission reduction, saving electricity output and operational performance (capture penalty, auxiliary consumption etc.). The scope and objective of this levels are available in Chapter 5. However, taking into consideration the time of this research tenure, evaluation for this specific level cannot be pursued.

6.4 Application of multi-objective constrained optimization strategy for black coal-fired power plant ERF project

Previously, in Chapter 5, the hybrid framework was evaluated via path constraint (apply for operational constraint). Where, the optimizer was executed discretely and independently throughout the planning horizon coincided to meet the objective function (maximize net operating revenue) at each time instant. This is called single objective optimization with single constraint strategy. However, to demonstrate the actual requirement of ERF policy imposes to the black coal-fired power plant in Australia, additional constraint namely end-point constraint is introduced into the framework. The end-point constraint is applied to the environmental constraint while path constraint is enforced for operational constraint. This strategy is called multi-objective optimization with multi-constraint strategy. The multi-objective optimization refers to the revenue of selling electricity and incentive gained from the emission abatement project as delineated

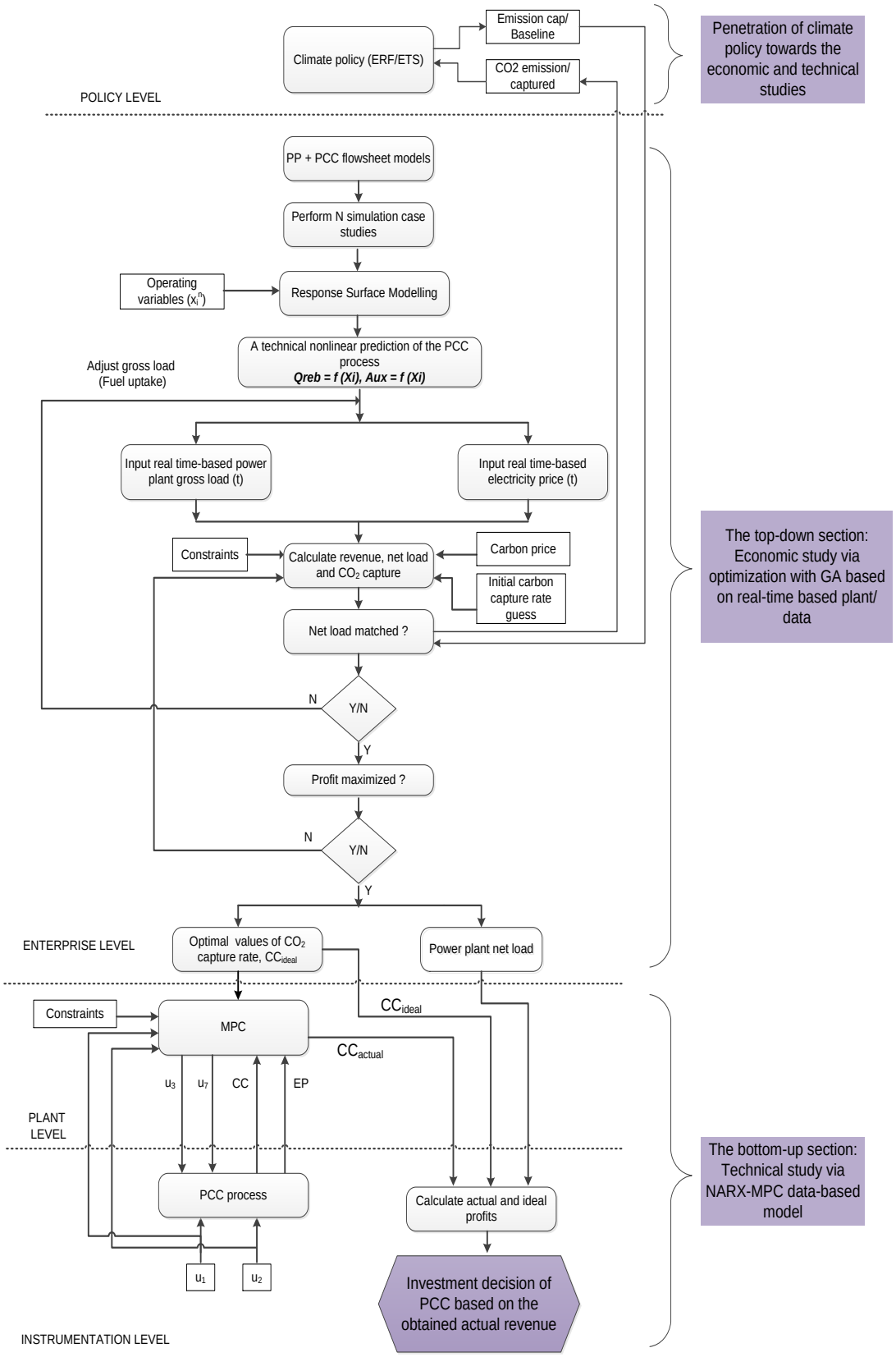

Figure 6.2: A multi-objective constrained optimization framework for the management decision-making of coal-fired power plant integrated with PCC plant under ERF scheme.

in Equation 6.3. Both terms have to be maximized in order to attain the global objective function (maximize net operating revenue). Where, the main objective function is linked with the two subsidiary optimization objectives. Contrariwise, single-objective optimization strategy demonstrated in Chapter 5 focused solely on maximizing the revenue of selling electricity as delineated in Equation 5.1.

Figure 6.3 illustrates the ideological touchstone for the black coal power generators towards economic and environmental liability in moving onto the clean energy pathway. The main challenge of the power plants is not only in technological and economic perspective alone, but rather on the managerial and organizational decisions. Where, the power generators have to ensure that it is able to deliver a perpetual and reliable supply of electricity generation coinciding to safeguard the excessive amount of CO_2 emission emitted from the electricity generation without incurred significant loss in the plant revenue. This balance requires a compromise between gaining the revenue from selling electricity and attaining incentive from the ERF project (based on the amount of emission abatement) by satisfying the corresponding constraints; operational and environmental constraints.

Fundamentally, coal-fired power plant's philosophy includes maximize revenue, generate optimal peak load and sustain the stability of power plant with minimal curtailment. While, the Government vision is to focus on the carbon emission abatement or/and maximize social welfare. Additionally, constraints (power plant load and CO_2 capture rate) are important to ensure process optimality under the presence of uncertainty. All these combined parameters were considered in this optimization problem to guarantee an accurate decision can be made to evaluate the relevance of ERF project in black coal-fired power generation.

Thus, two types of multi-objective constrained optimization strategies were de-

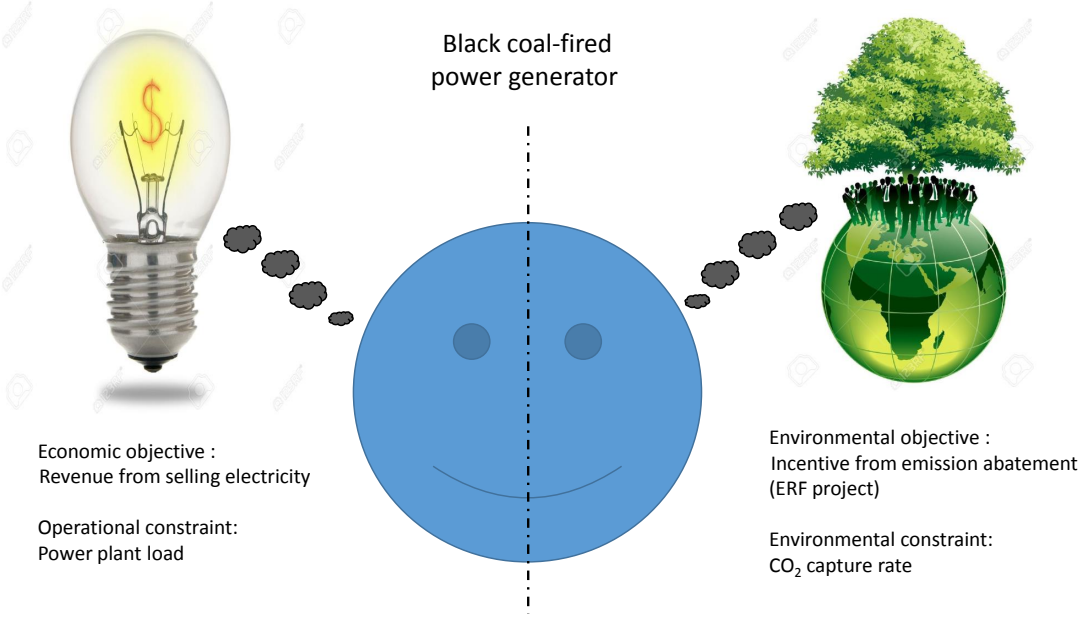

Figure 6.3: The ideological touchstone of the black coal-fired power generators considering the deployment of ERF scheme. A: Revenue from selling electricity, P_{ERF}: Incentive gained from ERF project

veloped to elucidate a scenario/dilemma faces by the black coal-fired power generators if they are about to consider the deployment of PCC technology as the ERF project as depicted in Figure 6.3. The strategies include multi-objective optimization subject to dual path constraint via using non-vectorize architecture (Strategy 1) and multi-objective optimization subject to path and end-point constraints via vectorize architecture (Strategy 2) as delineated in Table 6.1. As stated beforehand, multi-objective optimization refers to the revenue of selling electricity and incentive gains from the emission abatement. The path constraint indicates a certain restriction (CO_2 emission) that the process system (PCC plant retrofitted into power plant) must satisfy at each time instant/interval as delineated in Equation 6.1. While, the end-point constraint represents a certain restriction (total CO_2 emission) that the process system (PCC plant retrofitted

into power plant) must satisfy at the end of the planning/optimization horizon as delineated in Equation 6.2.

Table 6.1: Optimization strategies of flexible operation of PCC plant associated with black coal-fired power plant subject to ERF scheme.

Strategy	Strategy 1	Strategy 2
Objective function	Maximize net operating revenue	
Operational constraint	Path constraint	
Environmental constraint	Path constraint	End-point constraint
Optimization architecture	Non-vectorization	Vectorization
Interval time	30-minute	168-hour (weekly)
CPU time	36-hours	1-hour

In these strategies, different technique of optimization architectures (non-vectorize and vectorize) are used to imitate the ERF project requirement, which is the safeguard mechanism. In the ERF safeguard mechanism, power plants have to ensure that the total emission over the planning horizon is below than the regulated emission baseline over the crediting period. This represents by the vectorization architecture in Strategy 2. Whilst, a different hypothetical scenario from the safeguard mechanism was demonstrated in Strategy 1. Where, the power plant emissions cannot exceed the 30-minute emission baseline at each time interval over the planning horizon. This is executed via non-vectorization architecture. Essentially, the non-vectorization architecture evaluates all elements individually and independently throughout the planning horizon at each time instant/interval. While, the vectorization architecture evaluates all elements simultaneously (in a poll) throughout the planning horizon.

It should be noted that the developed optimization problems/strategies will generate many set of optimal solutions (possibly infinite) due to the nature of multi-

objective optimization algorithm. Since all the multi-objective optimization solutions are considered equally good (as vector cannot be ordered completely), thus a first simulation result was adopted and considered as the final optimal solution for this ERF project analysis [83]. Details of these two strategies and the outcomes from the simulation of multi-objective constrained optimization framework are explained in the next section.

6.4.1 Multi-objective optimization subject to dual path constraint (Strategy 1)

Strategy 1 illustrates a flexible operation of PCC plant associated with black coal-fired power plant subject to dual path constraint. These two constraints refer to operational and environmental constraints via non-vectorize optimization architecture. Where, the optimizer evaluates the input elements at each time instant/time interval in order to meet the objective function (maximize net operating revenue). In this strategy, a time interval is at every 30-minute through 7-year of planning horizon (crediting period) which consists of 122 646 x 2 of input variables (forecast electricity prices and historical power plant gross load) as illustrated in Figure 6.4. The forecast electricity prices for year 2016 to 2022 were calculated based on the projected index real retail electricity price which is 1.44 relative to based year 2009 [84], while the historical power plant gross loads were assumed to have similar yearly profile throughout the 7-year.

Operational and financial outcomes of the black coal-fired power plant ERF project are evaluated based on its financial and operational uncertainties. The operational uncertainty is illustrated by the competency of power plant to meet the energy demand and capability of PCC plant to capture CO_2 emissions to ensure the emissions from the power plant is below the ERF emission baseline

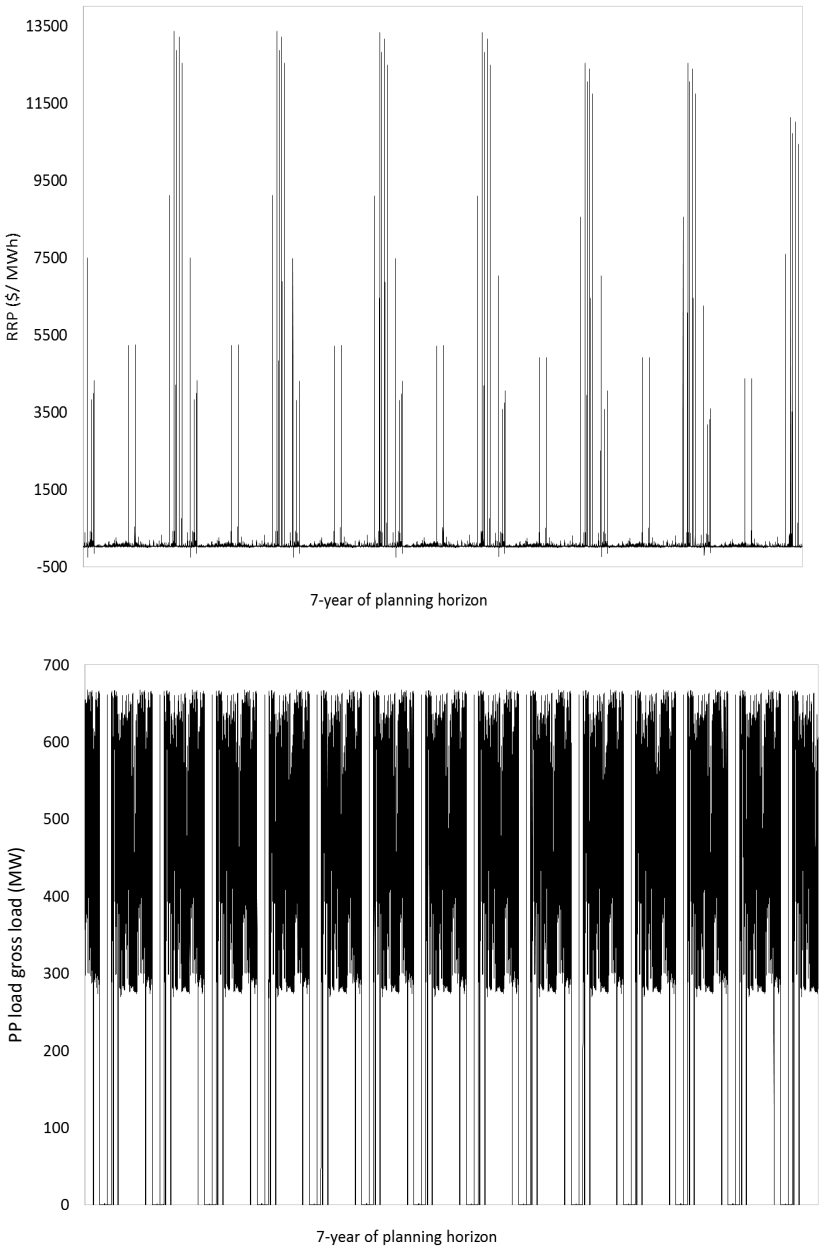

Figure 6.4: The electricity prices and historical power plant gross loads for 7-year of crediting period from 2016 to 2022 at every 30 minute.

as shown in Figure 6.6(a). While, the financial uncertainty represents by the net operating revenue generated from the deployment of ERF project as illustrated in Figure 6.8.

Figure 6.6(a) depicts the optimal solution (power plant load and CO_2 capture rate) generated from the optimization algorithm using 30-minute time interval. It can be seen, there were certain periods where the power plant load (represents the operational constraint) and CO_2 capture rate (represents the environmental constraint) performances were conflicting with each other as extracted in Figure 6.6(b). For instance, at low electricity prices, it is economically wise for power plant to operate at low load (generate low energy) while taking an advantage by enhancing the capacity of PCC plant via capturing maximum amount of CO_2 emission (90%). Where, at this time, more steam from the intermediate turbine can be provided for solvent regeneration process in the PCC system. However, based on the optimizer solution (Figure 6.6(b)), at selected period between year 2016 - 2022, power plant operated at almost maximum capacity (500 - 680 MW) coinciding capturing higher amount of CO_2 emissions (PCC plant simultaneously operated at maximum capacity).

This behaviour indicated that at certain condition when the integrated plant (power plant with PCC system) forces to meet the optimization objectives (by selling electricity and obtaining ERF incentive), the optimizer unable to determine the superiority performance between these two objectives. Concurrently, caused suboptimal trade-off between operational and environmental constraints (power plant load and CO_2 capture rate) which made both outputs to behave non sequentially. This solution underpinned with the study performed by Cristobel et al. [85], where they found that operational and environmental constraints are behaved diversely where improvement in one of the constraint can only be

achieved by compromising the other. However, the optimizer still managed to provide an optimal solution at some time instant as illustrated in Figure 6.6(a). As at high electricity prices, CO_2 was captured at low percentage coincides with a considerable increased of power plant loads in order for power plant to meet the energy demand (illustrated by the high electricity prices) and to obtain maximum net operating revenue. The result commensurate with the previous study conducted by [66, 41].

Figure 6.6 features the performance of the developed multi-objective constrained optimization algorithm in handling with the environmental constraint. It is elucidated based on the profile of CO_2 emission over the planning horizon (7-year of crediting period). It can be observed that the optimizer managed to regulate the power plant emission from exceeding the 30-minute emission baseline which is below the 57 tonne CO_2. Subsequently, limits the plant total emission below than 7 100 000 tonne CO_2. The computation time required for this analysis is approximately 36-hour.

Financial analysis of black coal-fired power plant and evaluation of ERF project is interpreted based on the plant net operating revenue. In this analysis, net operating revenue is normalized (similar normalization technique as in Chapter 5) to ease of the management decision of the power plant industries (especially black coal-fired power plants) and the Government (CER) to get a future insight of the financial reliability of the ERF project (PCC plant embedded with MPC) and feasibility of ACCU price proposed in this analysis. The financial evaluation conducted in this analysis can accommodate the extensive demand in the implementation of large-scale PCC plants in the present and future.

Calculation of net operating revenue is obtained based on Equation (6.3). It can

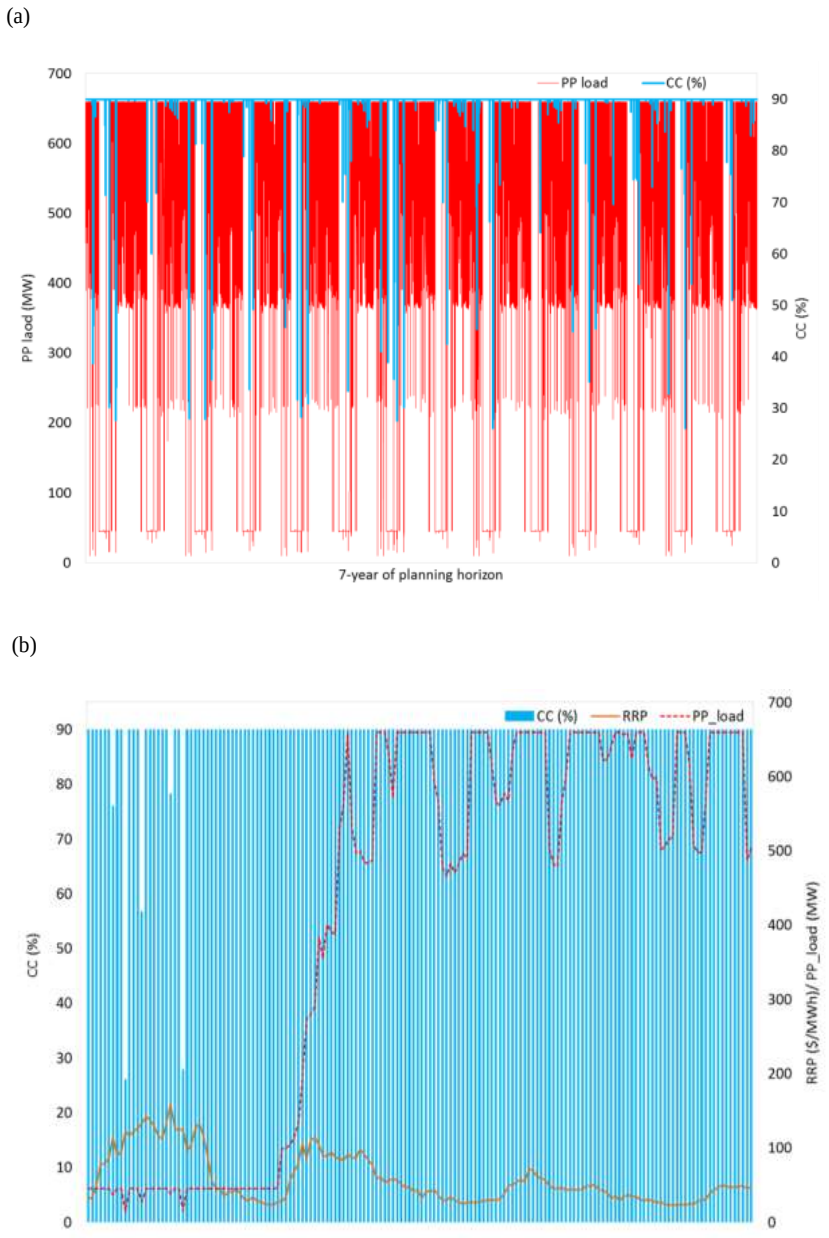

Figure 6.5: Profile of input and output variables from the multi-objective constrained optimization algorithm. (a) Multi-objective constrained optimization output responses (power plant load and CO_2 capture rate) from flexible operation mode of PCC plant retrofitted with existing black coal-fired power plant subject to ERF scheme from year 2016 to 2022. (b) Profile of electricity prices (RRP), power plant load and CO_2 capture rate at selected period from 2016 to 2022.

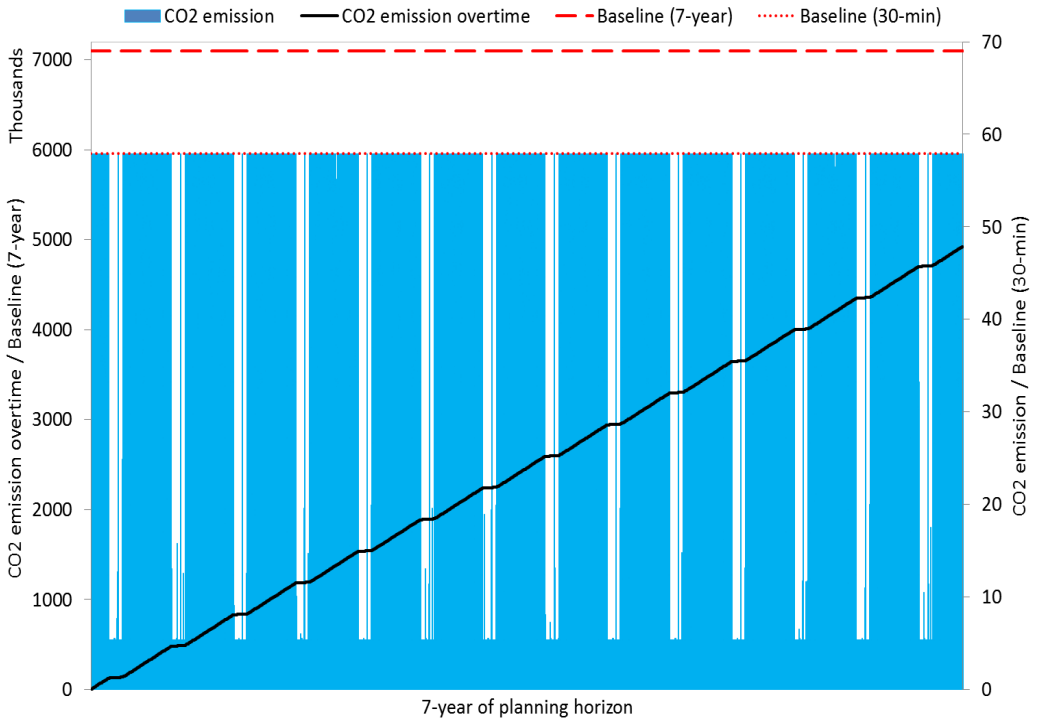

Figure 6.6: Performance of the environmental constraint via CO_2 emission over the planning horizon.

be segregated into four individual terms as given in Equation (6.4).

$$(PP+PCC)_{Rev} = A + E - C - D \tag{6.4}$$

Where A represents the plant revenue generated through selling of electricity, E is incentive obtained from the ERF project (based on the amount of CO_2 captured and ACCU price). Whilst, C and D represent the power plant and PCC operating costs respectively.

According to Figure 6.7, it is noticeable that via Strategy 1, the first objective (revenue from selling electricity) is seen to dominate the second objective which is

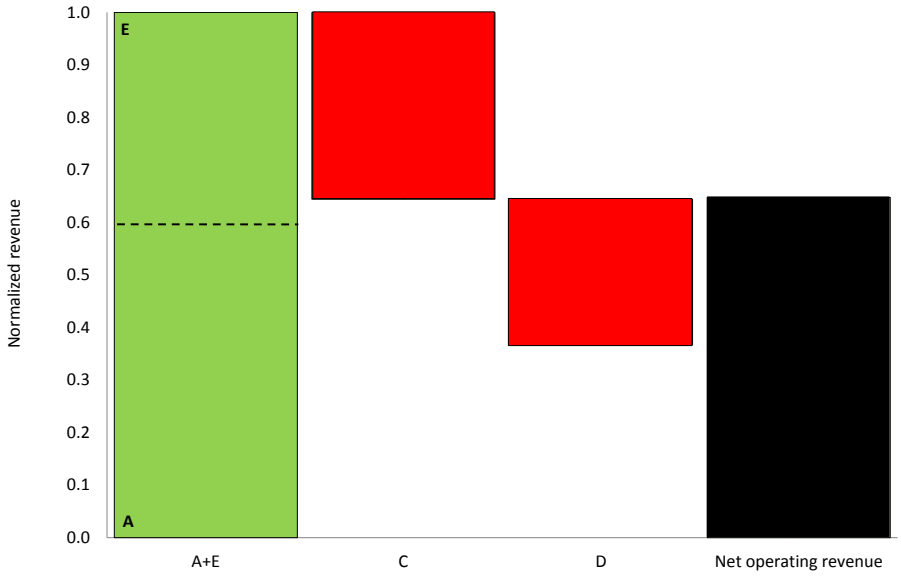

Figure 6.7: Revenue breakdown for power plant retrofitted with PCC system for 7-year of crediting period (2016 - 2022) at 30-minute time interval.

incentive from the ERF project (E). By means, the deployment of ERF project is able to added substantial profit to the power plant revenue for approximately 26% from the total net operating revenue. On the other hand, revenue from selling electricity accounted about 41% from the total net operating revenue while the rest (33%) was occupied by the power plant and PCC operating costs. The revenue obtained from this multi-objective constrained optimization strategy shows that the optimizer is capable to provide a feasible and reliable solution for the power plant management decision-making.

6.4.2 Multi-objective optimization subject to path and end-point constraints (Strategy 2)

Contrary to Strategy 1, Strategy 2 elucidates a flexible operation of PCC plant associated with black-coal fired power plant subject to path and end-point con-

straints. In this strategy, a path constraint is applied for operational constraint while the end-point constraint is enforced for environmental constraint. This strategy is executed via vectorize optimization architecture. The advantage of vectorization technique is it can reduce the computational time. However, executing the multi-objective algorithm in Matlab environment via vectorize architecture (122 646 x 2 of input variables at 30-minute time interval for 7-year of planning horizon) resulted to a large array size of 448 GB where, eventually exceeded the memory available in the Matlab system. This has caused a failure in convergence the optimization problem and led to an algorithm error as illustrated in Figure 6.8.

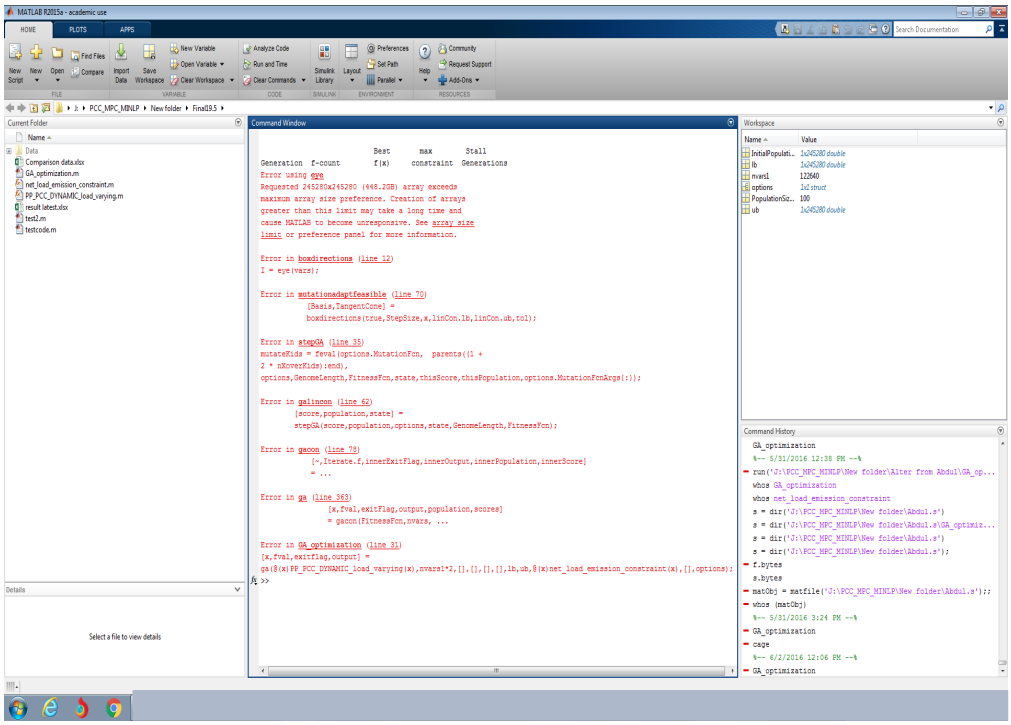

Figure 6.8: GA optimization error via vectorize optimization architecture (122 646 x 2 of input variables at 30-minute time interval for 7-year of planning horizon).

To overcome this problem, number of input variables are reduced to ensure Matlab is able to store the executed data during solving the optimization problem.

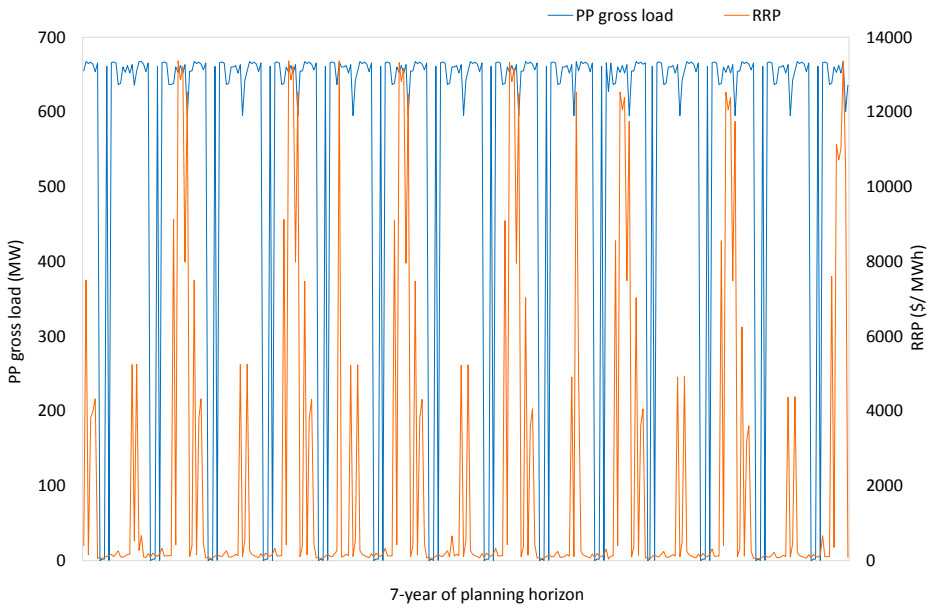

Figure 6.9: The electricity prices and historical power plant gross load for 7-year of crediting period from 2016 to 2022 at weekly time interval.

Therefore, alternatively, a longer time interval was chosen from 30-minute to 168-hour. It features a weekly time interval with similar planning horizon (7-year) and vectorization architecture. Through this condition, a 333 x 2 of input variables were generated (Figure 6.9) which based on the maximum value of weekly data extracted from the Figure 6.4.

Figure 6.10 shows the optimal solution (power plant load and CO_2 capture rate) generated from the optimizer for the black coal-fired power plant associated with PCC system under the ERF scheme using longer interval time (168-hour). It can be seen at low electricity prices (low power plant load demand), CO_2 was captured at high percentage which evident that more steam was distributed to the reboiler system for solvent regeneration process (elucidated by a lower power plant load at average 20 - 100 MW). This performance is zoomed out as illustrated in Figure 6.11 (in log scale). On the other hand, at high electricity prices, power

plant suppose to generate more energy (increase the load) and partially reduce the capacity of PCC plant in order to meet the electricity demand and gain revenue via selling the electricity. However, in this strategy, it can be observed that the average maximum power plant load throughout the crediting period is only 200 MW at most of the peak hours (high electricity prices) as illustrated in Figure 6.11. Where, at that period, the performance of power plant load and CO_2 capture rate were conflicting with each other. For instance, at period of A (high electricity prices), PCC plant is operated at its maximum capacity by capturing almost 90% of CO_2. Where practically, it is more economically wise if power plant generates more energy (selling the electricity during high electricity prices) instead of capturing more CO_2 (gaining the ERF incentive). Furthermore, this poor load forecasting performance may result in significant losses and even blackout events subsequently jeopardize the energy security system in the country [86]. This behaviour indicated that under the Strategy 2, when the optimizer has to abide the constraints (operational and environmental constraints) and meeting the objective function (maximize net operating revenue), one of the constraints might behave in a contradict way.

To improve the performance of the optimization outputs (power plant load and CO_2 capture rate), an initial condition for the optimization variable was adjusted from 200 MW to 250 and 300 MW (no changes was made for initial value of CO_2 capture rate). It can be seen, no feasible solutions (unsuccessful convergence) were found at this specific initial condition. Thus, it can be concluded that the optimal solution for Strategy 2 can only be achieved at the feasible domain by using 200 MW as the power plant initial optimization condition.

Figure 6.12 features the performance of the developed hybrid framework in handling with the environmental constraint. According to Figure 6.12, the optimizer

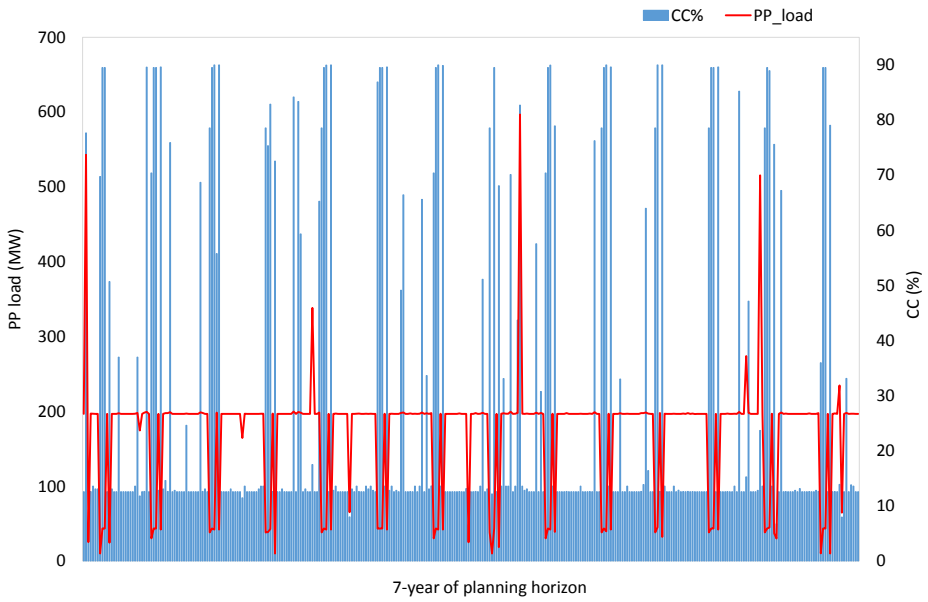

Figure 6.10: Multi-objective constrained optimization responses (power plant load and CO_2 capture rate) from flexible operation mode of PCC plant retrofitted with existing black coal-fired power plant subject to ERF scheme from year 2016 to 2022.

managed to regulate the power plant emissions from exceeding the emission baseline as required in the ERF scheme (emission baseline is 7 100 000 tonne CO_2). The spike appeared in CO_2 captured profile was due to the high power plant load generated from the power plant during that specific period as illustrated in Figure 6.10. Where, amount of CO_2 captured and CO_2 emission are strongly related to the load generation of the coal-fired power plant. The computation time required for this analysis is approximately 1-hour.

Financial analysis of black coal-fired power plant and evaluation of ERF project is interpreted based on the net operating revenue as delineated in Equation 6.4. According to Figure 6.13, it is noticeable that via Strategy 2, the second objective (E) is seen to dominate the first objective which is revenue of selling electricity (A) in order to maximize the net operating revenue of the integrated

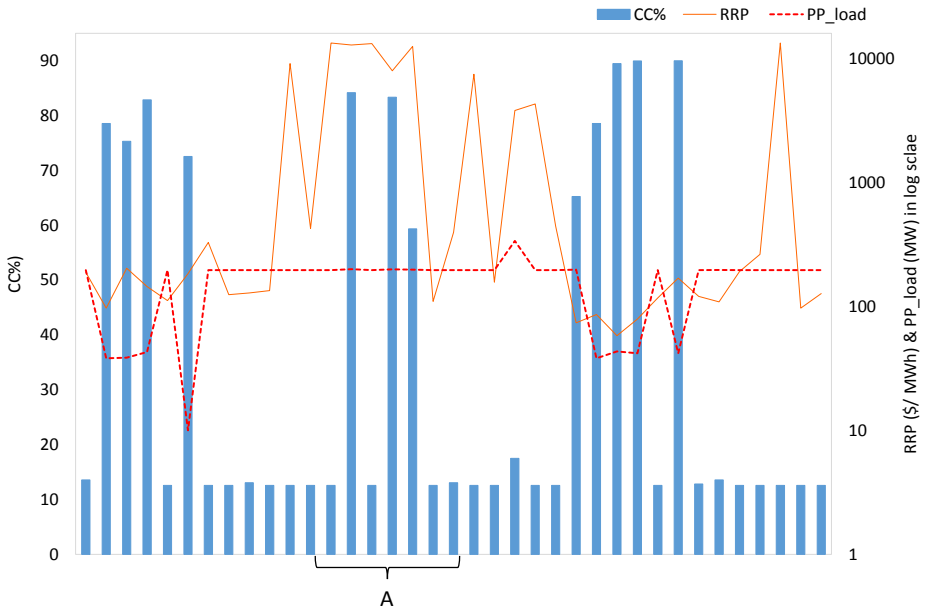

Figure 6.11: Profile of electricity prices (RRP), power plant load and CO_2 capture rate at selected period from 2016 to 2022.

plant. It is indicated that, to gain the global objective function (maximize net operating revenue), one of the other objective has to be sacrificed to obtain a feasible solution while satisfying the constraints. It is interestingly to note that even though the black-coal fired power plant able to obtain surplus revenue from the implementation of ERF project (using Strategy 2), but the conflict between economic and environmental decision-making leads to a difficulty in the deployment of ERF project. Where, it is unrealistic for coal-fired power plant to deploy PCC technology if only plant net revenue is gained from ERF incentive. This was translated in Figure 6.12 where the power plant showed poor load forecasting ability throughout the crediting period.

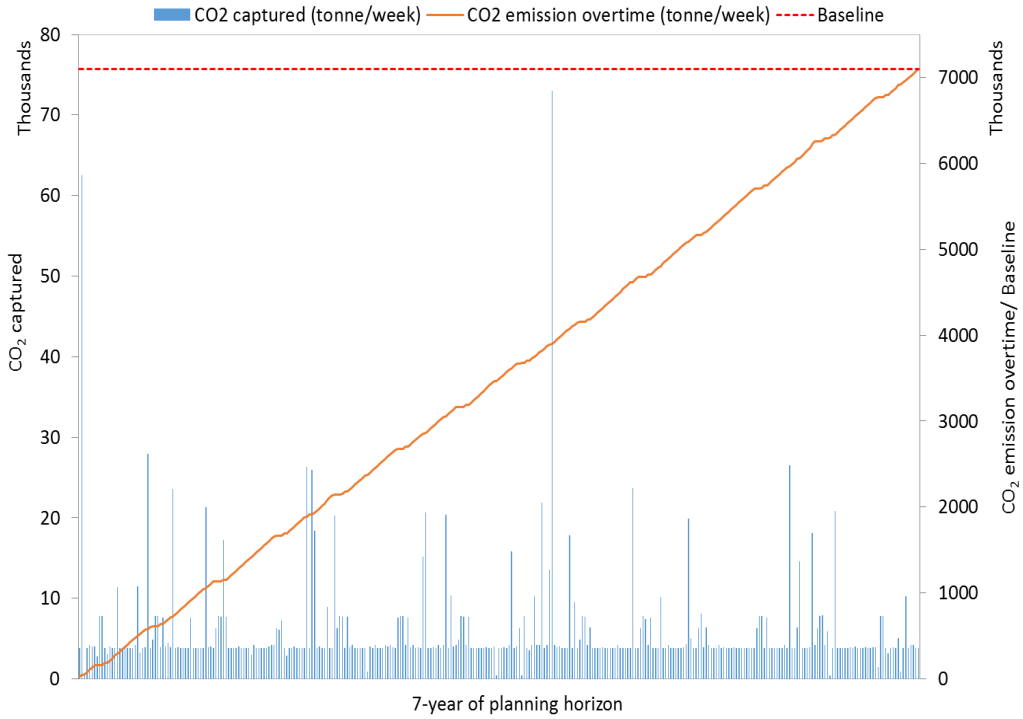

Figure 6.12: Performance of the environmental constraint via CO_2 emission over the planning horizon.

6.5 Optimization limitation of the multi-objective constrained optimization strategies

6.5.1 Resolution analysis (time interval/optimization interval)

Essentially, a smaller interval time will enhance the accuracy and resolution of the optimization solution (better objective function) and leads to larger flexibility. While, longer interval time makes the optimization solution infeasible and impair the objective function [87]. Furthermore, implementation of longer interval time contributes to a large model error since it is unable to replicate the actual physical characteristic of the developed model (refer to power plant retrofitted with PCC

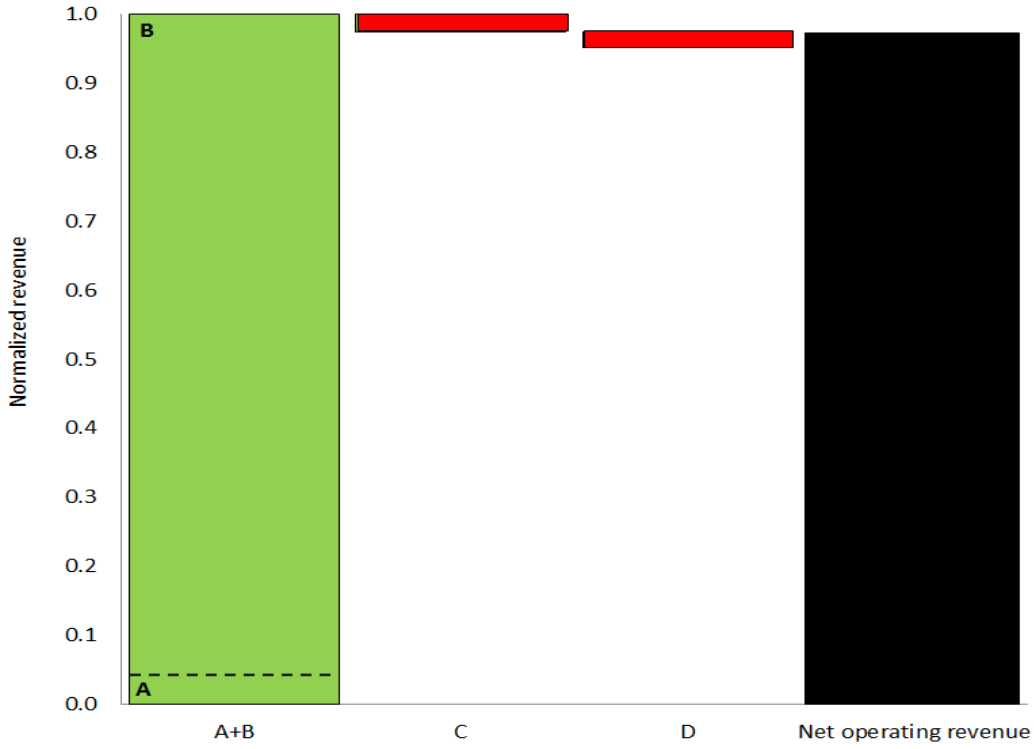

Figure 6.13: Revenue breakdown for power plant retrofitted with PCC system for 7-year of crediting period (2016-2022).

system) [87].

Due to the computational limitation of Matlab environment using GA technique, the optimization problem for 30-minute time interval via vectorization architecture (for 7-year of planning horizon) was unable to achieve an optimal feasible solution. Thus, a longer interval time (168-hour) has been used to overcome those issue as in Strategy 2. This is due to the limitation in Matlab memory to temporary store the intermediate data during execution time. Therefore, two resolution analyses were conducted to evaluate the exactitude and reliability of the optimization solutions at 30-minute and 24-hour interval time via vectorization architecture. This is to quantify the divergence of the optimization solutions based on different optimization interval/time interval.

6.5.1.1 Time interval: 30-minute

A 30-minute time interval for 7 days (1 week) of planning horizon was demonstrated for the resolution analysis with identical objective function and constraints as Strategy 2. The inputs of the optimization algorithm were extracted from Figure 6.4 (at maximum value) subject to weekly emission baseline, 91 000 tonne CO_2 via vectorization architecture. It consists of 336 x 2 of input variables as depicted in Figure 6.14.

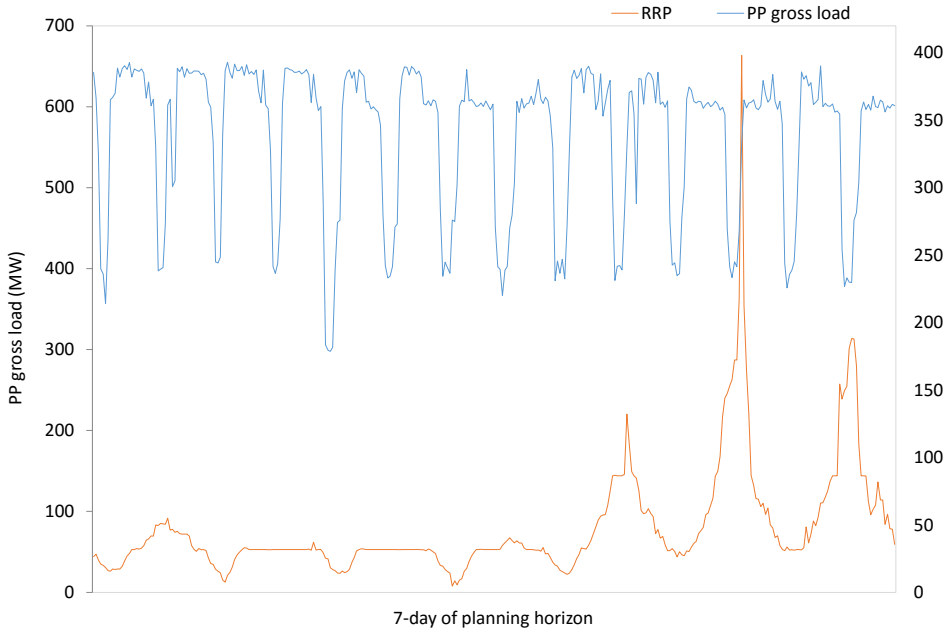

Figure 6.14: The electricity prices and historical power plant gross loads for 7-day of planning horizon at 30-minute time interval.

The outputs from the multi-objective constrained optimization algorithm are showed in Figure 6.16(a), which involve power plant load and CO_2 capture profile. It can be seen, at corresponding electricity and ACCU price ($ 50/tonne CO_2), capture rate was observed to decrease when the power plant load is in-

creased. Opposite profile was occurred when power plant operated at minimum capacity (PCC plant capacity is increased). These behaviours are comparable to the study conducted by [41, 71]. It presented a sensible proposition for the operation of coal-fired power plant integrated with PCC technology. Furthermore, power plant managed to control it emissions below the weekly emission baseline as illustrated in Figure 6.16(b).

Financial evaluation for this specific resolution analysis is depicted in Figure 6.16. It can be seen that the revenue from selling electricity is dominated the incentive gained from the ERF project. This is in favour with the black coal-fired power plant management decision on the ERF project. From the revenue breakdown, the incentive gained from the ERF project is about 22% from the total net operating revenue, while revenue from selling electricity is approximately 42% from the total net operating revenue.

6.5.1.2 Time interval: 24-hour

A 24-hour (1 day) time interval for 7 days (1 week) of planning horizon was demonstrated for the resolution analysis with identical objective function and constraints as Strategy 2. The inputs of the optimization algorithm were extracted from Figure 6.4 (at maximum value) subject to weekly emission baseline, 91 000 tonne-CO_2 via vectorization architecture. It consists of 7 x 2 of input variables as depicted in Figure 6.17.

The outputs from the multi-objective constrained optimization algorithm are showed in Figure 6.19(a), which involve power plant load and CO_2 capture profile. Similar performance as previous analysis (30-minute time interval) was forecasted for this analysis. Where, the power plant and PCC plant are operationally compromised in order to obtain maximum plant net operating revenue. On the other

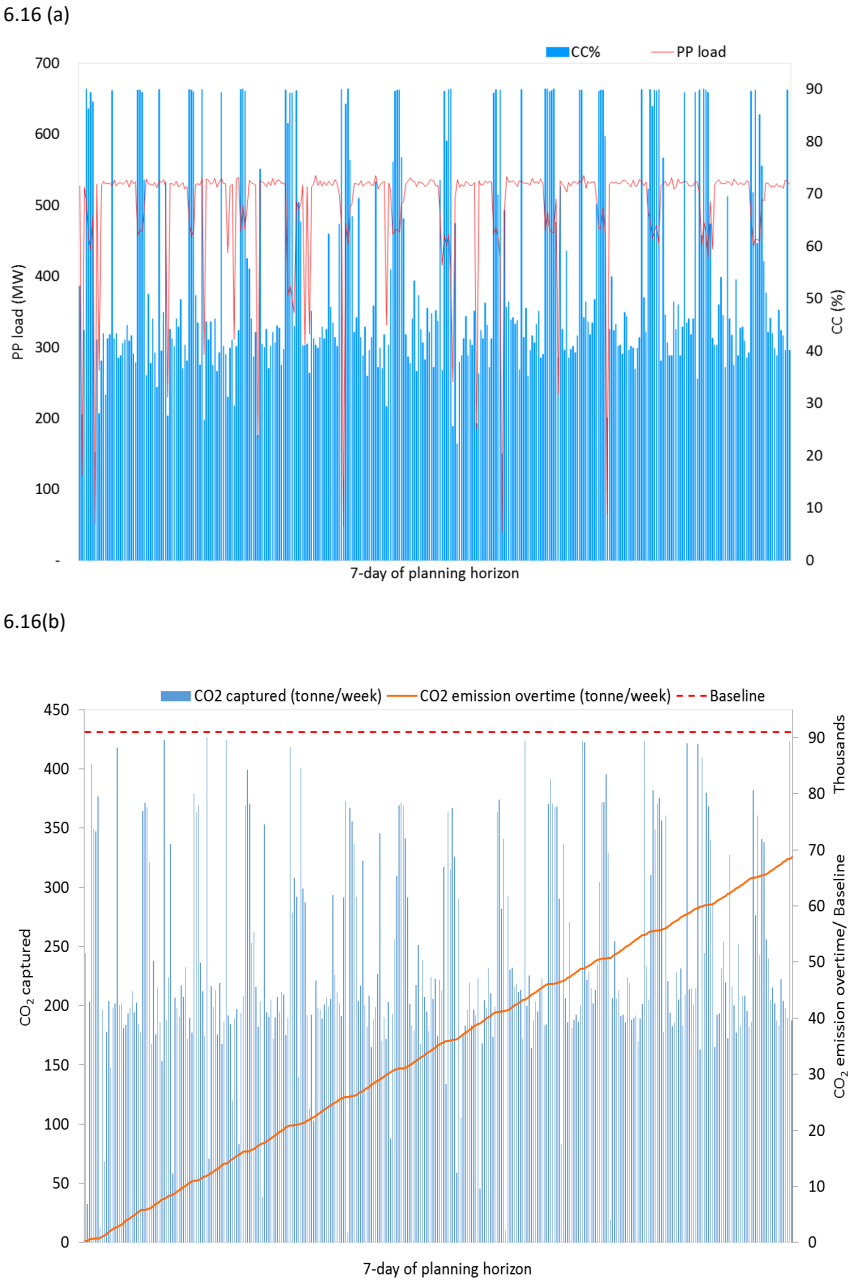

Figure 6.15: Multi-objective constrained optimization responses (power plant load and CO_2 capture rate) from flexible operation mode of PCC plant retrofitted with existing black coal-fired power plant subject to ERF scheme for 7-day of planning horizon at 30-minute time interval.

hand, the black coal-fired power plant managed to control it emissions below the weekly emission baseline as illustrated in Figure 6.19(b). The incentive gained

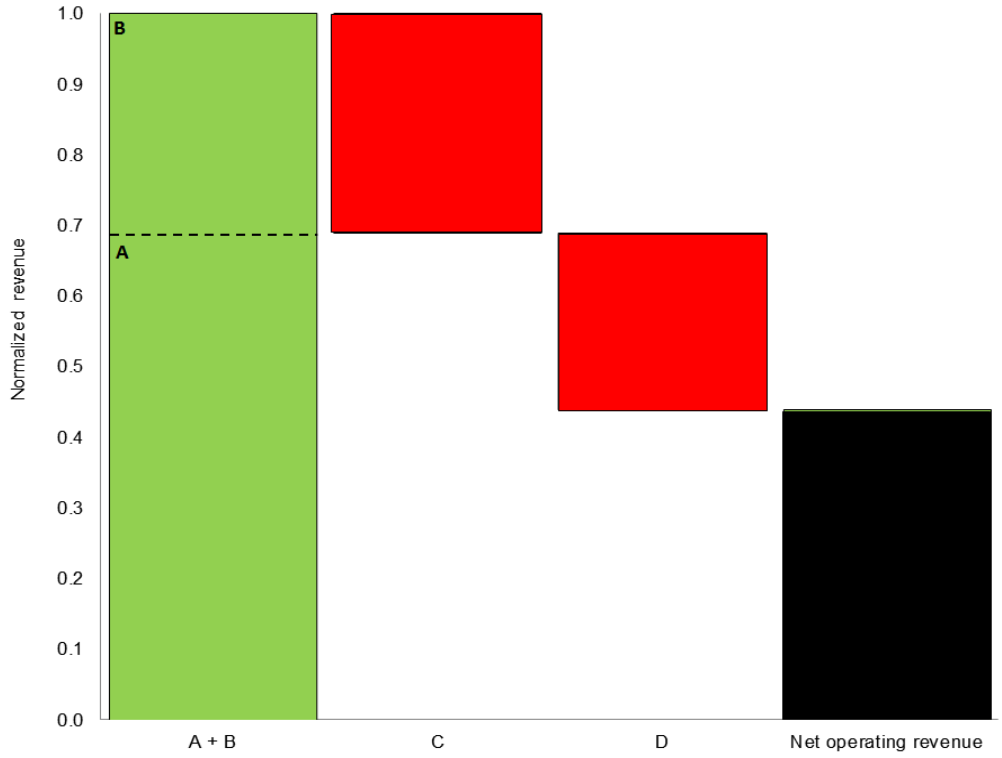

Figure 6.16: Revenue breakdown for power plant retrofitted with PCC system for 7-day of planning horizon at 30-minute time interval.

from the ERF project is about 9% while revenue from selling electricity is approximately 65% from the net operating revenue as depicted in Figure 6.19.

According to both resolution analyses, it can be concluded that an interval time plays a significant parameter for the optimization algorithm to attain a feasible optimal solution. For instance, total net operating revenue for 24-hour interval time is much more higher than the 30-minute interval time, with the percentage difference approximately 20%. Therefore, based on this outcome, it can be concluded that a longer interval time will result to a higher net operating revenue compare to a smaller interval time under identical optimization problem. Based on this ratio, the net operating revenue for 30-minute interval time for 7-year of planning horizon (122 646 x 2 of input variables via vectorization architecture) can be predicted to generate at least six times less than the net operating revenue

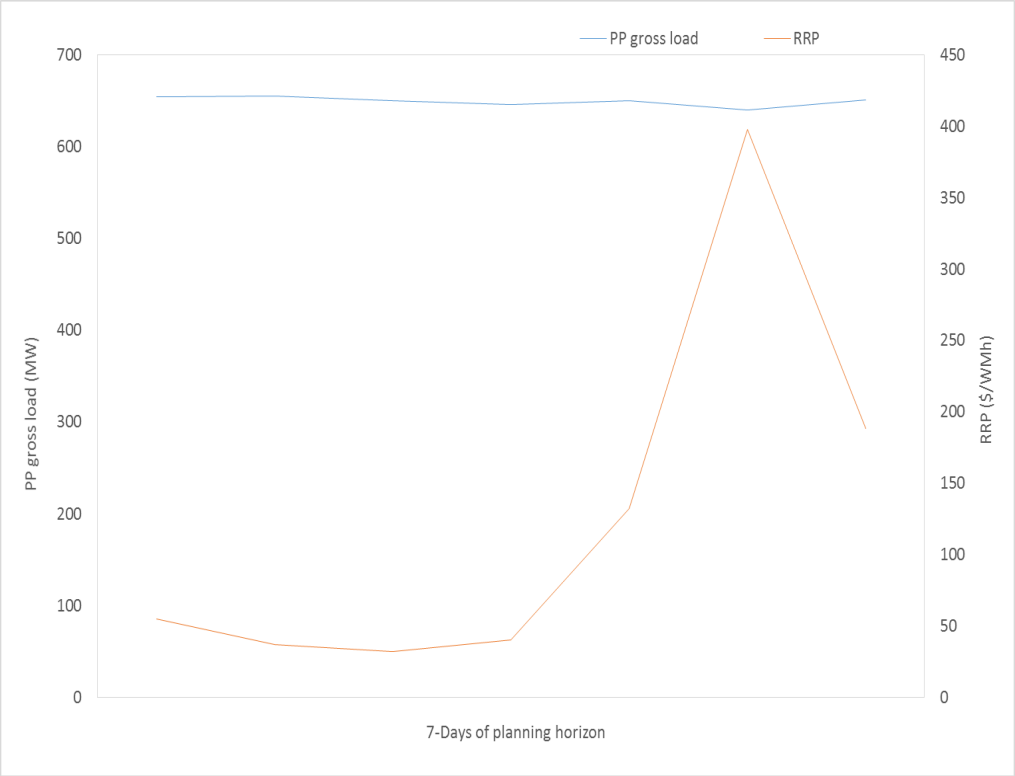

Figure 6.17: The electricity prices and historical power plant gross loads for 7-day of planning horizon at 1-hour time interval.

for Strategy 2 (333 x 2 of input variables via vectorization architecture).

6.5.2 Computational complexity: Pareto optimal solution

One of the challenges in the multi-objective constrained optimization strategies (Strategy 1 and 2) proposed in this chapter arises from the existence of different set of optimal solutions known as Pareto-optimal solutions [88]. In this analysis, Pareto-optimal solution features a trade-off between two objectives with the presence of dual constraints. Where, the optimization goal (global objective function: maximize net operating revenue) imposes a conflict between maximizing the revenue from selling electricity and raising the incentive from the ERF project (PCC technology) bounded to the corresponding constraints (operational and environmental) as illustrated in Figure 6.3. This has added computational complexity

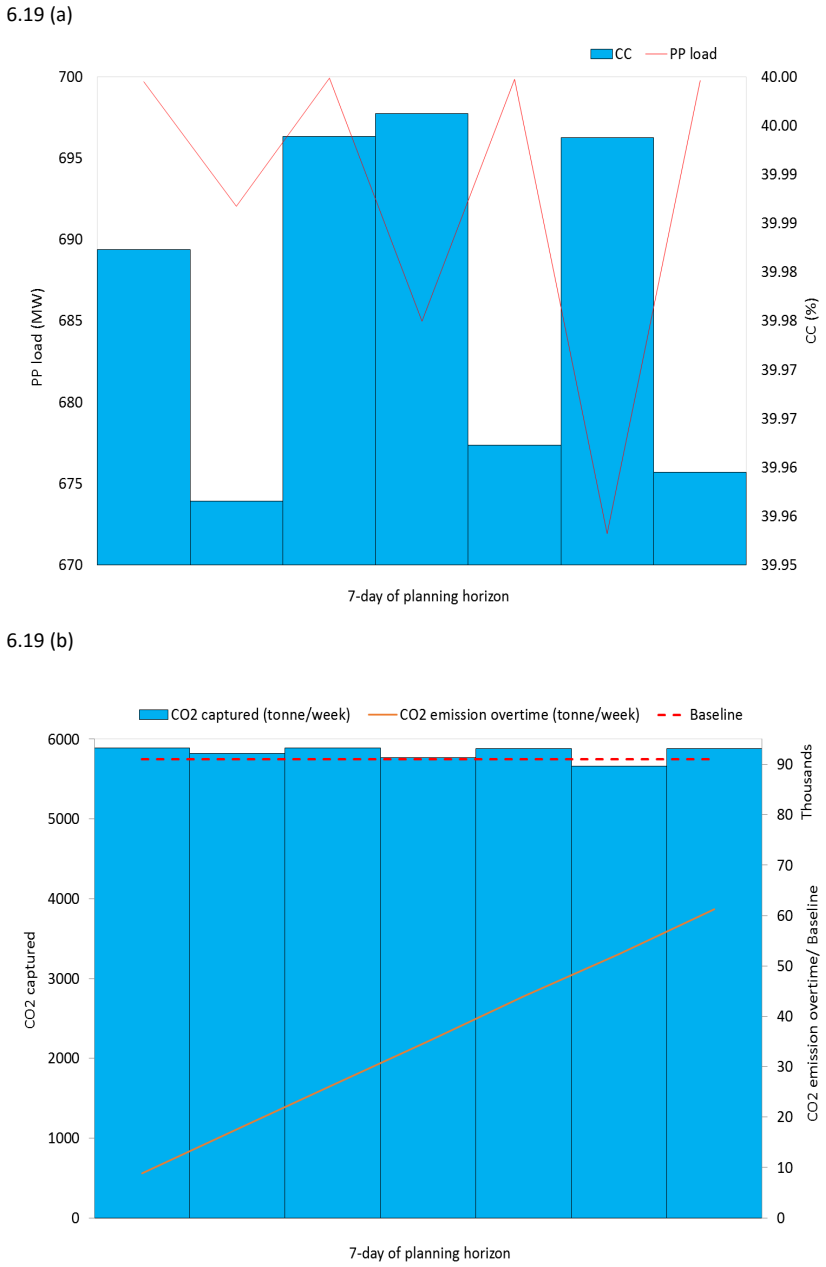

Figure 6.18: Multi-objective constrained optimization responses (power plant load and CO_2 capture rate) from flexible operation mode of PCC plant retrofitted with existing black coal-fired power plant subject to ERF scheme for 7-day of planning horizon at 1-hour time interval.

in solving the optimization problem, thus requires sensible decision-making philosophy from the operational and financial perspectives of black coal-fired power

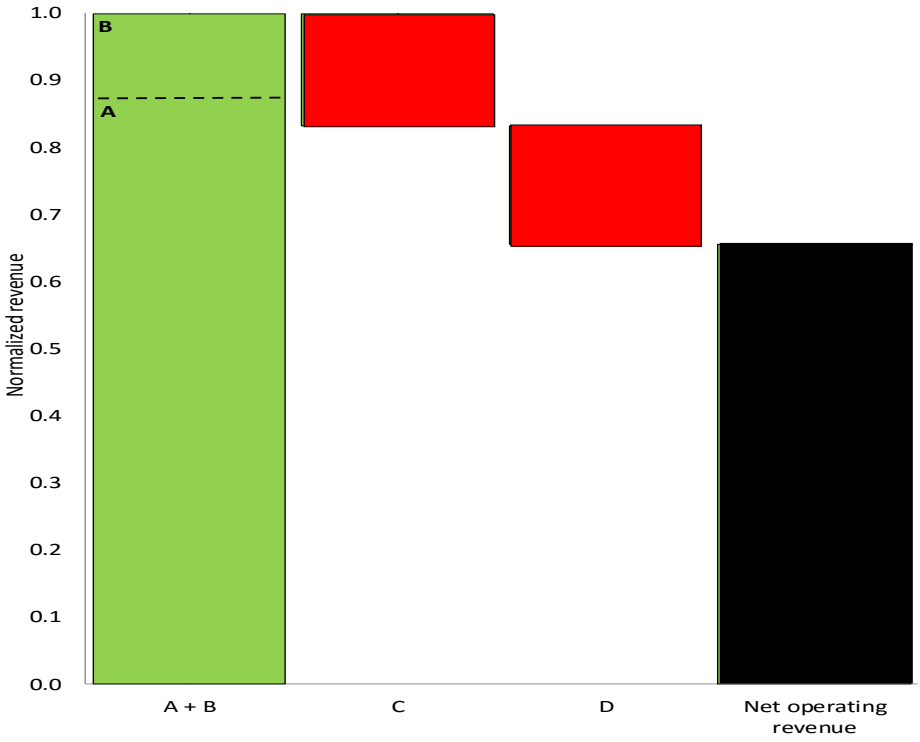

Figure 6.19: Revenue breakdown for power plant retrofitted with PCC system for 7-day of planning horizon at 1-hour time interval.

plant.

According to the optimization result and financial evaluation conducted in this analysis, the conflict occurred when the ERF incentive is superior to the revenue of selling electricity as illustrated in Strategy 2. This is because from the power plant's perspective; net operating revenue should be gained from selling electricity instead of the ERF project which underpinning the operational principal of power plant; to enhance the energy security via reliable supply demand. On the other hand, the fundamental deployment of ERF project (PCC technology) in coal-fired power plant is to embrace national environmental sustainability (by reducing the amount of CO_2 emission) as demanded by the Government concurrently could be as a secondary financial assistance to the coal-fired power plant. However, the financial analysis predicted in this analysis is solely deterministic

where thorough calculation should be focused on the capital cost of PCC technology (rate of return) and installation cost of the control system with consideration of the time value of money and future operational demand of black coal-based power generations throughout the crediting period.

Furthermore, the additional conflict also swayed by the constraints (power plant load and CO_2 capture rate) bounded on the optimization algorithm. As such, the power plant load forecasting is usually influenced by the exogenous variables accommodated in the optimization algorithm, for instance, time (peak or off-peak hours), electricity prices and policy (ERF scheme) [86]. While, the forecast of CO_2 capture rate is highly dependent on the power plant load. This interrelation (between power plant load and CO_2 capture rate) increased the complexity of optimization algorithm to find the optimal solution subject to the preference of human making decision (power plant managerial decision-making). This phenomenon featured in Strategy 1 and 2, where the conflict occurred when the integrated plant (power plant fitted with PCC system) forecasted to operate at maximum capacity during low electricity prices. Supposedly, the integrated plant should compliment each other for instance, when the power plant load increases the capture rate should be reduced and vice versa.

Generally, multi-objective constrained optimization problem (represented in Strategy 1 and 2) generates a number of optimal solutions (Pareto optimal solution) and thus require extensive technical information and prudent decision based on human/organisational preferences in order to attain the best and an exact optimization solution. One of the technique to solve this issue is by using numerical weight for respective objectives; revenue from selling electricity and incentive gained from the ERF project. This numerical weight can be obtained by finding all possible points in the feasible region in Pareto front [86] or by quantifying the

trade-off between two objectives by using trial and error [83]. However, further analysis to calculate the numerical weight (weighted factor) of this multi-objective constrained optimization problem is not possible in the tenure of this research work and may be explored in future studies.

6.6 The contemporary relevance of ERF scheme towards black coal-fired power plant

The multi-objective with dual path constraint strategy (Strategy 1) proposed in this chapter has shown to generate a feasible and reliable solution to predict the future insight of black coal-fired power plant ERF project compared to Strategy 2 (multi-objective with path and end-point constraints).

Based on Strategy 1, at the end of final crediting period (2022), the PCC plant is capable of capturing approximately 90% of total CO_2 emission throughout the crediting period. At this condition, the implementation of the ERF project (PCC technology) manages to limit the plant emissions below the regulated 7-year emission baseline (7 100 000 tonne CO_2). Deployment of PCC system has provided a surplus revenue of approximately 26% from the incentive gained from the ERF project. While, the power plant managed to obtain 41% revenue from selling the electricity. Under Strategy 1, the FAE for ERF project is approximately 10% from the total CO_2 emission of the BAU. This value can be used to represent the number of ACCU units to be issued during the auction process with estimated ACCU price per unit CO_2 is $AUD 50.

Based on the aforementioned result, it is financially and operationally viable for Australian black coal electricity generations to deploy PCC system under

the prevailing ERF scheme for crediting period between 2016 - 2022. However, a comprehensive analysis should be conducted regarding safeguard mechanism since the best decision for black coal-fired power plant ERF project can only be achieved if hourly emission (based on 30-minute emission baseline) is applied. Moreover, the outcome of this Strategy 1 is not deterministic (is only hypothetical) and warrants sensitivity analysis to evaluate the monetary value of a black coal electricity generation ERF project. Examples of parameters to be considered for sensitivity analysis are ACCU price, emission baseline and contract period. However, this study is believed to provide an insight to the Government and electricity generators towards advantage of the ERF project in term of economic and environmental perspectives.

Chapter 7

Conclusion and future work

7.1 Conclusion

The implementation of low emission technologies such as CCS system (i.e. amine-based PCC plant) at commercial scale power plant specifically coal-fired is of significant importance for the short and long-term global energy securities. Especially, when there is international pressure on the GHG abatement on top of the sporadic sources of renewable energy and rapid escalation of natural gas prices. Moreover, the uncertainty in technical and financial liabilities (in term of capital and operating expenditures) of the PCC plant have influenced and thus likely hindered the investment of the plant into large-scale deployment. Following that, a comprehensive managerial study that covers technical, economic, social, policy, safety and environmental perspectives are required towards the transformation of sustainable operation of clean fossil power generation and climate neutrality. Thus, this thesis explicates a development of computational management decision support framework for a coal-fired power plant associated with PCC system with the primary focus is to ensure the technology (amine-based PCC plant) is well worth considering for large-scale deployment.

At the initial stage, a mathematical black box model was developed to analyse the dynamic responses of a PCC pilot plant as illustrated in Chapter 3. The model identification reported the dynamics of variables of the key units in the plant; the absorber, rich/lean heat exchanger and desorber. Pilot plant dynamic data were used to develop a data-driven model (NLARX model) for each unit operation. Individual models were integrated to produce a simplified 4 x 3 PCC process model of the PCC plant. The fastest dynamic with a time constant ranging from 2 - 3 minutes featured in the relationship between power plant flue gas flow rate and CO_2 concentration in the absorber off gas. Whereas, the slowest response with a process time constant between 9 - 27 minutes occurred in CO_2 concentration at the top of the stripper due to changes in reboiler heat duty.

Process control analysis was then performed using the developed PCC-NLARX model in Chapter 4. Two control schemes were proposed which include a standard PID feedback control and a model-based control strategy in the form of MPC. Stepwise set point tracking and disturbance rejection scenarios imitated a real-time situation of power plant while considering retrofitting of the PCC system were employed to evaluate the performance of the proposed controllers for flexible operation, i.e. under variable plant load condition surrogate to electricity and carbon market prices patterns. Three elements of constraints include operational, economic and environmental were considered in selecting the best control strategy. The closed-loop simulation results showed that the MPC strategy handled very well the servo and regulator problems without violating the above mentioned constraints.

To ensure the reliability and feasibility of PCC technology, an algorithm that combines MPC with MINLP optimization (the hybrid MPC-MINLP algorithm) was developed in Chapter 5, and its application was demonstrated for coal-fired

power plants retrofitted with the solvent based PCC system. The developed algorithm, which featured a high sample frequency commensurate with electricity dispatch and control instrumentation levels was proposed as a decision support tool for flexible operation of the carbon capture plant while considering electricity and carbon price dynamics. Two techno-economic scenarios based on fixed (capture rate is constant) and flexible (capture rate is variable) operation modes were developed using actual (year 2011) and forecast (year 2020) electricity prices with two different carbon policy mechanisms for instance, fixed carbon prices (carbon tax) ($AUD 5, 25, 50/tonne-$CO_2$) for 24 hour period and ETS for one year planning horizon. Results showed that the integrated plant (power plant with PCC system) subject to forecast 2020 electricity and carbon prices were shown to generate yearly net operating revenue of approximately 12% of the gross revenue. While, the same integrated plant generated yearly net operating revenue loss of roughly 13% under 2011 electricity and carbon prices. These results underpin the strategy that employed the proposed optimization-based control framework for flexible operation of a PCC plant in the year 2020, because such framework captures financial benefits hidden in the dynamics of electricity load, electricity and carbon price trends, and does so at high temporal resolution.

Chapter 6 extended the techno-economic analysis performed in Chapter 5 for a real implementation in the emission abatement activity of Australia black-coal fired power plant. In this chapter, a multi-objective constrained optimization technique is used to evaluate the relevance of PCC technology as the ERF project for black coal power generations. The evaluation is conducted by incorporating economic and environmental objectives (design goals) to obtain maximum plant net operating revenue by generating the forecast of power plant load and CO_2 capture rate subject to dual constraint: operational and environmental. The results indicated that the multi-objective with dual path constraint strategy (Strategy

1) was able to generate a feasible and sensible solution to predict future insight of black coal fired power plant ERF project compared to Strategy 2 (multi-objective with path and end-point constraints) in term of operational and financial uncertainties. Throughout the seven years of the ERF contract period, the black-coal fired power plant capable to reduce plant emission approximately 10% from the total emission (from BAU) via Strategy 1. Moreover, coal-fired power plant obtained surplus revenue roughly 26% by the incentive gained from ERF project subject to carbon credit price of $AUD 50 per unit CO_2.

7.2 Future work

Although the outcomes of this thesis are able to provide a conceivable decision pertaining to the future deployment of CCS technology (i.e. PCC system) in term of operational, financial and policy point of views, more important aspects are still remains lacking. For instance, to ensure a realistic investment decision, a capital cost of CCS technology should be considered in the techno-economic analysis while adapting with the carbon-constrained world. This is because the cost of construction materials such as steel, cement and piping are fluctuated and thus can affect the total plant capital cost over time. Moreover, the cost of the control system package (i.e. hardware, software and services (maintenance, installation)) contributes to the elevation of PCC capital cost for an indeterminate return on capital if the plant flexibility is in demand. Beside the top-down managerial decisions propose in this thesis, there are other decisions that need to take into account by the power plant companies pertaining to the deployment of PCC technology. For instance, initial investment in transport and storage infrastructure is one of the vital decisions that can unlock the forecast unit cost reduction. Moreover, another critical decision is to obtain initial incentive either from government of non-government agencies to begin early PCC deployment.

On the other hand, this research can be extended by considering the uncertainty in CCS investment decisions (investment risk) for instance scale-up of CCS deployment, sequestration cost (onshore and offshore costs) and public acceptance. Additionally, one has to contemplate the extra cost emerges from the deployment of CCS technology such as the cost of coal and gas. Nevertheless, a highly sophisticated framework consists of comprehensive and wide-ranging internal and external uncertainties/parameters of the power plant and CCS technology will result in a high computational complexity, and thus require high-end computation software to deliver optimal and reliable solutions.

Appendix

Appendix A: A simplified 4 x 3 PCC linearized transfer function model.

From input "u_1" to output...

$$y_1 = \frac{0.0002285z^4}{z^5 - 0.9374z^4 + 4.895e^{-23}z^3 + 3.584e^{-47}z^2 + 2.469e^{-86}z}$$

$$9.256e^{-7}z^{31}-7.27e^{-6}z^{30}-2.752e^{-6}z^{29}+0.0001684z^{28}-0.0006914z^{27}+0.001443z^{26}-$$

$$0.001813z^{25}+0.001392z^{24}-0.0005707z^{23}+1.915e^{-5}z^{22}+9.985e^{-5}z^{21}-4.467e^{-5}z^{20}+$$

$$6.595e^{-6}z^{19}-2.581e^{-7}z^{18}+3.402e^{-7}z^{17}-1.466e^{-7}z^{16}+2.083e^{-8}z^{15}+2.063e^{-21}z^{14}+$$

$$1.236e^{-21}z^{13}+6.91e^{-23}z^{12}-5.63e^{-25}z^{11}+7.753e^{-25}z^{10}-2.34e^{-38}z^{9}+2.173e^{-39}z^{8}-$$

$$3.487e^{-53}z^{7}-1.057e^{-54}z^{6}+1.346e^{-68}z^{5}-6.228e^{-71}z^{4}+1.66e^{-85}z^{3}+9.717e^{-86}z^{2}-$$

$$8.358e^{-101}z + 1.744e^{-102}$$

$y_4 = ----------$

$$z^{33}-8.961z^{32}+36.22z^{31}-86.77z^{30}+135.7z^{29}-142.3z^{28}+95.52z^{27}-29.06z^{26}-15.68z^{25}+$$

$$25.27z^{24}-13.03z^{23}-1.02z^{22}+5.991z^{21}-3.68z^{20}+0.615z^{19}+0.3639z^{18}-0.2075z^{17}+$$

$$0.03178z^{16}+0.001128z^{15}-0.0003495z^{14}-8.876e{-}20z^{13}+2.042e^{-19}z^{12}-2.425e^{-21}z^{11}+$$

$$4.933e^{-22}z^{10}+3.771e^{-36}z^{9}-3.217e^{-37}z^{8}+7.334e^{-52}z^{7}-5.602e^{-53}z^{6}-5.589e^{-67}z^{5}+$$

$$4.508e^{-68}z^{4} + 3.619e^{-84}z^{3} - 2.501e^{-85}z^{2}$$

$$-2.657e^{-08}z^{32}-4.374e^{-07}z^{31}+1.4e^{-06}z^{30}+4.106e^{-06}z^{29}-2.687e^{-05}z^{28}+5.734e^{-05}z^{27}-$$

$$6.433e^{-05}z^{26}+3.868e^{-05}z^{25}-8.628e^{-06}z^{24}-2.91e^{-06}z^{23}+1.831e^{-06}z^{22}-$$

$$2.124e^{-07}z^{21}+2.602e^{-07}z^{20}-3.201e^{-07}z^{19}+1.383e^{-07}z^{18}-2.26e^{-08}z^{17}-$$

$$4.42e^{-23}z^{16}+4.386e^{-22}z^{15}-6.338e^{-23}z^{14}-9.359e^{-24}z^{13}+1.607e^{-24}z^{12}-$$

$$4.713e^{-38}z^{11}+3.185e^{-39}z^{10}+7.64e^{-41}z^{9}+8.852e^{-42}z^{8}+1.181e^{-55}z^{7}+$$

$$2.065e^{-56}z^{6}+4.012e^{-71}z^{5}+1.21e^{-71}z^{4}-8.466e^{-87}z^{3}+1.796e^{-88}z^{2}-$$

$$1.328e6-102z-8.722e-104$$

$$y_5 = ----------$$

$$z^{34}-8.577z^{33}+32.81z^{32}-73.13z^{31}+103.3z^{30}-92.15z^{29}+43.5z^{28}+5.415z^{27}-25.8z^{26}+$$

$$19.29z^{25}-3.813z^{24}-5.653z^{23}+5.528z^{22}-1.485z^{21}-0.7007z^{20}+0.5728z^{19}-0.07412z^{18}-$$

$$0.04196z^{17}+0.01222z^{16}+5.72e^{-05}z^{15}-0.0001223z^{14}+2.737e-19z^{1}3-1.035e-19z^{1}2-2.899e$$

$$1.278e^{-21}z^{10}+5.497e^{-36}z^{9}-3.304e^{-37}z^{8}+3.846e^{-52}z^{7}-1.301e^{-52}z^{6}+5.886e^{-68}z^{5}+$$

$$1.033e^{-68}z^{4}+1.306e6^{-86}z^{3}-3.968e^{-85}z^{2}$$

From input "u_2" to output...

$$y_1 = 0$$

$$y_4 = \frac{0.0007257z^{31} - 0.009656z^{30} + 0.05054z^{29} - 0.1447z^{28} + 0.2554z^{27} - 0.2884z^{26} + 0.2023z^{25} - 0.07302z^{24} - 0.003546z^{23} + 0.0157z^{22} - 0.00606z^{21} + 0.0006646z^{20} + 6.798e{-}05z^{19} + 6.785e^{-06}z^{18} - 1.132e^{-05}z^{17} + 3.552e^{-06}z^{16} - 4.452e^{-07}z^{15} - 3.764e^{-18}z^{14} - 1.496e^{-19}z^{13} + 3.014e^{-20}z^{12} - 4.424e{-}22z^{11} + 2.665e^{-22}z^{10} - 2.559e^{-36}z^{9} + 1.074e^{-36}z^{8} - 2.673e^{-51}z^{7} - 1.147e^{-54}z^{6} - 4.831e^{-67}z^{5} + 6.59e^{-69}z^{4} + 7.224e^{-83}z^{3} - 8.144e^{-84}z^{2} + 9.69e^{-99}z - 4.539e^{-100}}{z^{33} - 8.961z^{32} + 36.22z^{31} - 86.77z^{30} + 135.7z^{29} - 142.3z^{28} + 95.52z^{27} - 29.06z^{26} - 15.68z^{25} + 25.27z^{24} - 13.03z^{23} - 1.02z^{22} + 5.991z^{21} - 3.68z^{20} + 0.615z^{19} + 0.3639z^{18} - 0.2075z^{17} + 0.03178z^{16} + 0.001128z^{15} - 0.0003495z^{14} - 8.876e^{-20}z^{13} + 2.042e^{-19}z^{12} - 2.425e^{-21}z^{11} + 4.933e^{-22}z^{10} + 3.771e^{-36}z^{9} - 3.217e^{-37}z^{8} + 7.334e^{-52}z^{7} - 5.602e^{-53}z^{6} - 5.589e^{-67}z^{5} + 4.508e^{-68}z^{4} + 3.619e^{-84}z^{3} - 2.501e^{-85}z^{2}}$$

$$-2.083e^{-05}z^{32}-0.00022z^{31}+0.002038z^{30}-0.00651z^{29}+0.01105z^{28}-0.01088z^{27}$$

$$0.0009423z^{25}-0.000691z^{24}+0.0003993z^{23}-5.503e^{-05}z^{22}-2.096e-^{06}z^{21}-8.749e^{-06}z^{20}+$$

$$8.74e^{-06}z^{19}-3.411e^{-06}z^{18}+4.829e^{-07}z^{17}-4.728e^{-20}z^{16}-4.135e^{-20}z^{15}+$$

$$7.024e^{-21}z^{14}-6.734e^{-22}z^{13}+1.094e^{-22}z^{12}-1.971e^{-37}z^{11}+6.751e^{-38}z^{10}-$$

$$3.512e^{-39}z^{9}-5.685e^{-40}z^{8}-3.348e^{-54}z^{7}-3.799e^{-55}z^{6}-1.8e^{-69}z^{5}-3.116e^{-70}z^{4}-$$

$$1.286e-85z^{3}-6.087e^{-86}z^{2}-1.728e^{-102}z-3.265e^{-102}$$

$$y_5 = \frac{}{}$$

$$z^{34}-8.577z^{33}+32.81z^{32}-73.13z^{31}+103.3z^{30}-92.15z^{29}+43.5z^{28}+5.415z^{27}-25.8z^{26}+$$

$$19.29z^{25}-3.813z^{24}-5.653z^{23}+5.528z^{22}-1.485z^{21}-0.7007z^{20}+0.5728z^{19}-0.07412z^{18}-$$

$$0.04196z^{17}+0.01222z^{16}+5.72e^{-05}z^{15}-0.0001223z^{14}+2.737e^{-19}z^{13}-1.035e^{-19}z^{12}-$$

$$2.899e^{-21}z^{11}+1.278e^{-21}z^{10}+5.497e^{-36}z^{9}-3.304e-37z^{8}+3.846e-52z^{7}-1.301e-52z^{6}+$$

$$5.886e^{-68}z^{5}+1.033e^{-68}z^{4}+1.306e^{-86}z^{3}-3.968e^{-85}z^{2}$$

From input "u_3" to output...

$$y_1 = 0$$

$$-1.537e^{-06}z^{34} + 1.254e^{-05}z^{33} - 4.593e^{-05}z^{32} + 9.92e^{-05}z^{31} - 0.0001389z^{30} +$$

$$0.0001288z^{29} - 7.373e^{-05}z^{28} + 1.364e^{-05}z^{27} + 1.89e^{-05}z^{26} - 2.061e^{-05}z^{25} +$$

$$7.499e^{-06}z^{24} + 3.17e^{-06}z^{23} - 5.037e^{-06}z^{22} + 2.277e^{-06}z^{21} - 1.858e^{-07}z^{20} -$$

$$2.271e^{-07}z^{19} + 9.063e^{-08}z^{18} - 1.381e^{-08}z^{17} + 3.249e^{-09}z^{16} - 1.805e^{-09}z^{15} +$$

$$4.096e^{-10}z^{14} + 2.09e^{-24}z^{13} - 2.738e^{-25}z^{12} + 4.219e^{-26}z^{11} - 5.22e^{-27}z^{10} -$$

$$1.088e^{-40}z^{9} + 7.814e^{-42}z^{8} + 4.86e^{-56}z^{7} - 2.33e^{-57}z^{6} - 1.023e^{-71}z^{5} - 8.316e^{-73}z^{4} +$$

$$1.451e^{-87}z^{3} + 2.494e^{-88}z^{2} - 1.805e^{-103}z + 3.398e^{-104}$$

$$y_4 = \frac{}{}$$

$$z^{35} - 8.961z^{34} + 36.22z^{33} - 86.77z^{32} + 135.7z^{31} - 142.3z^{30} + 95.52z^{29} - 29.06z^{28} -$$

$$15.68z^{27} + 25.27z^{26} - 13.03z^{25} - 1.02z^{24} + 5.991z^{23} - 3.68z^{22} + 0.615z^{21} + 0.3639z^{20} -$$

$$0.2075z^{19} + 0.03178z^{18} + 0.001128z^{17} - 0.0003495z^{16} - 8.876e^{-20}z^{15} + 2.042e^{-19}z^{14} -$$

$$2.425e^{-21}z^{13} + 4.933e^{-22}z^{12} + 3.771e^{-36}z^{11} - 3.217e^{-37}z^{10} + 7.334e^{-52}z^{9} -$$

$$5.602e^{-53}z^{8} - 5.589e^{-67}z^{7} + 4.508e^{-68}z^{6} + 3.619e^{-84}z^{5} - 2.501e^{-85}z^{4}$$

$$-5.06e^{-06}z^{35}+5.376e^{-05}z^{34}-0.0002503z^{33}+0.0006773z^{32}-0.00118z^{31}+0.001372z^{30}-$$

$$0.001034z^{29}+0.0004049z^{28}+8.992e^{-05}z^{27}-0.0002486z^{26}+0.0001584z^{25}-1.272e^{-05}z^{24}-$$

$$5.652e-05z^{23}+4.291e^{-05}z^{22}-9.935e^{-06}z^{21}-3.414e^{-06}z^{20}+2.519e^{-06}z^{19}-$$

$$4.363e^{-07}z^{18}-1.057e-08z^{17}+4.251e^{-09}z^{16}-1.226e-^{23}z^{15}+1.019e^{-23}z^{14}-$$

$$6.535e^{-26}z^{13}-3.221e^{-26}z^{12}-1.072e^{-40}z^{11}+9.983e^{-42}z^{10}+8.119e^{-44}z^{9}-$$

$$4.85e^{-44}z^{8}-2.251e^{-58}z^{7}-3.618e^{-59}z^{6}+5.926e^{-73}z^{5}-2.367e^{-74}z^{4}-4.593e-88z^{3}+$$

$$4.804e^{-89}z^{2}-3.331e^{-104}z+3.442e^{-105}$$

$y_5 = ----------$

$$z^{36}-8.577z^{35}+32.81z^{34}-73.13z^{33}+103.3z^{32}-92.15z^{31}+43.5z^{30}+5.415z^{29}-$$

$$25.8z^{28}+19.29z^{27}-3.813z^{26}-5.653z^{25}+5.528z^{24}-1.485z^{23}-0.7007z^{22}+$$

$$0.5728z^{21}-0.07412z^{20}-0.04196z^{19}+0.01222z^{18}+5.72e^{-05}z^{17}-0.0001223z^{16}+$$

$$2.737e^{-19}z^{15}-1.035e^{-19}z^{14}-2.899e^{-21}z^{13}+1.278e^{-21}z^{12}+5.497e^{-36}z^{11}-$$

$$3.304e^{-37}z^{10}+3.846e^{-52}z^{9}-1.301e^{-52}z^{8}+5.886e^{-68}z^{7}+1.033e^{-68}z^{6}+$$

$$1.306e^{-86}z^{5}-3.968e^{-85}z^{4}$$

From input "u_4" to output...

$$y_1 = 0$$

$$y_4 = \frac{-0.001331z^{31}+0.01835z^{30}-0.1011z^{29}+0.3099z^{28}-0.5967z^{27}+0.7574z^{26}-0.6326z^{25}+0.3219z^{24}-0.06548z^{23}-0.02869z^{22}+0.02483z^{21}-0.007176z^{20}+0.0007504z^{19}+2.53e^{-05}z^{18}-3.994e^{-06}z^{17}-1.578e^{-07}z^{16}-6.056e^{-08}z^{15}-6.57e^{-19}z^{14}+7.725e^{-19}z^{13}-1.256e^{-19}z^{12}-9.969e^{-22}z^{11}-4.612e^{-23}z^{10}-2.694e^{-36}z^{9}+4.113e^{-37}z^{8}+8.96e^{-52}z^{7}-3.712e^{-52}z^{6}+1.855^{e}-66z^{5}+1.796e^{-69}z^{4}-2.341e^{-82}z^{3}+3.076e^{-83}z^{2}-1.379e^{-98}z-4.585e^{-101}}{z^{33}-8.961z^{32}+36.22z^{31}-86.77z^{30}+135.7z^{29}-142.3z^{28}+95.52z^{27}-29.06z^{26}-15.68z^{25}+25.27z^{24}-13.03z^{23}-1.02z^{22}+5.991z^{21}-3.68z^{20}+0.615z^{19}+0.3639z^{18}-0.2075z^{17}+0.03178z^{16}+0.001128z^{15}-0.0003495z^{14}-8.876e^{-20}z^{13}+2.042e^{-19}z^{12}-2.425e^{-21}z^{11}+4.933e^{-22}z^{10}+3.771e^{-36}z^{9}-3.217e^{-37}z^{8}+7.334e^{-52}z^{7}-5.602e^{-53}z^{6}-5.589e^{-67}z^{5}+4.508e^{-68}z^{4}+3.619e^{-84}z^{3}-2.501e^{-85}z^{2}}$$

$$3.821e^{-05}z^{32}+0.000386z^{31}-0.003946z^{30}+0.01383z^{29}-0.02633z^{28}+0.03038z^{27}-0.02123z^{26}-$$

$$0.007717z^{25}-4.267e^{-06}z^{24}-0.001286z^{23}+0.00055z^{22}-0.0001147z^{21}+2.037e^{-05}z^{20}-$$

$$4.068e^{-06}z^{19}+2.313e^{-07}z^{18}+6.569e^{-08}z^{17}+1.115e^{-18}z^{16}+4.723e^{-20}z^{15}-$$

$$5.351e^{-20}z^{14}-1.57e^{-21}z^{13}+3.04e^{-22}z^{12}-5.625e^{-36}z^{11}-6.466e^{-37}z^{10}+$$

$$7.433e^{-39}z^{9}+4.55e^{-39}z^{8}+4.862e^{-54}z^{7}+3.299e^{-54}z^{6}-2.672e^{-69}z^{5}+$$

$$4.535e-70z^{4}-3.301e^{-84}z^{3}+1.16e^{-85}z^{2}+5.941e^{-100}z-4.2e^{-101}$$

$$y_4 = ----------$$

$$z^{34}-8.577z^{33}+32.81z^{32}-73.13z^{31}+103.3z^{30}-92.15z^{29}+43.5z^{28}+5.415z^{27}-$$

$$25.8z^{26}+19.29z^{25}-3.813z^{24}-5.653z^{23}+5.528z^{22}-1.485z^{21}-0.7007z^{20}+0.5728z^{19}-$$

$$0.07412z^{18}-0.04196z^{17}+0.01222z^{16}+5.72e^{-05}z^{15}-0.0001223z^{14}+2.737e^{-19}z^{13}-$$

$$1.035e^{-19}z^{12}-2.899e^{-21}z^{11}+1.278e^{-21}z^{10}+5.497e^{-36}z^{9}-3.304e^{-37}z^{8}+$$

$$3.846e^{-52}z^{7}-1.301e^{-52}z^{6}+5.886e^{-68}z^{5}+1.033e^{-68}z^{4}+1.306e^{-86}z^{3}-3.968e^{-85}z^{2}$$

Bibliography

[1] V. Foster and D. Bedrosyan, "Understanding CO_2 emissions from the global energy sector," 2014.

[2] "World energy outlook 2014," *International Energy Agency (IEA).*

[3] "Australian Electricty Market Operator (AEMO). 12 February 2016." [Online]. Available: http://www.aemo.com.au.

[4] "Greenhouse gas inventory data. 2 June 2015." [Online]. Available: http://unfccc.int/ghg_data/items/3800.php.

[5] "National greenhouse gas inventory - Kyoto Protocol classifications. 16 February 2016." [Online]. Available: http://ageis.climatechange.gov.au/.

[6] "Climate change. 28 November 2016." [Online]. Available: http://www.climatechange.gov.au.

[7] "Emissions Reduction Fund White Paper," *Department of the Environment.*

[8] "What is energy security? 12 February 2015." [Online]. Available: http://www.iea.org/topics/energysecurity/subtopics/whatisenergysecurity/.

[9] "Analysis of impacts of climate change policies on energy security. Final report," *European Commission Environment*, 2009.

[10] "Carbon Pollution Reduction Scheme. 9 November 2016." [Online]. Available: http://www.aph.gov.au/About_Parliament/

Parliamentary_Departments/Parliamentary_Library/Browse_by_Topic/ClimateChangeold/governance/domestic/national/cprs.

[11] "Emission Reduction Fund." [Online]. Available: http://www.cleanenergyregulator.gov.au/ERF.

[12] "Carbon farming iniative review report," *Climate Change Authority, Australian Government*, December 2014.

[13] B. Banks and M. Bigland-Pritchard, "Saskpower's Carbon Capture Project. What Risk? What Reward? January 2015."

[14] E. Boot-Handford Matthew, C. Abanades Juan, J. Anthony Edward, J. Blunt Martin, S. Brandani, N. Mac Dowell, R. Fernandez Jose, M.-C. Ferrari, R. Gross, P. Hallett Jason, S. Haszeldine, P. Heptonstall, A. Lyngfelt, Z. Makuch, E. Mangano, J. Porter, Richard, M. Pourkashanian, T. Rochelle Gary, N. Shah, G. Yao Joseph, and S. Fennell Paul, "State and trends of carbon pricing 2014," *International Journal of Greenhouse Gas Control*, 2014.

[15] "The future of CCS. An IChemE energy centre green paper. 2 August 2016." [Online]. Available: http://www.icheme.org/~/media/Documents/icheme/Media%20centre/ccs-forum-report-summary-report-july%202016.pdf.

[16] J. Gaspar and M. Cormos A, "Dynamic modeling and validation of absorber and desorber columns for post-combustion CO_2 capture," *Computers & Chemical Engineering*, vol. 35, no. 10, pp. 2044–2052, 2011.

[17] A. Lawal, M. Wang, P. Stephenson, and O. Obi, "Demonstrating full-scale post-combustion CO_2 capture for coal-fired power plants through dynamic modelling and simulation," *Fuel*, vol. 101, pp. 115–128, 2012.

[18] A. Jayarathna S, B. Lie, and C. Melaaen M, "Dynamic modelling of the absorber of a post-combustion CO_2 capture plant: Modelling and simulations,"

Computers & Chemical Engineering, vol. 53, pp. 178–189, 2013.

[19] A. Lawal, M. Wang, P. Stephenson, and H. Yeung, "Dynamic modelling of CO_2 absorption for post combustion capture in coal-fired power plants," *Fuel*, vol. 88, no. 12, pp. 2455–2462, 2009.

[20] J. Gaspar and M. Cormos A, "Dynamic modeling and absorption capacity assessment of CO_2 capture process," *International Journal of Greenhouse Gas Control*, vol. 8, pp. 45–55, 2012.

[21] C. Biliyok, A. Lawal, M. Wang, and F. Seibert, "Dynamic modelling, validation and analysis of post-combustion chemical absorption CO_2 capture plant," *International Journal of Greenhouse Gas Control*, vol. 9, pp. 428–445, 2012.

[22] T. Neveux, Y. Le Moullec, P. Corriou J, and E. Favre, "Modeling CO_2 capture in amine solvents: Prediction of performance and insights on limiting phenomena," *Industrial & Engineering Chemistry Research*, vol. 52, no. 11, pp. 4266–4279, 2013.

[23] S. Posch and M. Haider, "Dynamic modeling of CO_2 absorption from coal-fired power plants into an aqueous monoethanolamine solution," *Chemical Engineering Research & Design*, vol. 91, pp. 977–987, 2013.

[24] N. Mac Dowell and N. Shah, "Dynamic modelling and analysis of a coal-fired power plant integrated with a novel split-flow configuration post-combustion CO_2 capture process," *International Journal of Greenhouse Gas Control*, vol. 27, pp. 103–119, 2014.

[25] J. Akesson, D. Laird C, G. Lavedan, K. Prolss, H. Tummescheit, S. Velut, and Y. Zhu, "Nonlinear model predictive control of a CO_2 post-combustion absorption unit," *Chemical Engineering & Technology*, vol. 35, no. 3, pp. 445–454, 2012.

[26] J. Lin Y, H. Pan T, H. Wong D S, S. Jang S, W. Chi Y, and H. Yeh C, "Plantwide control of CO_2 capture by absorption and stripping using monoethanolamine solution," *Industrial & Engineering Chemistry Research*, vol. 50, no. 3, pp. 1338–1345, 2011.

[27] A. Lawal, M. Wang, P. Stephenson, G. Koumpouras, and H. Yeung, "Dynamic modelling and analysis of post-combustion CO_2 chemical absorption process for coal-fired power plants," *Fuel*, vol. 89, no. 10, pp. 2791–2801, 2010.

[28] M. Kvamsdal H, P. Jakobsen J, and A. Hoff K, "Dynamic modeling and simulation of a CO_2 absorber column for post-combustion CO_2 capture," *Chemical Engineering and Processing*, vol. 48, no. 1, pp. 135–144, 2009.

[29] A. Arce, N. Mac Dowell, N. Shah, and F. Vega L, "Flexible operation of solvent regeneration systems for CO_2 capture processes using advanced control techniques: Towards operational cost minimisation," *International Journal of Greenhouse Gas Control*, vol. 11, pp. 236–250, 2012.

[30] T. Nittaya, L. Douglas P, E. Croiset, and A. Ricardez-Sandoval L, "Dynamic modelling and control of MEA absorption processes for CO_2 capture from power plants," *Fuel*, vol. 116, pp. 672–691, 2014.

[31] N. Harun, T. Nittaya, L. Douglas P, E. Croiset, and A. Ricardez-Sandoval L, "Dynamic simulation of MEA absorption process for CO_2 capture from power plants," *International Journal of Greenhouse Gas Control*, vol. 10, pp. 295–309, 2012.

[32] A. Jayarathna S, B. Lie, and C. Melaaen M, "Amine based CO_2 capture plant: Dynamic modeling and simulations," *International Journal of Greenhouse Gas Control*, vol. 14, pp. 282–290, 2013.

[33] J. Lin Y, C. Chang C, S. H. Wong D, S. Jang S, and J. Ou J, "Control strategies for flexible operation of power plant integrated with CO_2 capture

plant," *AiChe Journal*, vol. 31, pp. 1366–1371, 2012.

[34] N. Mac Dowell, J. Samsatli N, and N. Shah, "Dynamic modelling and analysis of an amine-based post-combustion CO_2 capture absorption column," *International Journal of Greenhouse Gas Control*, vol. 12, pp. 247–258, 2013.

[35] M. Kvamsdal H, A. Chikukwa, M. Hillestad, A. Zakeri, and A. Einbu, "A comparison of different parameter correlation models and the validation of an MEA-based absorber model," *Energy Procedia*, vol. 4, pp. 1526–1533, 2011.

[36] A. Jayarathna S, B. Lie, and C. Melaaen M, "NEQ rate based modeling of an absorption column for post combustion CO_2 capturing," *Energy Procedia*, vol. 4, pp. 1797–1804, 2011.

[37] S. Ziaii, T. Rochelle G, and F. Edgar T, "Dynamic modeling to minimize energy use for CO_2 capture in power plants by aqueous monoethanolamine," *Industrial & Engineering Chemistry Research*, vol. 48, no. 13, pp. 6105–6111, 2009.

[38] X. Zhang, I. J. Duncan, G. Huang, and G. Li, "Identification of management strategies for CO_2 capture and sequestration under uncertainty through inexact modeling," *Applied Energy*, vol. 113, no. 0, pp. 310–317, 2014.

[39] R. Khalilpour, "Flexible operation scheduling of a power plant integrated with PCC processes under market dynamics," *Industrial & Engineering Chemistry Research*, vol. 53, no. 19, pp. 8132–8146, 2014.

[40] R. Khalilpour, "Multi-level investment planning and scheduling under electricity and carbon market dynamics: Retrofit of a power plant with PCC (post-combustion carbon capture) processes," *Energy*, vol. 64, pp. 172–186, 2014.

[41] A. Qadir, M. Sharma, F. Parvareh, R. Khalilpour, and A. Abbas, "Flexible dynamic operation of solar-integrated power plant with solvent based post-

combustion carbon capture(PCC) process," *Energy Conversion and Management*, vol. 97, pp. 7–19, 2015.

[42] N. Mac Dowell and N. Shah, "The multi-period optimisation of an amine-based CO_2 capture process integrated with a super-critical coal-fired power station for flexible operation," *Computers & Chemical Engineering*, vol. 74, pp. 169–183, 2015.

[43] Y. Lee M and H. Hashim, "Modelling and optimization of CO_2 abatement strategies," *Journal of Cleaner Production*, vol. 71, no. 0, pp. 40–47, 2014.

[44] Z. Wang, H. Huang G, P. Cai Y, C. Dong, and G. Sun H, "The identification of optimal CO_2 emissions-trading strategies based on an inexact two-stage chance-constrained programming approach," *International Journal of Green Energy*, vol. 11, no. 3, pp. 302–319, 2014.

[45] R. Anantharaman, S. Roussanaly, F. Westman S, and J. Husebye, "Selection of optimal CO_2 capture plant capacity for better investment decisions," *Ghgt-11*, vol. 37, pp. 7039–7045, 2013.

[46] J. Cristobal, G. Guillen-Gosalbez, L. Jimenez, and A. Irabien, "MINLP model for optimizing electricity production from coal-fired power plants considering carbon management," *Energy Policy*, vol. 51, pp. 493–501, 2012.

[47] H. Hashim, P. Douglas, A. Elkamel, and E. Croiset, "Optimization model for energy planning with CO_2 emission considerations," *Industrial & Engineering Chemistry Research*, vol. 44, no. 4, pp. 879–890, 2005.

[48] N. Abdul Manaf, A. Cousins, P. Feron, and A. Abbas, "Dynamic modelling, identification and preliminary control analysis of an amine-based post-combustion CO_2 capture pilot plant," *Journal of Cleaner Production*, vol. 113, pp. 1–19, 2015.

[49] A. Cousins, A. Cottrell, A. Lawson, S. Huang, and P. Feron, "Model verification and evaluation of the rich-split process modification at an Australian-based post combustion CO_2 capture pilot plant," *Greenhouse Gases: Science and Technology*, vol. 2, no. 5, pp. 329–345, 2012.

[50] N. Mac Dowell and N. Shah, "Identification of the cost-optimal degree of CO_2 capture: An optimisation study using dynamic process models," *International Journal of Greenhouse Gas Control*, vol. 13, pp. 44–58, 2013.

[51] S. Ziaii, S. Cohen, G. T. Rochelle, F. Edgar T, and E. Webber M, "Dynamic operation of amine scrubbing in response to electricity demand and pricing," *Greenhouse Gas Control Technologies*, vol. 1, no. 1, pp. 4047–4053, 2009.

[52] M. Mokhtar, T. Ali M, R. Khalilpour, A. Abbas, N. Shah, A. Al Hajaj, P. Armstrong, M. Chiesa, and S. Sgouridis, "Solar-assisted post-combustion carbon capture feasibility study," *Applied Energy*, vol. 92, pp. 668–676, 2012.

[53] B. Rao A and S. Rubin E, "A technical, economic, and environmental assessment of amine-based CO_2 capture technology for power plant greenhouse gas control," *Environmental Science and Technology*, vol. 36, no. 20, pp. 4467–4475, 2002.

[54] J. Gaspar and M. Cormos A, "Dynamic modeling and validation of absorber and desorber columns for post-combustion CO_2 capture," *Computers and Chemical Engineering*, vol. 35, pp. 2044–2052, 2011.

[55] M. Saimpert, G. Puxty, S. Qureshi, L. Wardhaugh, and A. Cousins, "A new rate based absorber and desorber modelling tool," *Chemical Engineering Science*, vol. 96, pp. 10–25, 2013.

[56] A. Tobiesen Finn, O. Juliussen, and F. Svendsen Hallvard, "Experimental validation of a rigorous desorber model for post-combustion capture," *Chemical Engineering Science*, vol. 63, no. 10, pp. 2641–2656, 2008.

[57] A. Cybulski, M. Sharma M, A. Sheldon R, and A. Moulijn J, *Fine Chemicals Manufacture: Technology and Engineering.* Gulf Professional Publishing, 2001.

[58] Q. Zhang and L. Ljung, "Multiple steps prediction with nonlinear arx models," 2007.

[59] N. Abdul Manaf, A. Cousins, P. Feron, and A. Abbas, "Control analysis of post combustion carbon dioxide capture process (PCC)," *International Journal of Chemical and Environmental Engineering*, vol. 5 (4).

[60] M. T. Luu, N. Abdul Manaf, and A. Abbas, "Dynamic modelling and control strategies for flexible operation of amine-based post-combustion CO_2 capture systems," *International Journal of Greenhouse Gas Control*, vol. 39, pp. 377–389, 2015.

[61] M. Karimi, M. Hillestad, and F. Svendsen H, "Investigation of the dynamic behavior of different stripper configurations for post-combustion CO_2 capture," *International Journal of Greenhouse Gas Control*, vol. 7, pp. 230–239, 2012.

[62] L. Darby Mark and M. Nikolaou, "Multivariable system identification for integral controllability," *Automatica*, vol. 45, no. 10, pp. 2194–2204, 2009.

[63] E. Haggblom K, "Integral controllability and integrity for uncertain systems," *American Control Conference*, vol. 1-12, pp. 5192–5197, 2008.

[64] B. Metz, *IPCC Special Report on Carbon Dioxide Capture and Storage.* Cambridge University Press for the Intergovernmental Panel on Climate Change, 2005.

[65] "Australia Energy Market Operator (AEMO). 10June 2014." [Online]. Available: http://www.aemo.com.au

[66] N. A. Manaf and A. Abbas, "Temporal multiscalar decision support framework for flexible operation of carbon capture plants targeting low-carbon management of power plant emissions." *Journal of Applied Energy*, vol. 169, pp. 912–926, 2016.

[67] N. A. Manaf, A. Qadir, and A. Abbas, "The hybrid MPC-MINLP algorithm for optimal operation of coal-fired power plant with solvent based post-combustion CO_2 capture." *Petroleum*, Accepted. 2016.

[68] M. Sharma, F. Parvareh, and A. Abbas, "Highly integrated post-combustion carbon capture process in a coal-fired power plant with solar repowering," *International Journal of Energy Research*, vol. 39, pp. 1623–1635, 2015.

[69] *Electric Power from Competitive Sources. Darra, Australia: Ultra-Systems Technology Pty Ltd.*, 1999.

[70] Z. Li, M. Sharma, R. Khalilpour, and A. Abbas, "Optimal operation of solvent-based post-combustion carbon capture processes with reduced models," *Energy Procedia*, vol. 37, pp. 1500–1508, 2013.

[71] M. Zaman and J. H. Lee, "Optimization of the various modes of flexible operation for post-combustion CO_2 capture plant," *Computers & Chemical Engineering*, vol. 75, pp. 14–27, 2015.

[72] P. C. Van der Wijk, A. S. Brouwer, M. van den Broek, T. Slot, G. Stienstra, W. van der Veen, and A. P. C. Faaij, "Benefits of coal-fired power generation with flexible CCS in a future northwest European power system with large scale wind power," *International Journal of Greenhouse Gas Control*, vol. 28, pp. 216–233, 2014.

[73] "Australian Energy Market Operator (AEMO). 10 June 2014." [Online]. Available: http://www.aemo.com.au.

[74] "The impact of congestion on bidding and inter-regional trade in the NEM. special report. Australian Energy Regulator." 2012.

[75] "Intercontinental exchange futures data. 5 April 2051." [Online]. Available: https://www.quandl.com/data/ICE/CZ2014-ECX-EUA>.

[76] "Strong growth, low pollution: Modelling a carbon price: Australian Government." 2011.

[77] N. Mac Dowell and N. Shah, "The multi-period optimisation of an amine-based CO_2 capture process integrated with a super-critical coal-fired power station for flexible operation," *Computers & Chemical Engineering*, vol. 74, 2015.

[78] R. D. Brasington, "Integration and operation of post-combustion capture system on coal fired power generation: load following and solvent storage," *Master Thesis. Massachusettes Istitute of Technology*, 2007.

[79] S. A. Lefton and P. Besuner, "The potential for renewable energy to provide baseload power in Australia, Parliamentary Library (Australia).5 April 2015."

[80] A. S. Brouwer, M. van den Broek, A. Seebregts, and A. Faaij, "Operational flexibility and economics of power plants in future low-carbon power systems," *Applied Energy*, vol. 156, pp. 107–128, 2015.

[81] L. Hirth and J. C. Steckel, "The role of capital costs in decarbonizing the electricity sector," *Environmental Research Letters*, vol. 11, no. 11, p. 114010.

[82] "Modelling and Analysis of Australia Abatement Opportunities. 10 March 2017." [Online]. Available: http://www.environment.gov.au/system/files/resources/b8540c8a-8a31-4aba-a8b5-63cc46466e33/files/modelling-and-analysis-australias-2030-abatement-opportunities.pdf.

[83] J. Stjepandic, N. Wognum, and W. J. C. Verhagen, "Concurrent Engineering in the 21^{st} Century: Foundations, Developments and Challenges," *Springer International Publishing*, 2015.

[84] *National and state economic forecasts to 2034-35.* National Institute of Economic and Industry Research (NIEIR).

[85] J. Cristobal, G. Guillen-Gosalbez, L. Jimenez, and A. Irabien, "Optimization of global and local pollution control in electricity production from coal burning," *Applied Energy*, vol. 92, pp. 369–378, 2012.

[86] L. Xiao, W. Shao, C. Wang, K. Zhang, and H. Lu, "Research and application of a hybrid model based on multi-objective optimization for electrical load forecasting," *Applied Energy*, vol. 180, pp. 213–233, 2016.

[87] Z. Pan, Q. Guo, and H. Sun, "Impacts of optimization interval on home energy scheduling for thermostatically controlled appliances," *CSEE Journal of Power and Energy Systems*, vol. 1, pp. 90–100, 2015.

[88] K. Deb, "Multi-objective optimisation using evolutionary algorithms: An introduction," *Multi-objective* E*volutionary* O*ptimisation for* P*roduct* D*esign and* M*anufacturing, Springer International Publishing*, pp. 3–34, 2011.